Selection and Characterization of Engineered Binding Proteins to α-Synuclein

Inaugural dissertation

for the attainment of the title of doctor
in the Faculty of Mathematics and Natural Sciences

at the Heinrich Heine University Düsseldorf

presented by

Hamed Shaykhalishahi

from Yazd, Iran

Düsseldorf, November 2014

from the institute for Physikalische Biologie

at the Heinrich Heine University Düsseldorf

Published by permission of the
Faculty of Mathematics and Natural Sciences at

Heinrich Heine University Düsseldorf

Supervisor: Dr. Wolfgang Hoyer

Co-supervisor: Prof. Dr. Dieter Willbold

Date of the oral examination: 25.11.2014

Table of Contents

Summary

Selection and Characterization of Engineered Binding Proteins for α-Synuclein

Amyloidogenesis or formation of amyloid fibrils is associated with more than 20 human diseases including Parkinson's disease (PD), Alzheimer's disease (AD), and type 2 diabetes (T2D). PD is characterized by brain deposition of Lewy bodies, mainly composed of α-synuclein fibrils. Increasing evidence establishes the involvement of α-synuclein aggregation in the pathogenesis of PD. Despite extensive research on protein aggregation, the exact mechanisms controlling or triggering this process remain unknown. Identification of specific binding proteins may provide a precious tool for the study of protein-protein interactions in the aggregation process. Previous studies using a selected binding protein against amyloid-β (Aβ) peptide, ZAβ$_3$, resulted in the identification of a β-hairpin-forming region critical for Aβ aggregation. ZAβ$_3$ inhibits Aβ aggregation via shielding this β-hairpin region inside its tunnel-like cavity. The overall aim of the present thesis is focused on the selection of engineered binding proteins for α-synuclein and characterization of their interactions with α-synuclein and other amyloidogenic proteins.

Chapter 2 and chapter 3 deal with the selection and characterization of binding proteins from a ZAβ$_3$-based β-wrapin library using phage display technology. Chapter 2 describes the selection of AS69, a specific β-wrapin protein with nanomolar affinity to α-synuclein. Similar to ZAβ3, dimeric AS69 forms a hydrophobic tunnel-like cavity in which α-synuclein adopts a β-hairpin conformation. The β-hairpin region comprises residues 37 to 54 in N-terminal domain of α-synuclein amino acid sequence and is composed of two β-strands which are similar to those identified in the fibril core. Location of these β-strands in the core of α-synuclein oligomers and the presence of 5 familial mutations linked to early-onset PD highlight the importance of the

identified β-hairpin forming region. Here, it is shown that sequestration of the β-hairpin structure inside of AS69 impedes α-synuclein aggregation and toxicity. Remarkably, sub-stoichiometric amounts of AS69 prolong lag time of aggregation via interference with primary and/or secondary nucleation events.

Chapter 3 reports the characterization of additional β-wrapin proteins with affinity for α-synuclein. Out of this set, the β-wrapin AS10 interacts not only with α-synuclein but also with Aβ and Islet amyloid polypeptide (IAPP) with sub-micromolar affinity. Our NMR data demonstrate that AS10 binding is accompanied by the formation of β-hairpin structure in all three target proteins. AS10 is able to inhibit aggregation and toxicity of the three amyloidogenic proteins. These results emphasize the similarity of these amyloidogenic proteins with respect to conformational properties and molecular recognition motifs.

AS69 is a homodimer protein linked via Cys-28 residues of the subunits. Chapter 4 describes the generation of AS69-GS3, a head-to-tail construct of dimeric AS69 with a glycine-serine-rich linker. Employing AS69-GS3 construct reveals the importance of Cys-28 for the binding affinity to α-synuclein. Our biophysical data demonstrate an increase in structural compaction and stability induced by formation of interamolecular Cys-28 linkage.

In Chapter 5, the β-hairpin region identified by AS69 is further investigated. The impact of the β-hairpin region on α-synuclein aggregation is elucidated using α-synCC, a double-cysteine mutant of α-synuclein. Here, stabilization of contact between the β1 and β2 segments of α-synuclein via introduction of an intramolecular disulfide bond leads to the loss of aggregation propensity of α-synuclein. This chapter also demonstrates the inhibitory effect of α-synCC on the fibrillation process of α-synuclein, Aβ and IAPP. In our in vitro experiments, the reduced α-synCC shows an inhibitory effect against fibril formation to the same level as that of wild-type α-synuclein, while oxidized α-synCC exhibits a significantly increased inhibitory effect. Taken together, we propose that the β1-β2 contact in α-synuclein entails an inhibitory effect against

amyloid formation and that disulfide bond-assisted stabilization of this contact in α-synCC strengthens this effect.

This thesis demonstrates how engineered binding proteins can be applied to (i) identify sequence regions critical for protein aggregation, (ii) elucidate common interaction motifs of intrinsically disordered amyloidogenic proteins, (iii) devise novel therapeutic strategies for protein misfolding disorders.

Chapter 1: Introduction

1.1. Protein folding and misfolding

Proteins, the workhorse molecules of the cells, are the most abundant and functionally versatile macromolecules nearly involved in all biological processes [1]. Briefly, different genes encode different messenger RNAs (mRNAs). In the cytoplasm, ribosomes bind to mRNA transcripts and use it as a template for protein synthesis [2]. Due to various mRNA sequences, ribosomes translate different polypeptide chains containing amino acids as building units. Therefore, different proteins are distinguished by different amino acid compositions and sequences. To carry out biological functions, most newborn polypeptides are folded into a particular three-dimensional structure, the so-called native state. Functionality of most proteins is critically dependent on a compact native structure with buried hydrophobic regions [3]. However, several biologically active proteins are disordered in their monomeric, free states. Low mean hydrophobicity and high net charge are key features of the amino acid sequences of these intrinsically disordered proteins (IDPs) [4]. Therefore, amino acid sequence intrinsically defines the protein structure to fold or to remain unfolded. Healthy cells, with the assistance of molecular chaperones, control the freshly synthetized polypeptides to adopt their native structure. Failure of proper protein folding results in formation of misfolded and thus inactive proteins which is harmful to cellular homeostasis. The misfolded state of proteins can either enter a degradation pathway after recognition by the cellular quality-control system or self-assemble in special forms [3, 5-7]. In bacteria, accumulation of misfolded proteins leads to formation of insoluble aggregates, known as inclusion bodies. In humans, deposition of misfolded proteins in form of highly ordered aggregates, the so-called amyloid fibrils, is associated with pathology of a growing number of diseases. For example, aggregation of α-synuclein, amyloid beta (Aβ) peptide, human islet amyloid polypeptide, and prion protein (PrP) play a role in

Parkinson's disease (PD), Alzheimer's disease, diabetes type II (T2D), and transmissible spongiform encephalopathy (TSE), respectively [6, 8].

1.2. Amyloid formation and human diseases

All or at least the majority of proteins have been suggested to be potentially capable of amyloid fibril formation. High propensity for formation of β-sheet secondary structure and low net charge are general features of protein sequence driving fibril formation [6, 9]. The fibrillation process of globular proteins is different from that of IDPs, considering the fact that partial unfolding is required for fibrillation of globular proteins, whereas IDPs need to adopt an amyloid-compatible secondary structure prior to fibril formation. Regardless of amino acid sequence and composition, amyloid fibrils formed by different proteins show high similarity in structural features [6, 8, 10], suggesting a common mechanism applied to fibril formation and toxicity.

1.2.1. Amyloid fibrils

In 1854, Rudolf Virchow used the term "Amyloid" to explain the human pathological mass stained with iodine, resembling starch [11]. Amyloid fibrils are highly ordered assemblies with unbranched thread-like structure of a few nanometers in diameter and up to several micrometers in length as characterized by microscopy studies (figure 1A). Mature fibrils are typically composed of several protofilaments twisted together [12-16]. X-ray diffraction (XRD) studies of different amyloid fibrils have demonstrated a cross-β core structure with a meridional reflection at 4.7-4.8 A° and an equatorial reflection at about 11 Å. The cross-β signature reflects the presence of elongated β-sheets, which are composed of hydrogen-bonded β-strands that are oriented perpendicularly to the fibril axis and continuously repeated all along the fibril [10, 17-20] (figure 1B). The cross-β structure nature of amyloid fibril is based on the intrinsic

propensity of polypeptide chains for adopting β-sheet secondary structure via backbone hydrogen bonding. Therefore, high content of β-sheet structure is indicative of amyloid fibrils and is simply detectable by low resolution techniques like CD (Circular Dichroism) and Fourier Transform Infrared (FTIR) spectroscopies [9]. Moreover, the β-sheet-fibril binding property of Thioflavin T (ThT) and Congo red dyes is applied for the research on amyloid fibrils [21, 22]. The cross-β architecture is compatible with the continuous formation of hydrogen bonds across the fibril length.

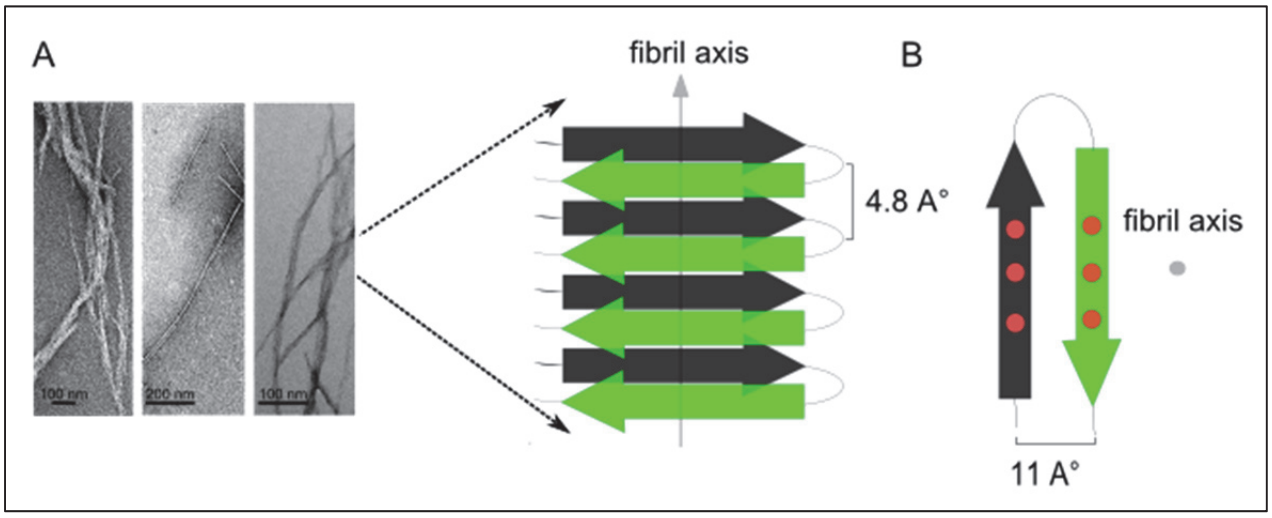

Figure 1: The structure of amyloid fibrils. A, electron micrographs of amyloid fibrils formed by IAPP (left), α-syn (middle), and Aβ1-42 (right, taken from [23]). B, schematic representation of cross-β architecture in amyloid fibrils [20]. Cross-β architecture is composed of hydrogen-bonded β-strands perpendicularly oriented to the fibril axis. In top view (right), potential hydrogen bonds are shown by red circles, respectively.

Within the protofilaments, β-sheets are typically arranged on top of each other (in-register) which not only facilitates the backbone hydrogen bonding between β-sheets, but also assists tight interdigitation of amino acid side chains in mated β-sheets. The motif formed by a tight pair of two neighboring β-sheets is termed as steric zipper [8, 24]. Interface between two β-sheets is devoid of water, the so-called dry steric zipper, representing an important contribution

of hydrophobic residues to fibril stability. The great content of hydrogen bonds in the fibril core and potential side chain interactions result in high stability of amyloid fibrils [19, 25].

1.2.2. Amyloid fibril formation

Upon misfolding, proteins may undergo a dramatic transition from a native soluble state to an extremely stable amyloid state featuring β-sheet structure. Therefore, fibril formation process is triggered by structural conversions leading to formation of oligomeric and eventually fibril structures [25] (figure 2A). Amyloid fibril formation is a complex process and its mechanism is not yet fully discovered. However, fibril formation typically follows a nucleation-dependent polymerization manner. In vitro fibrillation kinetics monitored by ThT fluorescence (figure 2B) typically show an initial lag phase, reflecting the slow formation of aggregation nuclei (primary nucleation), which could be misfolded monomers, oligomeric species, or small protofibrils. In this phase, amyloid fibrils are not detectable and ThT fluorescence is comparable to that for buffer sample devoid of protein. The lag phase length is variable and dependent on the amyloidogenic propensity of protein, protein concentration and environmental conditions such as pH, temperature and ionic strength [13]. Moreover, addition of preformed fibrils reduces or even eliminates the lag time [26, 27]. In growth phase, fibril growth from nuclei results in a rapid increase in ThT signal [28, 29]. Finally, the process reaches a stationary phase representing the constant ThT signal (figure 2B). Fibril fragmentation has been demonstrated to accelerate the fibrillation process by increasing the number of fibril ends [30]. In addition to fibril fragmentation, formation of new nuclei on the fibril surface is a secondary nucleation event [28, 31, 32].

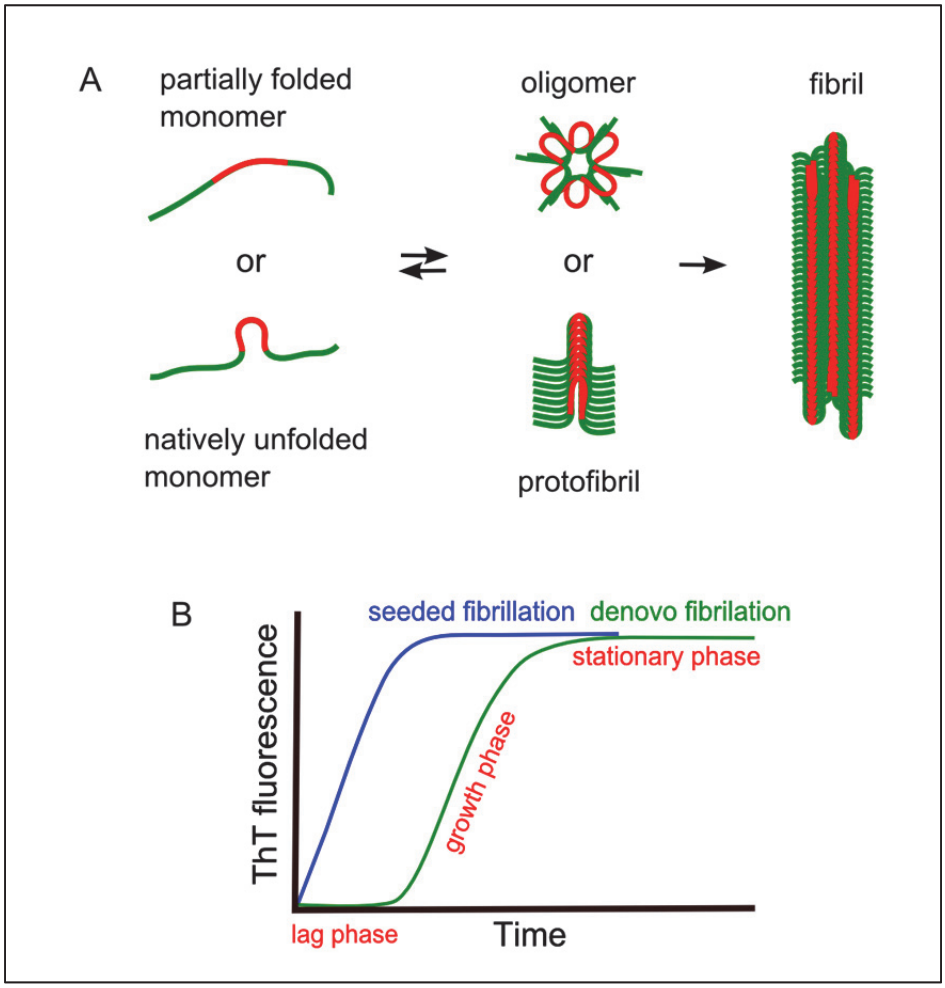

Figure 2: Fibril formation reaction. A, Aggregation pathway. Conversion of natively unfolded monomer into partially folded structure leading to the formation of oligomeric species or protofibrils and eventually fibrils. **B**, Fibrillation kinetics monitored by ThT fluorescence.

1.2.3. Human diseases

Deposition of amyloid fibrils in brain and other tissues, known as amyloidoses is associated with the pathogenesis of more than 20 human degenerative diseases (table 1) [6, 8], for which no effective cure has been yet developed. To set up an effective treatment strategy, the basic mechanisms of amyloid formation and amyloid-induced toxicity need to be well studied and understood.

1.2.3.1. Alzheimer's disease

Alzheimer's disease (AD) is characterized by irreversible and age-dependent progressive impairment of memory activities (dementia) caused by gradual damage in the hippocampus and the neocortex of brain. AD as the most common neurodegenerative disease accounts for 70 percent of dementia cases [33]. Post mortem studies on AD brains have defined the presence of intracellular neurofibrillary tangles (NFTs) and senile plaques as the main histological hallmarks of AD [34]. Tau is a microtubule-stabilizing protein and its intracellular accumulation results in formation of NFTs. Senile plaques are mainly composed of amyloid beta (Aβ) aggregates. Therefore, Aβ aggregation is believed to be the main pathological process involved in AD. Aβ peptides, the most frequent variants being $A\beta_{1\text{-}40}$ and $A\beta_{1\text{-}42}$, are derived from amyloid-β precursor protein (APP), encoded by a gene located on chromosome 21. Overproduction of aggregation-prone Aβ peptides leads to deposition of protein aggregates. For instance, triplication of chromosome 21 and, thus, of the APP gene accelerates the formation of Aβ fibrils in patients with Down's syndrome [35]. Several other factors have been shown to be involved in the pathology of AD. However, and despite the extensive research, the exact mechanism of the disease remains unknown.

1.2.3.2. Type II diabetes

Type II diabetes (T2D) is the most common form of diabetes and is characterized by an elevation of glucose level in blood which damages nerves and blood vessels in the long term. In addition, type II diabetes is associated with some secondary complications such as stroke, heart attack, blindness and kidney diseases. Islet amyloid polypeptide (IAPP) or amylin is a pancreatic peptide consisting of 37 amino acids. Under normal conditions, IAPP is co-secreted with Insulin from pancreatic β-cells. T2D is associated with progressive loss of β-cells and consequently, overproduction and secretion of Insulin (and IAPP) by the remaining cells. Additional release of IAPP can result in formation of amyloid aggregates and secondary complications of T2D have

been suggested to be associated with deposition of IAPP amyloid aggregates [36]. Early histological studies indicated the extracellular location of IAPP deposits in T2D, whereas transgenic rodent models overexpressing the IAPP propose the intracellular deposition [37].

1.2.3.3. Parkinson's disease

Parkinson's disease (PD) was first medically described in 1817 by James Parkinson [38]. PD is the second most common neurodegenerative disease after AD and it affects 1-2 percent of people over 65. Neuropathologically, PD is characterized by a progressive loss of muscle control caused by a gradual loss in dopaminergic neurons of substantia nigra (SN) part of brain. PD is clinically characterized by tremor even at rest, impaired balance and bradykinesia. Moreover, patients may also show non-motor symptoms such as sleeping difficulties, dysautonomia and cognitive problems. Intracellular accumulation of amyloid aggregates, known as Lewy bodies (LBs), was first described by Friederich Lewy in 1912, as the main pathological hallmark of PD. In 1919, Tretiakoff reported the particular abundance of LBs in SN and a correlation between degradation of cells in SN and pathological symptoms. Later, LBs were also identified in the post-mortem brains of patients with other dementia diseases [39]. LBs are proteinaceous inclusions mainly composed of α-synuclein aggregates and also some additional proteins including α-synuclein binding proteins, cytoskeleton proteins, proteins associated with signal transduction and phosphorylation, cell cycle proteins, and others. α-synuclein aggregation is believed to be the precursor event responsible for the formation of LBs nuclei in which additional proteins are captured and deposited [40, 41].

Diseases	Aggregating polypeptide	Number of amino acids	Native structure of polypeptide	Hallmark	Location of aggregates
Parkinson's disease	α-synuclein	140	Disordered	Lewy bodies	Intracellular
Dementia with Lewy bodies	α-synuclein	140	Disordered	Lewy bodies	Intracellular
Alzheimer's disease	Aβ	40-42	Disordered	Senile plaques, neurofibrillary tangles	Extracellular Intracellular
Type II diabetes	IAPP	37	Disordered	Amyloid deposits	Extracellular Intracellular
Amyotrophic lateral sclerosis	Superoxide dismutase 1	153	All β-sheet	Hyaline inclusions	Intracellular
Transmissible Spongiform Encephalopathy	Prion	230	Disordered / α-helical	Prion plaques	Extracellular
Huntington disease	Huntingtin	3144	Mainly disordered	Inclusion bodies	Intracellular

Table 1: Selected list of human diseases associated with amyloid fibril formation, based on ref. [6, 8, 11, 42].

1.3. α-synuclein

1.3.1 History

In 1988, Maroteaux et al. identified a neuron-specific protein in cholinergic synaptic vesicles of Torpedo Californica. They designated this protein as "synuclein" because of its special localization to pre-synaptic terminals and nuclei of neuronal cells [43]. In 1991, Maroteaux et al.

identified a very similar protein in the rat brain [44]. In 1993, protease digestion of purified amyloid deposits from AD patients resulted in the identification of a peptide fragment of α-synuclein, termed non-Aβ component (NAC) [45]. Therefore, α-synuclein has been also termed as non-Aβ component protein (NACP) [46]. Following in vitro studies established the NAC segment as a highly aggregation-prone region required for the fibrillation of full length α-synuclein [47-49]. In 1995, FISH (fluorescence in situ hybridization) technique disclosed the synuclein expression from a gene, SNCA, located on the chromosome 4 (4q21.3-q22) [50]. In 1997, genetics analysis by Polymeropoulos et al. for the first time revealed an association between inherited PD and a mutation in the SNCA gene, resulting in substitution of the amino acid alanine by threonine at position 53 (A53T) [51]. Subsequent genetic studies on PD families led to the discovery of additional missense mutations (A30P, E46K, H50Q, G51D and A53E) and, hence, further emphasized the involvement of α-synuclein in PD pathogenesis [52-56]. Moreover, overexpression of α-synuclein induced by multiplication of the SCNA gene has been shown to be associated with familial PD [57]. Furthermore, Maraganore et al. in 2007 reported that a polymorphism in the promoter of SNCA gene increases the risk for PD [58]. These findings together with identification of α-synuclein as the main constituent of Lewy bodies in the post-mortem brain of patients with sporadic and familial PD [59-61] ascertain the involvement of α-synuclein in the PD pathogenesis.

1.3.1. Characteristics of α-synuclein

α-synuclein belongs to a highly conserved synuclein family (α-, β- and γ-synucleins) which is predominantly expressed in brain of vertebrates. Although synuclein proteins are encoded by three different genes, they are 55-62% identical in amino acid sequence and share some cellular localisations and functions [40]. In mice, knockout models of all synuclein family show a significant change in structure of synapses and age-dependent dysfunctions in CNS, indicating the critical role of these proteins in vertebrates [62]. Human α-synuclein (~14 kDa) is a heat-

resistant protein consisting of 140 amino acids and comprises 1% of cytoplasmic proteins in neuronal cells [43]. The α-synuclein amino acid sequence is classified into three different regions: 1) Amphipathic N-terminal region (1-60) containing four imperfect 11-mer repeats with conserved sequence KTKEGV (figure 3A), which is a highly conserved domain among all proteins in synuclein family and facilitates membrane interactions [63]. Remarkably, this region contains all so far discovered missense mutations in α-synuclein (figure 3B). 2) Hydrophobic middle region (61-95) including two additional KTKEGV repeats. As mentioned above, this region is a highly hydrophobic region required for α-synuclein fibrillation [47, 49]. In this region, amino acid residues 71-82, the so-called hydrophobic core, is sufficient for α-synuclein fibrillation [64]. Notably, non-amyloidogenic human β-synuclein lacks this hydrophobic stretch [40]. 3) Highly flexible C-terminal region (96-140), rich in proline and acidic residues (5 aspartates and 10 glutamates). At neutral pH, the C-terminus is negatively charged and impedes α-synuclein aggregation possibly by induction of electrostatic repulsions between two α-synuclein molecules. Consistent with this hypothesis, C-terminally truncated α-synuclein (1-108) shows higher aggregation propensity [65]. Moreover, several studies have established the presence of long-term interactions between the C-terminal and central region [66, 67]. Release of these interactions by deletion of the C-terminal region, addition of polyamines or lowering the solution pH accelerates α-synuclein aggregation. Therefore, electrostatic attractions between the negative charge of C-terminus and positive charge of central region have been proposed to be important for these interactions [65, 67]. In addition, this region has been shown to be involved in a chaperone-like activity of α-synuclein [68].

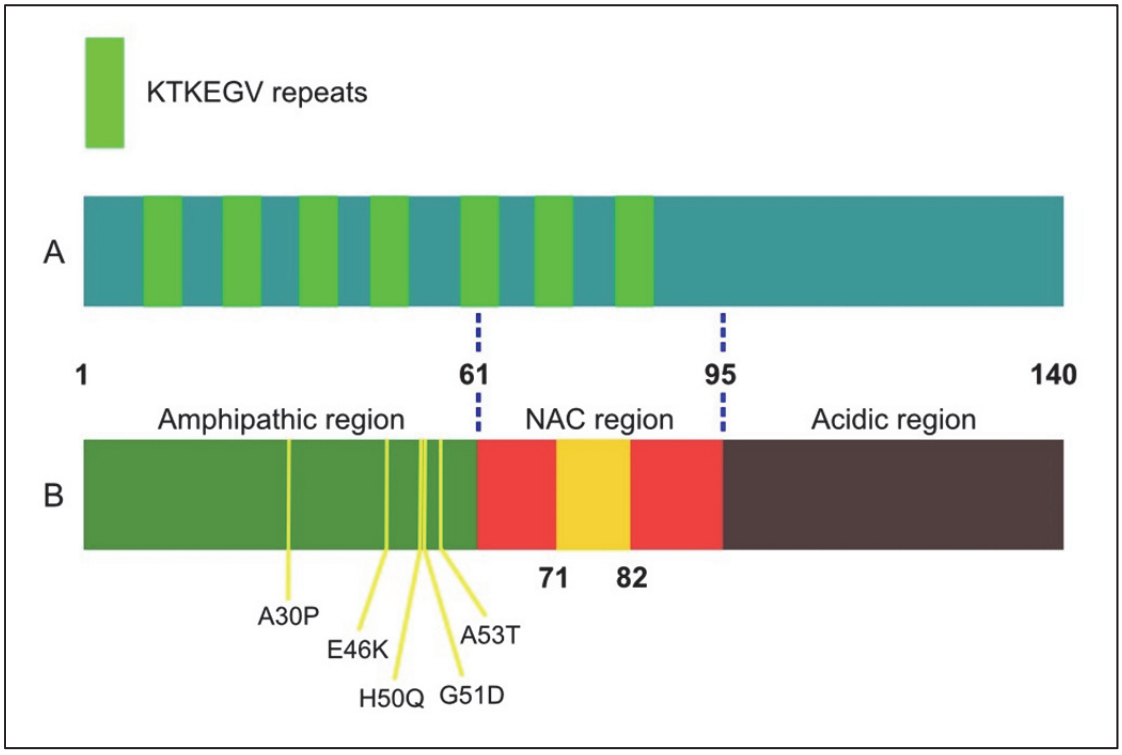

Figure 3: Amino acid sequence of α-synuclein. A, α-synuclein contains 7 imperfect KTKEGV repeats in N-terminal and central region. **B**, Amphipathic region encompasses all missense mutations linked to familial PD. NAC region comprises the most hydrophobic stretch in α-synuclein sequence.

1.3.1.1. Membrane-binding properties of α-synuclein

As mentioned above, the N-terminus of α-synuclein contains several imperfect 11-mer repeats with conserved KTKEGV sequence, resembling the amphipathic α-helices-forming region in apolipoproteins. Based on this similarity, the 5-helix model proposed by Davidson et al. suggested the potential propensity for formation of α-helix structure by the α-synuclein N-terminus and stabilization of this structure upon interaction with phospholipid membranes [63]. They experimentally observed a significant increase in α-helix content of α-synuclein (from 3% to about 80%) upon preferential its binding to small unilamellar vesicles (SUVs) containing acidic phospholipids [63]. Moreover, results obtained by Eliezer et al. using multi-dimensional NMR and SDS micelles indicated the formation of two α-helices (comprising residues 1-41 and 45-94) connected by a short linker [69]. Subsequent studies have shown that α-synuclein adopts

various α-helical structures upon binding to lipid membranes with different compositions. Binding to lipid membrane induces the extended or broken α-helices in α-synuclein (residues 1-100), depending on membrane composition and morphology [70-72]. On the other side, influence of α-synuclein interaction on the membrane integrity has been confirmed by NMR, EPR and fluorescence spectroscopy [73-75]. For instance, Varkey et al. reported that large vesicles transform into tubular and curved membranes upon interaction with α-synuclein, reminiscent membranes interacting with apolipoproteins [75]. Fibrillation propensity of α-synuclein can be accelerated [76] or inhibited [77] by membrane interaction. Moreover, α-synuclein aggregates induced by membrane interactions are rich in either α-helices [78] or β-sheets [79], depending on the experimental conditions and membrane compositions.

1.3.1.2. Metals binding

Accumulating evidence demonstrates an association between an elevation in the level of metal ions and pathology of PD. First, in 1987, Pall et al. observed an increase in total level of copper in cerebrospinal fluid (CSF) of people with PD [80]. Soon later, an alteration in the level of iron, aluminum and zinc was observed in brain of people with PD [81, 82]. In support of these findings, Youdim et al. observed that an injection of $FeCl_3$ into SN part of rat brain selectively reduces dopamine level which consequently results in brain dysfunction [83]. Furthermore, several studies have reported that metal ions directly bind to α-synuclein with low or high affinity [84-86]. Most of metal ions show a low binding affinity to the C-terminal region of α-synuclein, via electrostatic interactions and a metal binding site, ^{119}DPDNEA^{124} [86]. High affinity interactions target the N-terminal region of α-synuclein, albeit binding to His50 is of a low affinity. Several groups have established the binding of two Cu^{2+} ions to one α-synuclein molecule. In addition to low affinity binding to the C-terminal region, second copper ion binds to the N-terminal region with a nanomolar affinity. This interaction is coordinated by the N-terminal amine, the carboxylate side chain of Asp-2, and His-50 [87]. The redox activity of

Cu^{2+}:α-synuclein is able to form reactive oxygen species (ROS), leading to the oxidative stress condition [88]. In addition, Cu^{2+}:α-synuclein complex is able to reduce Fe^{3+} to Fe^{2+} [89]. Analysis of post-mortem brain of PD patients shows a decrease in the ratio of Fe^{2+}/Fe^{+3} in SN, indicating an increase in level of Fe^{3+} due to the change in redox state [81]. With respect to ferrireductase activity of α-synuclein, lack of this activity due to α-synuclein self-assembly might be involved in the elevation of Fe^{3+}. Like many metal ions, Fe^{2+} binds to C-terminal region of α-synuclein and resulting complex is able to generate ROS [90]. In many cases, binding to metal ions comes along with a transformation in α-synuclein structure and acceleration of its aggregation [91].

1.3.1.3. Conformational nature of monomeric α-synuclein

Initially, conformational analysis by Weinreb et al. proposed an intrinsically disordered structure for α-synuclein [46]. They observed that α-synuclein has a much larger stokes radius (34 Å) and slower sedimentation rate ($S_{20,\,W}$= 1.7 S) than the globular proteins of similar number of residues indicating an unfolded structure. Their FTIR and CD spectroscopy data also indicated the lack of significant secondary structure for α-synuclein. Furthermore, small-angle X-ray scattering (SAXS) and size exclusion chromatography (SEC) added further evidence for the unstructured nature of α-synuclein [92]. Inconsistent with previous findings, Bartels et al. [93] and Wang et al. [94] proposed an aggregation-resistant tetramer structure for the α-synuclein under native conditions. However, in-cell NMR studies by Binolfi et al. clearly indicated a disordered nature for α-synuclein inside bacteria cells [95]. Moreover, conformational analysis of native α-synuclein using SEC and CD spectroscopy indicated the disordered structure as previously shown for recombinant α-synuclein [96, 97]. Like other IDPs, α-synuclein possesses an amino acid sequence of a low mean hydrophobicity and high net charge. All these pieces of evidence undoubtedly set α-synuclein as being a largely unstructured protein. Like all IDPs, lack of a rigid structure predisposes α-synuclein toward adopting different partially folded structures, functional or pathological, under certain conditions. For instance, α-synuclein adopts a helical

structure upon binding to membranes [70] or forms a aggregation-prone compact structure at low pH or high temperature [92]. Employing paramagnetic resonance enhancement (PRE) and NMR dipolar couplings, Bertoncini et al. have shown that long-range interactions between C-terminal and NAC region prevent α-synuclein aggregation. In addition, they observed that release of these long-range interactions due to polyamine binding or an increase in temperature results in the formation of completely unfolded monomers which are highly prone to self-assembly and aggregation [67].

1.3.2. α-synuclein Functions

Despite the abundance of α-synuclein in brain, its physiological role is not yet well understood. With respect to the considerable portion of α-synuclein bound to membrane in presynaptic terminals, its role has been proposed to be associated with membrane structures at synaptic terminals [76]. For example, several studies have suggested that α-synuclein regulates neurotransmission of dopamine [98, 99], the size of presynaptic vesicles [100] and organization of phospholipid bilayers [73]. *In vitro* and *in vivo* results indicate a potential role of α-synuclein in assembly of SNARE complex [101]. As an inhibitor, α-synuclein regulates the activity of some neurotransmission-associated enzymes including phospholipase D2 (PLD2) [102] and tyrosine hydroxylase (TH) [99]. Furthermore, lipid membranes bound to α-synuclein have been shown to be protected against oxidation [103]. In cooperation with some chaperon proteins abundant in nerve terminals, α-synuclein assists the folding of proteins [104]. Sharing functional and physical homology with molecular chaperon 14-3-3 [105], α-synuclein exhibits a chaperon-like activity associated with potential binding affinity to various proteins. Thereby, α-synuclein modulates their folding and activity of several cellular proteins [68, 106-108].

1.3.3. α-synuclein aggregation

Protein aggregation has been shown to be associated with several neurodegenerative diseases. The Fibrillation process of α-synuclein is involved in the pathogenies of PD and other synucleinopathies, since α-synuclein amyloid aggregates have been identified as the major component of LBs [59]. Therefore, a detailed understanding of aggregation-triggering factors and also of the protein-protein interactions involved in the aggregation process will provide insights for the development of prevention and therapeutic approaches. As a chameleon protein, conformational fluctuations of α-synuclein are controlled by environmental factors [109, 110]. Under physiological condition, α-synuclein accepts different functional partially folded structures, conferring the binding potential to different partners [111]. Under fibrillation conditions, α-synuclein adopts an unstable partially folded intermediate structure [92]. To become energetically stable, misfolded structures self-assemble into oligomeric species and eventually form stable amyloid fibrils. In vitro studies have confirmed the α-synuclein tendency to form amyloid fibrils resembling those isolated from LBs [48]. Moreover, CD spectroscopy detects a transformation from random coil to β-sheet structure in α-synuclein under fibrillation conditions. The exact mechanism of the aggregation process and the mediating structures are not well understood, however, the formation of amyloidogenic partially folded structure has been proposed as the origin of this process [92]. Single molecule studies have revealed the conformational equilibrium for α-synuclein under different experimental conditions and a shift in this equilibrium in favor of formation of amyloid-forming conformers has been proposed to trigger α-synuclein aggregation [111-114]. Furthermore, these studies propose the α-synuclein aggregation to be dependent on the formation of nuclei [26, 92]. Several studies using AFM and EM microscopy have indicated that, under different experimental conditions, α-synuclein aggregation results in different products including soluble oligomeric species, insoluble amorphous aggregates and fibrils [13, 92].

1.3.4. Factors influencing α-synuclein aggregation

1.3.4.1. Environmental factors

The intracellular environment contains a high concentration (approximately 400 mg/ml) of different macromolecules [115]. High concentration of different solutes induces variable structural changes in different proteins. In the case of α-synuclein, high concentration of solutes, such as polysaccharides and polyethylene glycols, leads to the formation of a compact structure, and finally accelerates fibril formation [116]. Furthermore, aggregation of α-synuclein shows a dependency on the protein concentration so that an increase in the concentration enhances the aggregation rate probably through increasing the concentration of partially folded structures serving as nuclei [117, 118]. Uversky et al. observed that high temperature accelerates α-synuclein oligomerization through stabilization of partially folded structures [119]. Aggregation studies by Hoyer et al. demonstrate a significant decrease in the lag time of aggregation from about 60 hours at pH 7.0 to several minutes at pH 4.0 [13]. Diminishing the auto-inhibitory effect of C-terminal region at acidic pH due to neutralization of negative charge, driving electrostatic repulsions, has been suggested to accelerate the α-synuclein aggregation [65]. Data obtained by single molecule studies suggest that in low pH, α-synuclein forms a compact transient structure prone to aggregation [114]. Hoyer et al. observed the similar effect in the presence of high ionic strength (500 mM Tris-HCl buffer) [13] and later single molecule studies by Sandal et al. indicated a shift in equilibrium in favor of β-like structure formation, under the same condition [114]. Incubation of α-synuclein under agitation conditions with shaking and in presence of small glass beads accelerates the fibrillation process by fragmentation of preformed fibrils and increasing the number of nuclei [30]. Accumulating evidence indicate the influence of several metal ions and pesticides on α-synuclein aggregation. In vitro studies have established a stimulating effect for pesticides (eg. dieldrin, rotenone and paraquat) on α-synuclein fibril formation [120]. Pesticides directly interact with α-synuclein and induce formation of

amyloidogenic partially folded structures. In addition, administration of the herbicide paraquat to mice resulted in overexpression and consequently aggregation of α-synuclein [121]. In vitro studies demonstrate that interaction of several metal ions (iron, zinc, copper, lead and aluminum) to C-terminal domain of α-synuclein promotes the formation of collapsed structure prone to aggregation [91]. Moreover, metal ions and pesticides exhibit a synergistic effect on the α-synuclein aggregation [122]. An increase in the content of β-like structure for monomeric α-synuclein has been reported in the presence of Cu^{2+} [112]. Light scattering technique detected on-pathway oligomeric species formed in the presence of Al^{3+} [91]. Unlike the accelerating effect of heavy metal ions, magnesium not only prevents the aggregation of α-synuclein but also modulates the interaction of pesticides with α-synuclein [123]. Because of an association with brain and CSF of PD patients, low level of magnesium has been proposed as a high risk factor for PD [124]. Finally, numerous small molecules, particularly polyphenolic compounds, have been shown to interfere with the aggregation process of α-synuclein by stabilization or modification of different structures including partially folded monomer, on- or off-pathway oligomers and fibrils [125-127]. Despite the potent effect of small molecules reported by in vitro studies, there has been not yet any small molecule-based therapeutics developed.

1.3.4.2. Effect of post-translational modifications

Several lines of studies have demonstrated the influence of post-translational modifications (PTMS) on the α-synuclein aggregation. Mass spectroscopy analysis of α-synuclein isolated from the pathological samples indicated an extensive phosphorylation at Ser-129 whereas α-synuclein is non-phosphorylated in healthy brains [128]. Furthermore, H_2O_2-induced phosphorylation of α-synuclein at Ser-129 leads to formation of intracellular inclusion bodies in SH-SY5Y neuroblastoma cells [129]. In constrast, phosphorylation at Try-87 and Tyr-128 interferes with α-synuclein fibril formation [130, 131]. In addition to phosphorylation, α-synuclein fibrillation is affected by other modifications such as N-terminal acetylation, tyrosine nitration oxidation,

methionine oxidation, cross-linking and truncation [132]. C-terminal truncation of α-synuclein is one of the most common modifications associated with PD [133]. C-terminal truncation increases α-synuclein aggregation [65, 67, 134].

1.3.4.3. Effect of familial mutations

So far five amino acid substitutions (A30P, A53T, E46K, H50Q, G51D and A53E) have been identified in people with early on-set PD. In vitro studies indicate the higher aggregation propensity for PD associated α-synuclein mutants [135-139]. A30P enhances oligomerization whereas A53T accelerates both oligomerization and fibrillation [140]. Although analyses of these mutants by CD spectroscopy show the high content of random coil structure similar to the wild-type α-synuclein, single molecule studies indicate a shift in the conformational equilibrium of the monomer toward formation of β-like structure [112, 113, 138].

1.3.4.4. Interaction with other proteins

Being disordered enables α-synuclein to interact with several cellular proteins. In some cases, these interactions affect α-synuclein aggregation. Interestingly, AD-related proteins, Aβ and Tau have shown to promote α-synuclein aggregation [141], indicating a connection between AD and PD. Masliah et al. have shown that overexpression of Aβ in mice model results in the intraneuronal α-synuclein deposits and consequently, motor deficiency [142]. Moreover, in vitro experiments performed by Ono et al. indicate a dual cross-seeding effect of Aβ and α-synuclein [143]. PrP^{sc} is able to seed α-synuclein aggregation in an animal model [144]. Fibrillation of α-synuclein is also triggered upon interaction with other proteins such as tubulin [145], agrin [146], p25α [147] and HMGB1 [148]. Furthermore, β- and γ-synucleins can prevent α-synuclein aggregation by formation of stable hetero-oligomers [149]. The inhibitory effect of β-synuclein has been also established in animal models [150]. Several heat shock proteins (HSPs) have been identified in LBs [151]. Overexpression of torsin A and HSP70 has been shown to inhibit α-

synuclein aggregation. By binding to the NAC region HSP70 stabilizes oligomeric species and, thereby, inhibits fibril formation [151, 152]. A small HSP, αβ-crystallin, prevents elongation of α-synuclein fibrils by binding to partially folded monomers [153, 154].

1.3.5. α-synuclein amyloid fibrils

Upon fibril formation, α-synuclein undergoes a conformational transition from random coil to cross-β structures, confirmed by CD spectroscopy, electron and X-ray diffraction studies [92, 155]. Several studies using EM and AFM microscopy have characterized the in vitro α-synuclein fibrils with a thickness of about 10 nm and a length ranging from 100 nm to few micrometers, reminiscent of those extracted from LBs [13, 59, 156]. However, fibril morphology has been shown to be highly dependent on the experimental conditions [13, 118]. Protease digestion-assisted analysis of both in vitro and brain-extracted fibrils has revealed that the central region (residues 31-109) is protease K-resistant whereas peripheral regions, N- and C-terminus, are prone to digestion [157]. Moreover, an initial spin-labeling study characterized α-synuclein within fibrils as possessing a highly ordered central region (residues 34-101), heterogeneous N-terminus and highly disordered C-terminus [158]. As aforementioned, within fibrils, amyloidogenic proteins adopt β-strands-turn-β-strand motifs which align to form different spatial arrangements [8, 159]. As a common structure evidenced by different NMR, EPR and spin-labeling techniques, the core of α-synuclein consists of approximately five separate β-strands folded in a parallel, in-register cross-β structure (figure 4) [160-164]. It has been shown that different fibrillation conditions lead to morphologically different α-synuclein fibrils [13, 92]. Moreover, solid-state NMR studies indicate the presence of several distinct structures available in a single fibril solution, which is called fibril polymorphism. Heise et al. [160] and Vilar et al. [162] have identified two distinct types of fibril structures (figure 4A, 4B and 4C). These two studies assumed the Glu-46 to be located in the loop region because of the absence of signal for this residue and neighboring ones. Further assignments performed by Comellas et al. (figure 4D)

proposed a novel model of secondary structure for the fibrils, which consists of two repeats of long β-strands and 4 smaller β-strands [163]. In contrast to previous results, the full assignment of the structured region in the fibril core of this polymorph indicates that Glu-46 and Ala-53 residues reside in the β-strand regions whereas Ala-30 is located in a loop region. In agreement with this finding, Lemkau et al. observed a specific perturbation in fibril structure derived by α-synuclein mutations A53T and E46K not A30P [165].

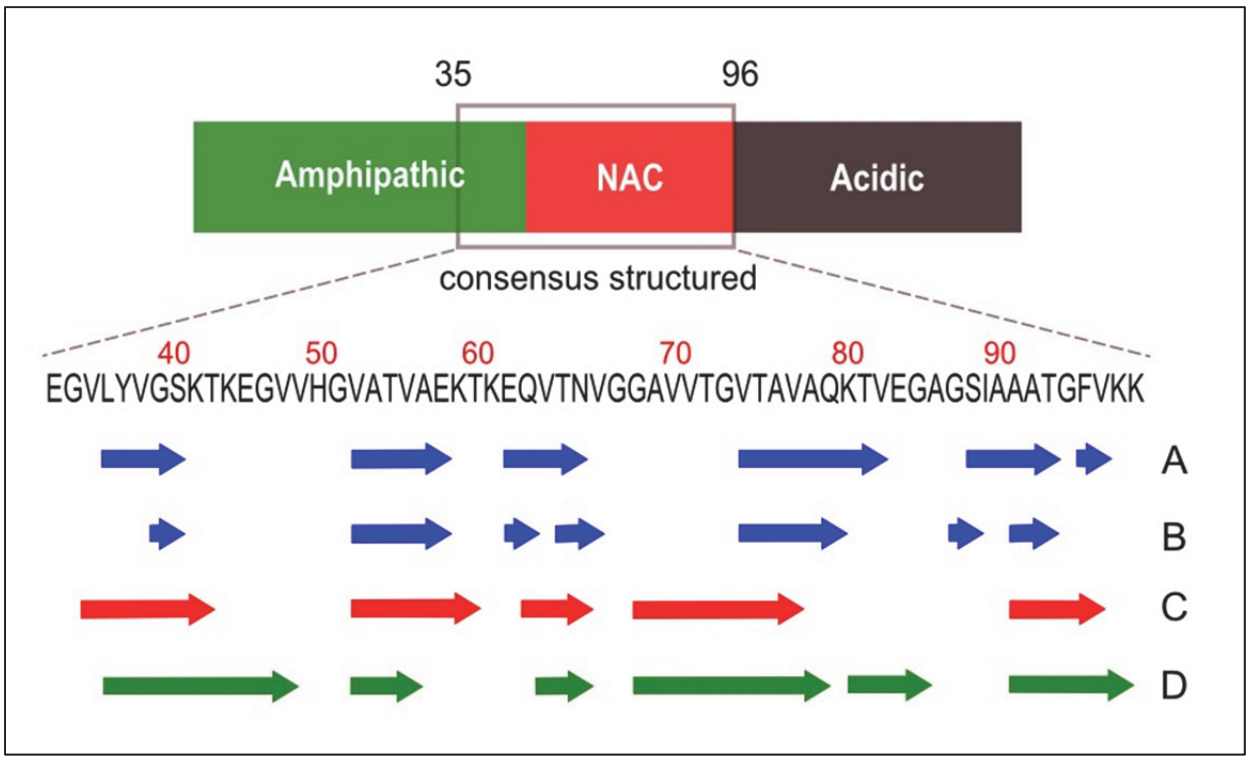

Figure 4: Secondary structure of α-synuclein fibrils. Arrows demonstrate β-strand regions identified by NMR spectroscopy in fibrils. **A** and **B** show the β-strand regions in two distinct α-synuclein fibril polymorphs studied by Heise et al. [160]. **C** and **D**, indicate β-strands identified by Vilar et al. [162] and Comella et al [163], respectively.

1.3.6. α-synuclein toxic species

Pathology of LBs has been associated with different α-synuclein aggregates including oligomers, protofibrils and fibrils [166-168]. Although several lines of in vivo and in vitro studies have established the toxicity of α-synuclein aggregates, the exact mechanism of toxicity remains to be elucidated. The complexity of the toxicity mechanism arises from the heterogeneity of aggregated species inducing different toxicity levels. Despite the toxicity effects observed for mature fibrils, several in vivo and in vitro studies have proposed a higher toxicity level for the oligomeric species [140, 169-171] and thus, conversion of highly toxic oligomeric species into less toxic fibrillar assemblies has been postulated as a defense process exerted by neuronal cells. Notably, a high level of α-synuclein oligomers has been detected in post-mortem brain extracts, plasma and CSF in PD patients [172-175]. Moreover, familial PD-linked mutations accelerate α-synuclein oligomerization in vitro and in vivo [140, 169, 176]. α-synuclein oligomers are highly unstable and rapidly convert into insoluble fibrils. However, oligomerization of α-synuclein has been reported to be induced and stabilized in the presence of several chemical additives [177-180]. Oligomeric species formed under different *in vitro* conditions are of distinct morphologies such as tubular, spherical and chain-like [140, 177, 180]. Toxic mechanism of oligomers is yet not known but the most accepted toxicity model is based on the lipid-binding propensity of α-synuclein which is higher for oligomers than monomers and fibrils [181, 182]. Interaction with α-synuclein oligomers increases the permeability of the cell membrane and consequently disrupts the ionic homeostasis resulting in cell death. Toxic oligomers, particularly annular and tubular oligomers, show a high propensity of pore formation. Additionally, familial mutations such as A30P and A53T strengthen the pore-like activity of oligomeric species [177, 181, 183]. In addition to their pore-like activity, α-synuclein oligomers have shown to inhibit SNARE-mediated vesicle docking [184] and chaperone-like activity of HSP70 [185].

Despite the fact the LBs are intracellular inclusions, α-synuclein aggregates have been reported to be secreted to the extracellular environment through calcium-dependent exocytosis [186-

188]. Extracellular secretion of α-synuclein has been shown to be promoted under stress conditions. In addition, increasing evidence establishes the prion-like transfer of misfolded forms of α-synuclein from one cell to another [188-190]. In agreement, exogenous oligomers and fibrils are able to seed formation of LB-like intracellular inclusions in cells [191-193]. Furthermore, prion-like transmission as an age-dependent pathology-spreading factor appears to be a common process among neurodegenerative diseases [194, 195].

1.4. Engineered binding proteins for amyloid research

Antibodies or immunoglobulins are conventional binding proteins with widespread therapeutic and diagnostic applications. High specificity is the main advantage of antibodies and there are a variety of biotechnological approaches developed for selection and preparation of recombinant monoclonal antibodies against a specific target. An antibody molecule (figure 5A) is composed of four polypeptide chains including two identical light chains and two identical heavy chains. Heavy and light chains contain highly conserved (C_H and C_L) and variable (V_H and V_L) domains. Moreover, antibodies are big molecules (on average 150 kDa) of a complex structure stabilized by multiple disulfide bonds. Therefore, researchers have made continuous efforts to engineer functional antibodies of smaller size. These efforts have yielded in development of several antibody derivatives with high affinity for the target proteins. In addition, several other proteins have been reported to provide ideal scaffolds for engineering libraries of potential binders, using random mutagenesis. Library screening via phage display technology and other techniques have resulted in identification of high affinity binders. Compared with antibody molecules, these scaffold proteins are normally small, stable, and offer convenient production in E.Coli. In neurodegenerative research, discovery of high affinity binding proteins have been constantly of profound interest. Here, engineered binding proteins not only provide insights into protein-protein interactions in aggregation process, but also could be regarded as diagnostic tools and therapeutics.

1.4.1. Antibody-derived binding proteins

Size engineering strategies have resulted in development of several antibody-derived fragments including Fab, scFv, nanobody, etc. (reviewed in [196]). In amyloid research, several antibody fragments have been so far engineered for amyloidogenic proteins. Fab or antigen-binding fragment with a size of about 55 kDa consists of one variable and one constant domain of light and heavy chains. ScFv or single-chain variable fragment is smaller than Fab (ca. 28 kDa) and contains only the variable regions of one heavy and one light chain. An Aβ-specific Fab antibody distinguishes different conformers of Aβ oligomers [197]. Similarly, syn-10H scFv (Fig 5C) detects morphologically different oligomeric species of α-synuclein [198]. Nanobody or single domain antibody (sdAb) is the smallest fragment (12-15 kDa) devoid of the light chain, therefore also called heavy chain antibody. There are two types of nanobodies, VHH (containing the variable domain of the heavy chain, also called heavy antibody, see figure 5D) and VNAR (containing the variable domain of shark new antigen receptor, see figure 5E). There are several nanobodies selected against different amyloidogenic proteins [199-201]. A VHH nanobody binding to the non-amyloidogenic region of lysozyme inhibits amyloid fibril formation [201]. A4, a specific nanobody for oligomeric Aβ, inhibits fibrillation and toxicity [200].

1.4.2. Alternative protein scaffolds

To date, more than 50 non-antibody scaffolds have emerged for molecular recognition applications [202]. The most progress has been made on protein scaffolds including Kunitz domains (ca. 6 kDa, figure 5F), monobodies (ca. 10 kDa), DARPins (14-21 kDa, figure 5G), anticalins (ca. 20 kDa, figure 5H), SH3 domain (ca. 8 kDa, figure 5I) and Z-domain-based affibody binders (ca. 7 kDa, figure 5J). The main focus of this thesis is on selection of a specific protein binder from a β-wrapin library derived from a Z-domain affibody.

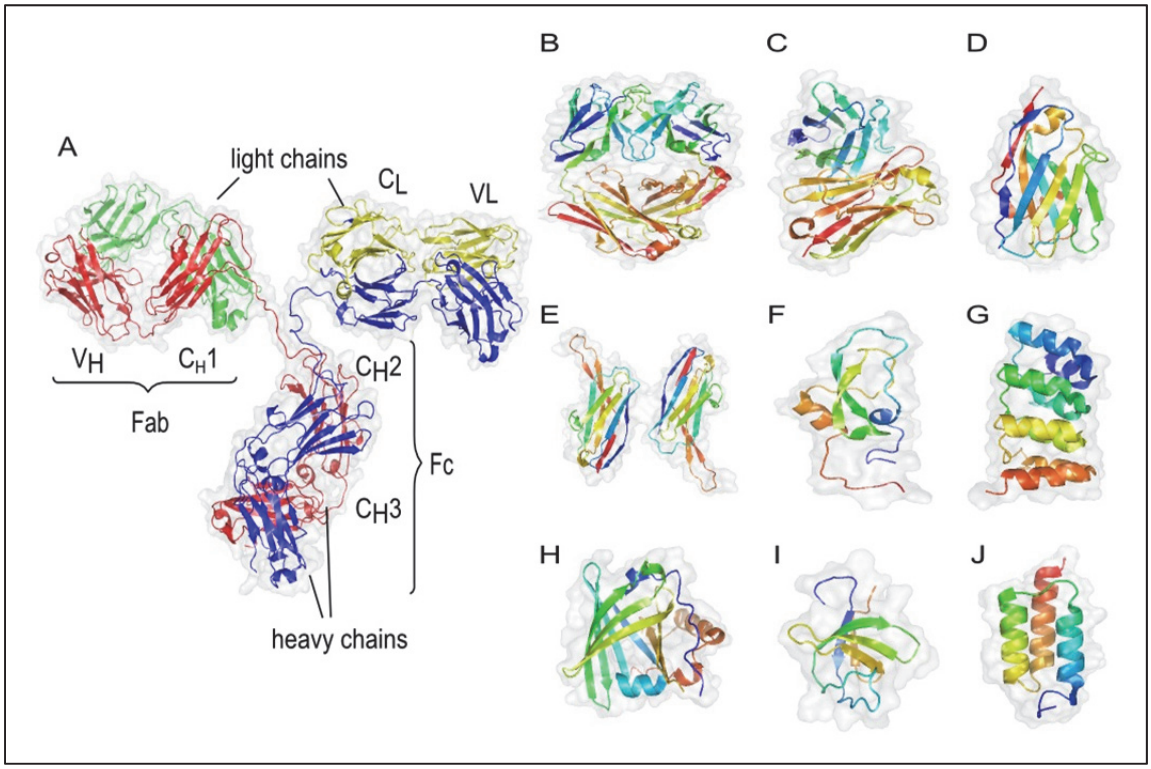

Figure 5: Representative examples of protein scaffolds for molecular recognition. For each molecule, backbone cartoons and transparent surface are generated by Pymol software and the corresponding PDB ID which is specified in the bracket. **A**, the structure of a typical IgG (1IGT) composed of two light chains and two heavy polypeptide chains. Digestion of IgG by papain results in formation of Fab and Fc fragments. **B**, Fab (4HBC). **C**, scFv (1P4I). **D**, VHH nanobody (1OP9). **E**, VNAR nanobody (1VES). **F**, Kunitz domain (2DDI). **G**, DARPin (1MJ0). **H**, anticalins (1LKE). **I**, SH3 domain (2O31). **J**, Z-domain (2SPZ).

1.4.2.1. Affibody molecules

In 1995, the affibody scaffold, also called Z-domain, was generated from the B-domain (comprising 58 amino acids) of staphylococcal protein A (SPA). SPA is a 42 kDa surface protein consisting of five homologous IgG-binding domains (E, D, A, B and C) which share a three-helix bundle structure (figure 6) and binding affinity to the Fc region of IgG molecules [203]. Fc-binding has been the basis for protein A applications in purification of antibodies. Through direct interaction with Fc region, SPA captures IgG molecules in an inverted orientation and thereby, assists bacteria to escape from host immune system [204]. In 1987, Nilsson et al. engineered the SPA B-domain by Gly-29 and Val-1 to alanine substitutions [205]. The engineered B-domain,

denoted as Z-domain, is resistant to hydroxylamine digestion and more stable than the B-domain, while keeping the α-helical structure binding to the Fc region of human IgG. The Z-domain is a cysteine-free, soluble and small molecule (about 7 kDa) and thus, it features rapid folding and convenient production. To generate an affibody ligand library, 13 surface-exposed residues in α-helix-1 and α-helix-2 were randomized [206]. Introduction of these mutations gave rise to the loss of Fc-binding affinity in the affibody molecule (figure 6). To date, several binders have been selected by screening affibody library against target proteins such as AD-related Aβ peptide and HER2 (human epidermal growth factor receptor 2) [207-210]. Affibody molecules have been studied as potential candidates in wide range of biotechnology, imaging and therapeutic applications. For instance, preclinical studies on mice showed promising results using HER2:342, a HER2-specific affibody, as a tracer for imaging of tumors overexpressing HER2 [211].

1.4.2.1.1. ZAβ$_3$

In 2005, phage display-assisted screening of the affibody library against Aβ$_{1-40}$ resulted in discovery of ZAβ$_3$ [209]. ZAβ$_3$ is an affibody molecule (~14 kDa) which specifically binds to Aβ, residues 17-36, with nanomolar affinity (17 nM), measured by isothermal titration calorimetry

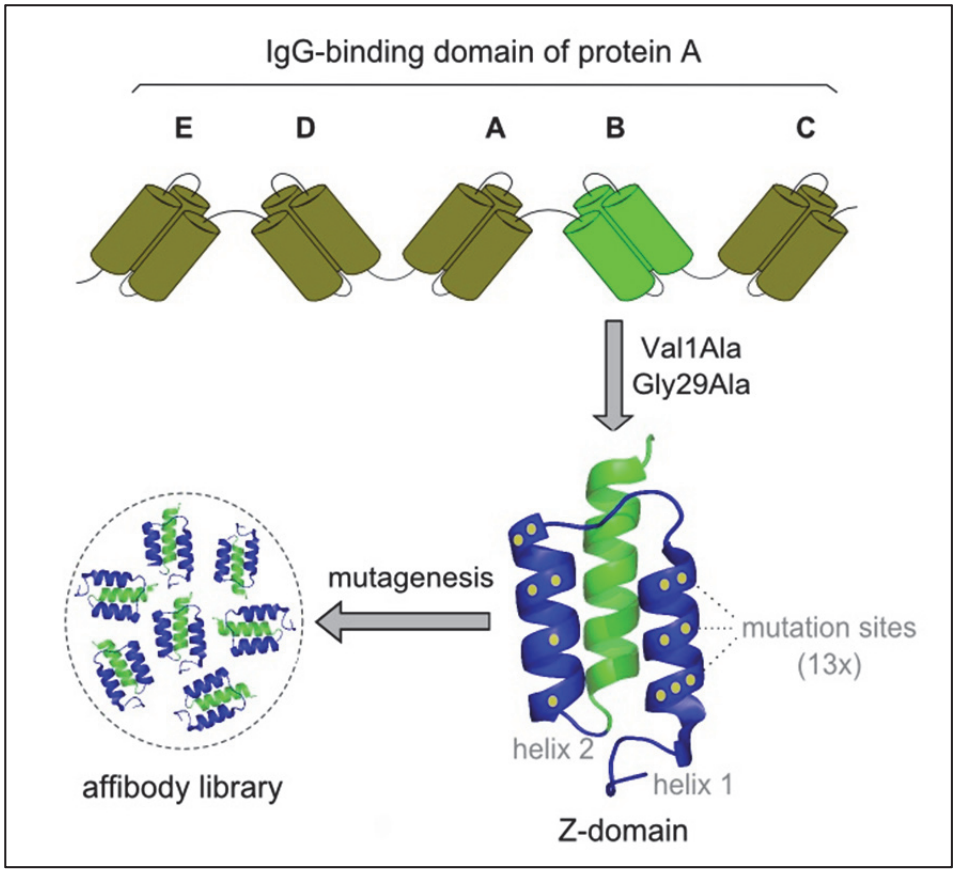

Figure 6: Schematic illustration of the development of the affibody library. The IgG-binding domain of staphylococcal protein A is composed of 5 α-helical protein domains (E, D, A, B and C) from which the B-domain was used as the protein scaffold for generation of the Z-domain (PDB code: 2SPZ) [205]. To generate the Z-domain, amino acids Valine1 and Glycine 29 in the B-domain were mutated to Alanine. Like the B-domain, the Z-domain consists of three α-helices. To create the affibody library, 13 amino acid positions in helix-1 and helix-2 of the Z-domain were targeted by random mutagenesis [206].

(ITC). The maturation process of ZAβ$_3$ from the Z-domain scaffold came along with 11 amino acid substitutions, including appearance of a cysteine residue at position 28. Cysteine-linked dimerization of ZAβ$_3$ is required for high affinity binding to Aβ. Structural characterization of the ZAβ$_3$:Aβ complex using NMR spectroscopy revealed that dimeric ZAβ$_3$ forms a hydrophobic cavity in which Aβ folds into a β-hairpin structure (figure 7A, B) [212]. The identified β-hairpin is composed of two antiparallel β-strands (β1: residues 17-23 and β2: residues 30-36) connected by a short linker. The β-strands resemble those identified in the Aβ fibrils. Sequestration of this

β-hairpin, inside the complex, results in inhibition of Aβ fibrillation and toxicity [212, 213]. Furthermore, stabilization of this β-hairpin via introduction of an intramolecular disulfide bond (Figure 7C) leads to formation of highly toxic oligomeric species [170]. Overexpression and aggregation of Aβ peptide has been shown to be associated with pathogenesis of AD [34, 35]. Like other neurodegenerative diseases, the exact mechanism of protein aggregation and its induced toxicity remains unknown. In the case of Aβ, using ZAβ$_3$ as a study tool resulted in the identification of a β-hairpin forming region critical for aggregation [170, 212-214]. Therefore, the identification of specific affibody binders against other amyloidogenic proteins could likewise provide structural insights into their aggregation process.

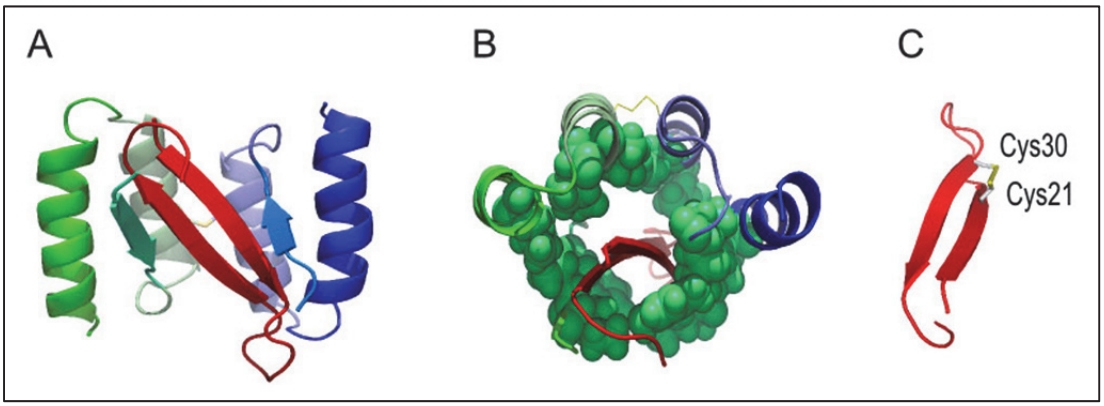

Figure 7: The structure of the ZAβ3:Aβ complex, the Aβ β-hairpin, and AβCC design strategy. The structures are generated using Pymol software. **A**, the structure of Aβ in complex with ZAβ$_3$ (PDB ID: 2OTK). ZAβ$_3$ is a homodimer protein containing 2 α-helices and one short β-strand in each subunit. Subunits are linked by a disulfide bond (in yellow). As shown in side view (**B**), ZAβ3 forms a hydrophobic tunnel-like cavity (in green spheres) in which Aβ folds into a β-hairpin structure [212]. (**C**) In AβCC, mutation of Alanine-30 and Alanine-21 to Cysteine residues results in stabilization of β-hairpin structure via an intramolecular disulfide bond (in yellow) [170].

1.5. Selection of engineered binding proteins

To select specific binding proteins, first of all a DNA-library is generated using random mutagenesis techniques and second, binders expressed from this library are screened against the target. The selection system needs to create a connection between the selected protein binders and their corresponding DNA sequence. Different selection systems include three common steps including: first, mixing the library with protein target, second, capture of binders with affinity to target and third, amplification of selected binders and repetition of the previous steps in order to achieve high affinity binders. Selection systems can be classified into three major classes [215]: cell-free systems (e.g. mRNA display, DNA display and ribosomal display), cell-dependent systems (e.g. bacteria surface display, yeast display and phage display) and non-display systems e.g. yeast-two-hybrid. In present thesis, phage display is applied as the selection technique which is thus explained more in detail in the following section.

1.5.1 Phage display

In phage display technology, the connection between phenotype and genotype is provided by insertion of the gene coding for the protein of interest into a filamentous bacteriophage and display of the corresponding protein on the phage surface. First in 1985, Smith et al. used M13 bacteriophage display for screening of protein libraries [216]. M13 phage display is still the most commonly used system, albeit the appearance of other systems such as T4, T7 and lambda [215]. M13 bacteriophage contains a circular single-stranded DNA (ssDNA) and several coat proteins. PVIII (with about 2700 copies) is the major coat protein and minor proteins with few copies are pIII, pVI, pVII and pIX. All coat proteins have been evaluated as potential protein display site, showing that all have advantages and disadvantages. For instance, due to the high number of pVIII copies, display in fusion with pVIII is limited to small peptides. PIII (42 kDa) is the most commonly used site suitable for display of proteins with different sizes. All five copies of protein III are localized at the tip of M13 particle and mediate its attachment to pilus F, which is

required for infection of *E.coli* cells [217]. In pIII display, for expression of fusion protein, either a complete phage vector or a phagemid assisted by a helper phage can be used. In 3+3 system, a phagemid vector carries the pIII gene C-terminally fused with the gene encoding the protein of interest [217]. In addition, the phagemid vector contains the M13 origin sites for replication of M13 ssDNA and a standard *E.coli* origin for replication of the vector inside bacterial cells. Using these origins, the phagemid is only able to replicate inside *E.coli* but it cannot make phages. Addition of helper phage, M13KO7, provides the proteins required for replication and assembly of M13 phage. Therefore, a combination of phagemid and helper phage results in assembly of recombinant phage particles expressing pIII fusion protein. Selection of potential binders displayed on the surface of phage particles is known as phage display selection or biopanning cycle [215] which is performed via several steps (figure 8): first, the phage library is incubated with biotinylated target protein, followed by capturing the biotinylated target using paramagnetic streptavidin beads. After the capturing step, unbound phage particles are washed away and bound particles are eluted using low pH buffer. Next, *E.coli* cells are infected with eluted phage particles. As mentioned above, addition of helper phage in this step results in propagation of phage particles. To select potent binders, the panning cycle is repeated for several times, along with a step-wise increase in washing stringency and a decrease in the concentration of target protein. Lastly, the gene sequences and binding properties of the selected clones are analyzed.

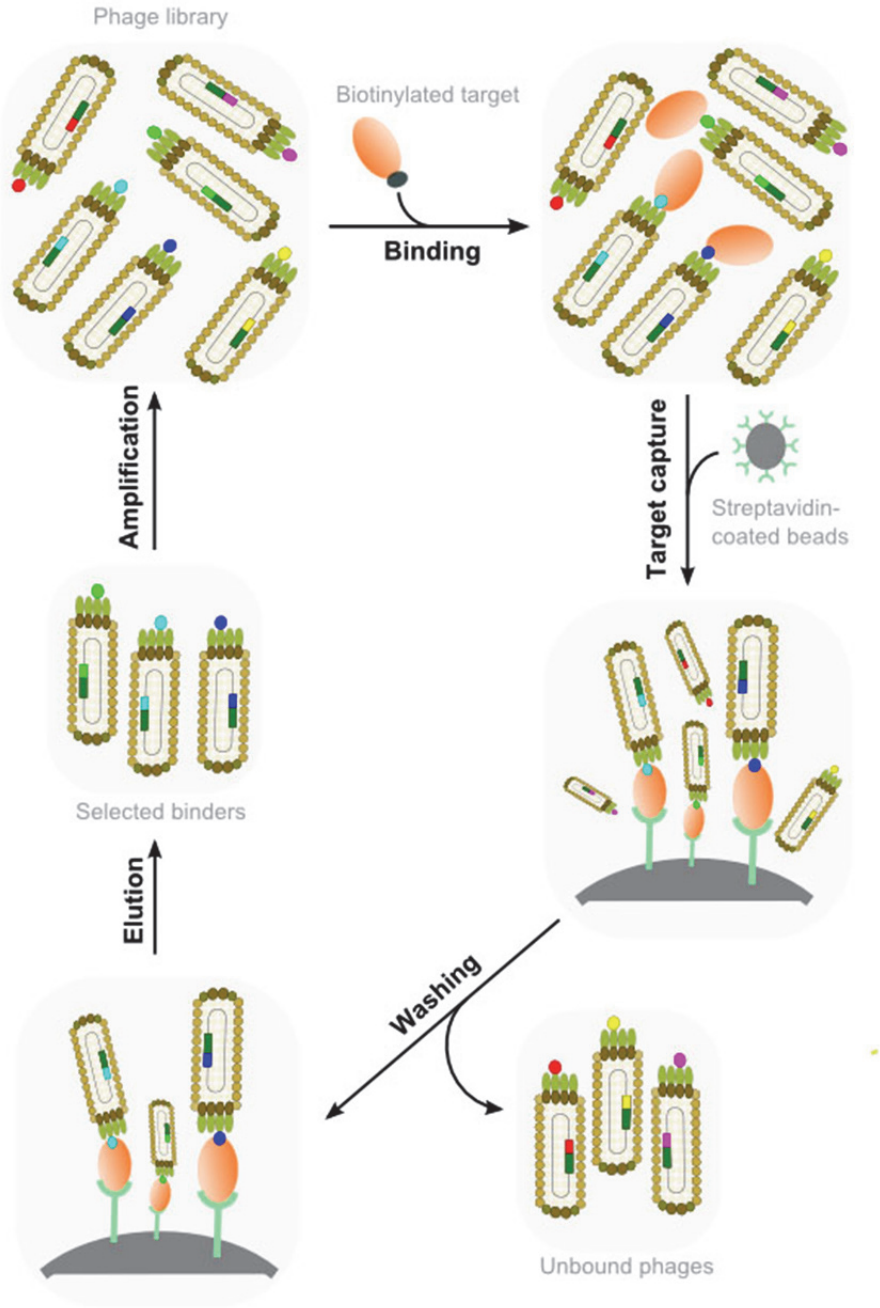

Figure 8: Schematic illustration of phage display. In the phage library, each phage displays a protein variant encoded by the corresponding gene from the library fused to pIII. The phage library is screened in a biopanning cycle. In the first step, phages are allowed to bind to the biotinylated target protein. Next, bound phages are captured by streptavidin coated beads and unbound phages are removed by washing steps. Lastly, the selected phages are eluted and amplified in *E.coli* for the next round of the biopanning cycle.

1.6. Scope of this thesis

Protein aggregation is believed to play an important role in the pathogenesis of several human diseases, particularly of neurodegenerative diseases such as AD and PD. However, the mechanism of protein aggreagtion is not fully known and, therefore, development of efficient therapeutics demands a better understanding of conformations and eptiopes that are critical in this process. Increasing number of studies validate the benefit of the application of engineered binding proteins for understanding molecular recognition and conformational properties of proteins. For instance, investigations on the AD-related Aβ peptide using an engineered binding protein, ZAβ3, led to the identification of a critical β-hairpin structure involved in aggregation and toxicity.

In the present thesis, the primary aim is to select an eningeered binding protein for the PD-related protein α-synuclein using phage display technology. For this purpose, the ZAβ3 sequence is considered as an ideal scaffold for the generation of a combinatorial library due to two main reasons: Firstly, different amyloidogenic proteins form fibrils of common structure. Secondly, the ZAβ3 scaffold already shows an affinity to an amyloid protein. Therefore, randomization of the ZAβ3 sequence might result in maturation of affinity to other amyloidogenic proteins. In addition to binder selection, this thesis will attempt to identify and study critical protein motifs involved in protein aggregation.

Chapter 2: Sequestration of a β-Hairpin for Control of α-Synuclein Aggregation

Ewa A. Mirecka*, Hamed Shaykhalishahi*, Aziz Gauhar, Serife Akgül, Justin Lecher, Dieter Willbold, Matthias Stoldt, and Wolfgang Hoyer

* Both authors equally contributed to this work

Status: published in *Angewandte Chemie* 12 March 2014

Impact factor: 13.7 (2012)

Own contribution to this work: 50%

Design, cloning, expression and purification of α-synuclein constructs; biotintylation of C-terminally truncated α-synuclein (1-108); selection, expression and purification of AS69; isothermal titration calorimetry; aggregation studies, sample preparations for NMR measurements.

Angewandte International Edition Chemie

Protein Aggregation

DOI: 10.1002/anie.201309001

Sequestration of a β-Hairpin for Control of α-Synuclein Aggregation**

*Ewa A. Mirecka, Hamed Shaykhalishahi, Aziz Gauhar, Şerife Akgül, Justin Lecher, Dieter Willbold, Matthias Stoldt, and Wolfgang Hoyer**

Abstract: *The misfolding and aggregation of the protein α-synuclein (α-syn), which results in the formation of amyloid fibrils, is involved in the pathogenesis of Parkinson's disease and other synucleinopathies. The emergence of amyloid toxicity is associated with the formation of partially folded aggregation intermediates. Here, we engineered a class of binding proteins termed β-wrapins (β-wrap proteins) with affinity for α-synuclein (α-syn). The NMR structure of an α-syn:β-wrapin complex reveals a β-hairpin of α-syn comprising the sequence region α-syn(37–54). The β-wrapin inhibits α-syn aggregation and toxicity at substoichiometric concentrations, demonstrating that it interferes with the nucleation of aggregation.*

The conversion of specific peptides and proteins into amyloid fibrils has been identified as a causative mechanism underlying several neurodegenerative conditions. Monomeric and oligomeric misfolding intermediates are key species on the aggregation pathway;[1] thus, the stabilization of partially folded states of amyloid proteins has been suggested as an approach for drug development.[1c,d]

The protein α-synuclein (α-syn) is the major protein component of the intracellular neuronal deposits observed in Parkinson's disease and related synucleinopathies.[2] A role of α-syn aggregation in the pathogenesis is supported by various genetic studies showing the enhanced propensity of α-syn to aggregate as a result of disease-related mutation or multiplication of the α-syn gene. Structurally, α-syn is characterized by high conformational flexibility. Free monomeric α-syn is intrinsically disordered; however, some regions of the protein show intramolecular long-range interactions.[3] When bound to synthetic or biological membranes, α-syn can readily adopt α-helical conformation.[4] In the fibrillar form, the central region of α-syn forms several β-strands which assemble into in-register parallel β-sheets in the fibril core, whereas the N-terminal part of the protein is less ordered and the C-terminus remains unfolded.[5] In contrast to the parallel arrangement of α-syn in fibrils,[5b,6] α-syn oligomers have been shown to adopt an antiparallel β-sheet structure.[7]

To stabilize partially structured α-syn, we generated binding ligands to α-syn using $ZA\beta_3$, a binding protein to the amyloid-β peptide (Aβ), as a scaffold. $ZA\beta_3$ is a disulfide-linked homodimer derived from the Z domain of protein A.[8] According to isothermal titration calorimetry (ITC), $ZA\beta_3$ binds Aβ with a dissociation constant of 20 nM but shows no affinity to α-syn (Figure S1). To generate binding affinity to α-syn, we created a new phage display library through random mutagenesis of the gene encoding $ZA\beta_3$. The binding ligands selected from this library are referred to as β-wrapins (β-wrap proteins). The β-wrapin clone AS69 harboring four amino acid substitutions in each subunit, that is, G13D, V17F, I31F, and L34V, was found to bind α-syn with a K_d value of 240 nM (Figure S1). In comparison to the original $ZA\beta_3$, the affinity of AS69 towards Aβ was 400-fold reduced. ITC indicated that the AS69:α-syn interaction follows a 1:1 stoichiometry. The binding of AS69 to α-syn was confirmed by (^{1}H-^{15}N) HSQC NMR spectroscopy. The spectra of free [U-^{15}N]-α-syn obtained at 30 °C showed only a few resonance signals stemming from the C-terminus, whereas cross-peaks from the N-terminal and central regions were not detected due to intermediate exchange.[9] However, upon addition of [NA]-AS69 to [U-^{15}N]-α-syn, several well-dispersed resonance signals appeared, indicating partial folding of α-syn (Figure 1a). The new resonances were assigned to the region α-syn(35–56).

To identify the conformation of α-syn(35–56), we determined the structure of full-length α-syn in complex with β-wrapin AS69 by high-resolution liquid-state NMR spectroscopy (Figure 1b,d, Tables S1 and S2). α-syn(35–56) folds into a β-hairpin comprising residues ^{37}VLYVGSK^{43} (β1) and ^{48}VVHGVAT^{54} (β2), connected by a β-turn formed by amino acids ^{44}TKEG^{47} (Figure 1b). The aromatic amino acids Tyr-39 and His-50 are located at the center of one β-hairpin face with their side chains hydrogen-bonded by the hydroxy proton of Tyr-39 and the N^{δ}-nitrogen of His-50 (Figure 1b). The H^{η} of Tyr-39 and $H^{\varepsilon 2}$ of His-50 are protected from exchange with solvent as inferred from their detectability in the NMR spectra.

The sequence positions of the β-strands are in good agreement with those of the β1 and β2 strands (designated according to Vilar et al.)[5d] of fibrillar α-syn (Figure 1c). Long-range interactions between the side chains Tyr-39 in β1 and His-50 in β2 have also been detected in α-syn amyloid

[*] Dr. E. A. Mirecka,[+] H. Shaykhalishahi,[+] A. Gauhar, Ş. Akgül, Dr. J. Lecher, Prof. Dr. D. Willbold, Dr. M. Stoldt, Dr. W. Hoyer
Institut für Physikalische Biologie
Heinrich-Heine-Universität Düsseldorf
40204 Düsseldorf (Germany)
E-mail: Wolfgang.Hoyer@uni-duesseldorf.de
Dr. J. Lecher, Prof. Dr. D. Willbold, Dr. M. Stoldt, Dr. W. Hoyer
Strukturbiochemie (ICS-6), Forschungszentrum Jülich
52425 Jülich (Germany)

[+] These authors contributed equally to this work.

[**] We thank Torleif Härd and Stephen F. Marino for valuable discussions. This work was supported by the Ministerium für Innovation, Wissenschaft und Forschung des Landes Nordrhein-Westfalen. The structure of the α-syn:AS69 complex has been deposited in the Protein Data Bank as entry 4BXL. Chemical shifts of the α-syn:AS69 complex have been deposited in the Biological Magnetic Resonance Bank under accession code 19353.

Supporting information for this article is available on the WWW under http://dx.doi.org/10.1002/anie.201309001.

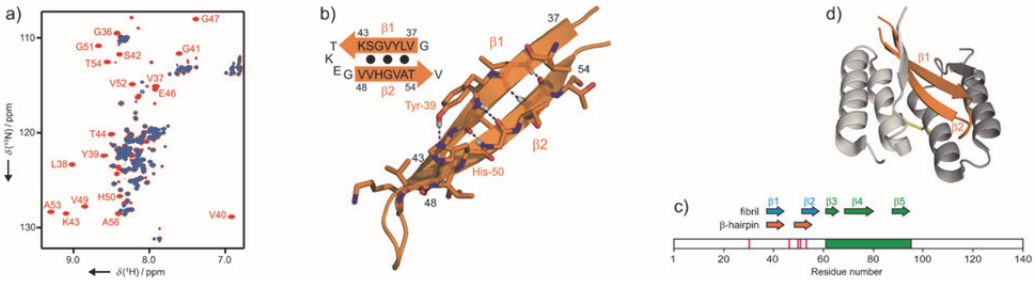

Figure 1. β-hairpin structure of α-syn in complex with β-wrapin AS69. a) (^{1}H-^{15}N) HSQC NMR spectra of [U-^{15}N]-α-syn recorded at 30 °C in the absence (blue) and presence (red) of an excess of [NA]-AS69. Assignments of peaks appearing upon complex formation are indicated. b) Ribbon drawing illustrating the β-hairpin of α-syn (orange). Amino acids forming the β1 and β2 strands are shown as sticks. The hydrogen bond between the hydroxy proton of Tyr-39 and the N^{δ}-nitrogen of His-50 is indicated as a dashed blue line. Backbone hydrogen bonds are marked as dashed black lines. The corresponding amino acid sequence is shown and backbone hydrogen bonding across the strands is indicated with black dots. c) Features of the α-syn primary structure. The central NAC region is shown in green. The positions of disease-related mutations are given in magenta. The location of β-strands in α-syn within fibrils as identified by EPR and solid-state NMR analysis[5] is approximated by blue and green arrows. The location of the β-strands within the β-hairpin of α-syn is given by orange arrows. d) The α-syn:AS69 complex illustrated by ribbon drawing. Residues 13–58 of the two AS69 subunits are shown in light and dark gray, respectively. The disulfide bond is shown in yellow. The β-hairpin of α-syn is shown in orange.

fibrils.[5d] The NAC region comprising β-strands β3 to β5, including the aggregation-prone sequence stretches with the highest hydrophobicity and β-sheet propensity,[10] is unaffected by AS69 binding (Figure S2). This demonstrates the specificity of the interaction of AS69 with the β1–β2 region.

Contacts between β1 and β2 are among the most prevalent transient tertiary interactions in monomeric α-syn according to paramagnetic relaxation enhancement data.[3c] Moreover, nascent β-structure was detected in the β1–β2 region of α-syn monomers.[1c] These findings suggest that structural features of the AS69-bound β-hairpin are present within a subset of the conformational ensemble sampled by free α-syn. This is in line with the observation that the binding mechanism of intrinsically disordered proteins is not solely of the induced-fit type, but also involves conformational selection.[11]

A comparison of the structures of the α-syn:AS69 and Aβ:ZAβ$_3$ complexes confirmed that the introduced mutations did not affect the overall structure of the β-wrapin protein scaffold in the bound state. The AS69 molecule is a dimer of two identical subunits covalently linked by a disulfide bond involving the Cys-28 residues of both subunits. The folding topology of AS69 comprises two β-strands and four α-helices forming a large hydrophobic tunnel-like cavity in which the β-hairpin of α-syn is buried (Figure 1d). Most of the exchanged amino acids are in direct contact with the β-hairpin (Figure S3). For example, the Phe-31 residues of both AS69 subunits are involved in aromatic–aromatic interactions with Tyr-39 and His-50 of α-syn.

The potency of AS69 to inhibit α-syn aggregation was evaluated by a Thioflavin T fluorescence assay. In the absence of AS69, a 35 μM solution of α-syn aggregated after a lag phase of roughly 10 h. However, the aggregation of α-syn was completely inhibited in the presence of an equivalent concentration of AS69 within an 8 day experiment (Figure 2a). Addition of an equimolar amount of AS69 to α-syn aggregation reactions at different time points prevented further fibrillation of α-syn (Figure 2b). These observations indicate that sequestration of the β-hairpin renders α-syn monomers incompetent to aggregate. In addition, AS69 inhibited fibrillation of α-syn at substoichiometric concentrations. For AS69:α-syn molar ratios of 1:10, 1:100, and 1:1000, AS69 prolonged the lag time of α-syn fibrillation 9-fold, 6-fold, and 2-fold, respectively (Figure 2d and Figure S4). Size-exclusion chromatography confirmed that the binding of β-wrapin AS69 to α-syn delayed fibrillation at substoichiometric ratios and furthermore revealed that during the lag time of the aggregation experiment stable oligomeric species were not formed (Figure 2c). The substoichiometric inhibition cannot be explained by monomer sequestration. Thus, a second inhibitory mechanism must be operative which interferes with the nucleation of aggregation. This mechanism might involve the binding of AS69 to the β1–β2 region of α-syn within early aggregates. However, other α-syn epitopes may also be crucial for the substoichiometric inhibition. In this context, it is of note that α-syn oligomers exhibit antiparallel β-structure.[7] With the present data the mechanism of substoichiometric inhibition cannot be elucidated. Possible mechanisms include: 1) a small fraction of AS69-bound α-syn molecules within oligomers precludes the concerted conformational conversion to ordered amyloid fibrils; 2) AS69 binds with high affinity to fibril ends, thereby blocking fibril growth.

To evaluate the effect of AS69 on α-syn toxicity, the viability of human SH-SY5Y neuroblastoma cells was analyzed upon addition of α-syn samples aged in the absence and presence of β-wrapin AS69. For fibrillar α-syn samples, we observed a concentration-dependent decrease in the cellular viability as assessed by an MTT assay (Figure 2e). The viability of SH-SY5Y cells was rescued when α-syn samples were incubated in the presence of AS69. The viability rescue was dependent on the concentration of AS69, with complete

Mira, A. Consiglio, E. Pham, E. Masliah, F. H. Gage, R. Riek, *Proc. Natl. Acad. Sci. USA* **2011**, *108*, 4194–4199; g) N. Zijlstra, C. Blum, I. M. Segers-Nolten, M. M. Claessens, V. Subramaniam, *Angew. Chem.* **2012**, *124*, 8951–8954; *Angew. Chem. Int. Ed.* **2012**, *51*, 8821–8824.

[2] a) H. A. Lashuel, C. R. Overk, A. Oueslati, E. Masliah, *Nat. Rev. Neurosci.* **2013**, *14*, 38–48; b) L. Breydo, J. W. Wu, V. N. Uversky, *Biochim. Biophys. Acta Mol. Basis Dis.* **2012**, *1822*, 261–285.

[3] a) C. W. Bertoncini, Y. S. Jung, C. O. Fernandez, W. Hoyer, C. Griesinger, T. M. Jovin, M. Zweckstetter, *Proc. Natl. Acad. Sci. USA* **2005**, *102*, 1430–1435; b) M. M. Dedmon, K. Lindorff-Larsen, J. Christodoulou, M. Vendruscolo, C. M. Dobson, *J. Am. Chem. Soc.* **2005**, *127*, 476–477; c) S. Esteban-Martín, J. Silvestre-Ryan, C. W. Bertoncini, X. Salvatella, *Biophys. J.* **2013**, *105*, 1192–1198.

[4] D. Eliezer, E. Kutluay, R. Bussell, Jr., G. Browne, *J. Mol. Biol.* **2001**, *307*, 1061–1073.

[5] a) H. Heise, W. Hoyer, S. Becker, O. C. Andronesi, D. Riedel, M. Baldus, *Proc. Natl. Acad. Sci. USA* **2005**, *102*, 15871–15876; b) M. Chen, M. Margittai, J. Chen, R. Langen, *J. Biol. Chem.* **2007**, *282*, 24970–24979; c) G. Comellas, L. R. Lemkau, A. J. Nieuwkoop, K. D. Kloepper, D. T. Ladror, R. Ebisu, W. S. Woods, A. S. Lipton, J. M. George, C. M. Rienstra, *J. Mol. Biol.* **2011**, *411*, 881–895; d) M. Vilar, H. T. Chou, T. Luhrs, S. K. Maji, D. Riek-Loher, R. Verel, G. Manning, H. Stahlberg, R. Riek, *Proc. Natl. Acad. Sci. USA* **2008**, *105*, 8637–8642.

[6] A. Loquet, K. Giller, S. Becker, A. Lange, *J. Am. Chem. Soc.* **2010**, *132*, 15164–15166.

[7] M. S. Celej, R. Sarroukh, E. Goormaghtigh, G. D. Fidelio, J. M. Ruysschaert, V. Raussens, *Biochem. J.* **2012**, *443*, 719–726.

[8] C. Grönwall, A. Jonsson, S. Lindstrom, E. Gunneriusson, S. Stahl, N. Herne, *J. Biotechnol.* **2007**, *128*, 162–183; b) W. Hoyer, C. Grönwall, A. Jonsson, S. Ståhl, T. Härd, *Proc. Natl. Acad. Sci. USA* **2008**, *105*, 5099–5104.

[9] B. C. McNulty, A. Tripathy, G. B. Young, L. M. Charlton, J. Orans, G. J. Pielak, *Protein Sci.* **2006**, *15*, 602–608.

[10] a) B. I. Giasson, I. V. Murray, J. Q. Trojanowski, V. M. Lee, *J. Biol. Chem.* **2001**, *276*, 2380–2386; b) S. Zibaee, G. Fraser, R. Jakes, D. Owen, L. C. Serpell, R. A. Crowther, M. Goedert, *J. Biol. Chem.* **2010**, *285*, 38555–38567.

[11] a) P. Csermely, R. Palotai, R. Nussinov, *Trends Biochem. Sci.* **2010**, *35*, 539–546; b) M. Fuxreiter, I. Simon, P. Friedrich, P. Tompa, *J. Mol. Biol.* **2004**, *338*, 1015–1026.

Angewandte International Edition Chemie

Communications

Protein Aggregation

E. A. Mirecka, H. Shaykhalishahi, A. Gauhar, Ş. Akgül, J. Lecher, D. Willbold, M. Stoldt, W. Hoyer* ——— ■■■■–■■■■

Sequestration of a β-Hairpin for Control of α-Synuclein Aggregation

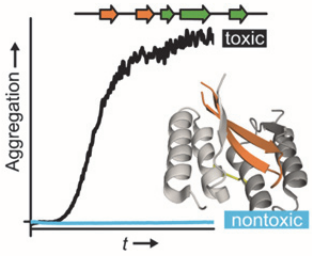

Wrapping the hairpin: NMR spectroscopy identifies a β-hairpin conformation of α-synuclein in complex with an engineered β-wrapin. The β-wrapin inhibits α-synuclein aggregation and toxicity at substoichiometric concentration. Sequestration of a β-hairpin is a novel approach to interfere with the initial steps of the aggregation reaction.

Angewandte Chemie
Eine Zeitschrift der Gesellschaft Deutscher Chemiker

Supporting Information

69451 Weinheim, Germany

Sequestration of a β-Hairpin for Control of α-Synuclein Aggregation**

*Ewa A. Mirecka, Hamed Shaykhalishahi, Aziz Gauhar, Şerife Akgül, Justin Lecher, Dieter Willbold, Matthias Stoldt, and Wolfgang Hoyer**

anie_201309001_sm_miscellaneous_information.pdf

Table of contents

Supporting Experimental Section

Library construction and phage display selection. A second generation β-wrapin library based on the $ZA\beta_3$ scaffold[1] was generated by error-prone PCR. The library construct in a pComb3HSS vector backbone (provided by C. F. Barbas, The Scripps Research Institute, La Jolla, USA) contained OmpA leader, AQHDEA peptide derived from the region E of protein A followed by the gene encoding β-wrapin clones, c-myc-tag, albumin-binding domain from streptococcal protein G and protein III(230-406) of M13 filamentous phage. Error-prone PCR was performed with the GeneMorph II Random Mutagenesis Kit (Stratagene) in a reaction containing 200 fg of the vector template containing the gene encoding for $ZA\beta_3$ monomer and vector-specific primers flanking the $ZA\beta_3$ gene: 5′GCCGAGCTCGCGCAACACGATGAAGCC and 5′CGCTGATCAGTTTTTGTTCCTCGAG (MWG Biotech). The DNA was amplified for 40 cycles (95 °C 30 s, 54 °C 30 s, 72 °C 1 min) and used as a template in the second PCR with DreamTaq DNA Polymerase (Thermo Scientific) and the same set of primers. The mutated $ZA\beta_3$ gene was gel purified and digested with SacI and XhoI (New England Biolabs) followed by ligation into the corresponding sites of a modified pComb3HSS vector. The library was transformed into electrocompetent *E. coli* XL1-Blue cells (Stratagene) resulting in 7×10^7 transformants. The phage library was produced by superinfection of bacteria harboring the library with M13KO7 phage (New England Biolabs) and precipitation by PEG/NaCl. In order to remove streptavidin-binding phage, a negative selection in which the phage preparation was incubated with streptavidin magnetic beads at room temperature for 1 h preceded each selection round. The library (10^{11}–10^{13} colony-forming units) was then subjected to successive rounds of panning with biotinylated α-syn(1-108). During each round, the phage library was incubated with α-syn(1-108) at a concentration of 500, 300, 50 and 10 nM in rounds 1-4, respectively. In the first panning round, the incubation was carried out overnight at 4 °C whereas the subsequent selection rounds were done for 1 h at room temperature. The phage-target complexes were captured on streptavidin magnetic beads and following washing (1-, 5-, 8- and 20-times in rounds 1-4, respectively) with PBST-BSA (PBS, 0.1% (w/v) Tween 20, 3% (v/v) BSA) and once with PBS, bound phages were eluted by lowering the pH to 2.0. Following neutralization with 1 M Tris-HCl, pH 8.0, the eluted phages were amplified in *E. coli* XL1-Blue cells and subjected to the following panning round. After the fourth selection round, the DNA pool was subcloned into pET302/NT-His vector (Invitrogen) and DNA from 90 single colonies was sequenced (MWG Biotech).

Protein preparation. Full-length α-syn and α-syn(1-108) were expressed from pT7-7 vector and purified essentially as described.[2] Briefly, cell lysates were obtained from *E. coli* BL21(DE3) cells cultivated in M9 minimal medium supplemented with NH_4Cl (1 g/l) and glucose (2 g/l), followed by IPTG (isopropyl-β-D-1-thiogalactopyranoside) induction. Both proteins were purified using anion exchange chromatography on a HiTrap Q FF column (GE Healthcare). Full-length α-syn was eluted with a salt gradient at approximately 300 mM NaCl, whereas α-syn(1-108) was collected in the flow-through. Further purification was achieved by size-exclusion chromatography on a HiLoad 16/60 Superdex 75 column (GE Healthcare) in 20 mM sodium phosphate, 50 mM NaCl, pH 7.4. Biotinylation was performed with Sulfo-NHS-LC-Biotin (Thermo Scientific) in a reaction containing ~200 μM of α-syn(1-108) in 20 mM sodium phosphate, pH 6.5 and a 5-fold molar excess of biotinylation reagent. After incubation at 4 °C for 3 h, the protein sample was passed through a Zeba Spin desalting column (Thermo Scientific) followed by affinity purification on monomeric avidin agarose

(Thermo Scientific). The level of biotinylation was quantified by HABA assay (Thermo Scientific), yielding an average value of 2 biotin molecules incorporated per α-syn(1-108) monomer.

Aβ(1-40) was produced with an N-terminal methionine by recombinant coexpression with $ZA\beta_3$.[3]

AS69 and $ZA\beta_3$ containing an N-terminal His6-tag were expressed from pET302/NT-His vector in *E. coli* BL21(DE3) cells. Head-to-tail linked AS69 dimer (termed AS69-GS3) used for cell culture experiments was expressed from the same vector. Expression cultures were grown in LB medium. Protein expression was induced with 1 mM IPTG at OD 0.6-0.8 for 4 h at 37 °C. Following centrifugation at 4,000 x g, the cell pellet was resuspended in 20 mM sodium phosphate, pH 8.3, 500 mM NaCl, containing EDTA-free protease inhibitor (Roche Applied Sciences) and lysed by a cell disrupter (Constant Systems). Insoluble material was removed by centrifugation at 28,000 x g and the supernatant was loaded on a HisTrap FF column (GE Healthcare). The dimeric fractions of AS69 or $ZA\beta_3$ as well as AS69-GS3 were collected from a HiLoad 16/60 Superdex 75 size-exclusion chromatography column (GE Healthcare) in 20 mM sodium phosphate, 50 mM NaCl, pH 7.4.

For NMR experiments, proteins were expressed in M9 minimal medium supplemented with ^{15}N-NH_4Cl (1 g/l) and $^{13}C_6$-glucose (2 g/l) and purified as described for the non-isotopically enriched proteins.

Isothermal titration calorimetry (ITC). ITC was performed on a Microcal iTC200 calorimeter (GE Healthcare) at 30 °C. The buffer was 20 mM sodium phosphate, 50 mM NaCl, pH 7.4. For determination of affinities to α-syn, AS69 or $ZA\beta_3$ were used as titrant in the cell at a concentration of ~60 μM, and α-syn at approximately 10-fold higher concentration as titrant in the syringe. For determination of affinities to Aβ, Aβ was used as titrant in the cell at a concentration of 10 μM, and AS69 or $ZA\beta_3$ at 100 μM as titrant in the syringe. The heat of post-saturation injections was averaged and subtracted from each injection to correct for heats of dilution and mixing. Data were processed using MicroCal Origin software provided with the calorimeter. Dissociation constants were obtained from a nonlinear least-squares fit to a 1:1 binding model.

Aggregation assay. Fibrillation of α-syn was followed by thioflavin T fluorescence. The reaction contained 35 or 70 μM of α-syn and 40 μM thioflavin T in 20 mM sodium phosphate, 50 mM NaCl, pH 6.0, 0.04% Na-azide, in a final volume of 150 μl. Aggregation was performed at 37° C with continuous orbital shaking (300 rpm) in a round-bottom 96-well black plate (Nunc) containing a 2 mm glass bead in each well. Thioflavin T emission was recorded at 480 nm (excitation 440 nm) on an Infinite M1000 plate reader (Tecan). For background correction, the signal of a buffer sample containing thioflavin T was subtracted. The lag-time was defined as the incubation time at which the fluorescence intensity for the first time reaches 5% of the final steady state fluorescence of α-syn in the absence of AS69. Protein samples were analyzed before and after the aggregation assay by size-exclusion chromatography on a Superdex 75 10/300 GL column (GE Healthcare) in 20 mM sodium phosphate, 50 mM NaCl, pH 7.4.

MTT cell viability assay. The viability of SH-SY5Y neuroblastoma cells in the presence of α-syn was tested with an MTT assay (Cell Proliferation Kit I, Roche Diagnostic). SH-SY5Y cells (purchased from DSMZ) were seeded in 96-well tissue culture plate at a density of 20,000 cells/well in 100 μL of media (DMEM-F12, 10% fetal calf serum) and incubated for 24 h. Following application of the protein samples at the indicated concentrations, cells were further incubated for 24 h. Untreated cells and cells either exposed to monomeric α-syn or AS69 were considered as controls. To assess the effects of test samples on the cells, MTT was added to the cells at a final concentration of 0.5 mg/mL in PBS followed by incubation for an additional 4 h at 37 °C. Next, 100 μL of the solubilization solution (10% SDS and 0.01 M HCl) was added and incubation was continued overnight at 37 °C followed by measuring the absorbance at 565 nm in an Infinite M1000 plate reader (Tecan). The data was normalized to the value of untreated control cells. All cell cultures were maintained in a 5% CO_2 humidified atmosphere at 37 °C.

NMR and structure determination. NMR experiments were performed at 10 or 30 °C on Varian VNMRS instruments at proton frequencies of 800 and 900 MHz, each equipped with a cryogenically cooled Z-axis pulse-field-gradient (PFG) triple resonance probe. NMR samples contained [U-^{13}C,^{15}N]-α-syn or [U-^{13}C,^{15}N]-AS69 at a concentration of 0.7 mM and a 20% molar excess of the respective non-isotopically enriched binding partner in 20 mM sodium phosphate, 50 mM NaCl, pH 7.4. NMR data were processed using NMRPipe[4] and analyzed with CcpNmr.[5] Mean weighted chemical shift displacements were calculated as $[(\Delta\delta^1H)^2 + (\Delta\delta^{15}N)^2/25]^{1/2}$. Backbone assignments were obtained using BEST-TROSY experiments[6] and side-chain assignments were

obtained using standard triple resonance heteronuclear NMR techniques. Histidine side chain protonation states were determined using a long-range (^{1}H-^{15}N)-HMQC experiment.[7] Nuclear Overhauser enhancement (NOE) based distance restraints for structure calculation were derived from 3D (^{1}H-^{1}H-^{15}N)-NOESY-HSQC (120 ms mixing time), (^{1}H-^{13}Cali-^{1}H)-HSQC-NOESY (100 ms mixing time) and (^{1}H-^{13}Caro-^{1}H)-HSQC-NOESY (100 ms mixing time) experiments and 2D NOESY for protons H^{η} of Tyr-39 and $H^{\varepsilon 2}$ of His-50 of α-syn. Backbone dihedral angle constraints were derived from chemical shifts, using TALOS+.[8] Structure calculations based on NOE distance restraints and dihedral angle restraints were accomplished with a modified version of CNS v. 1.2.1[9] using an optimized version of the PARALLHDG force field. The MD protocol contained 30 ps high-temperature torsion angle dynamics (10,000 K) and 20,000 steps during two cooling phases (2,000 K and 50 K). Ten lowest energy structures (overall CNS energy) out of 100 calculated were selected and validated using Molprobity.[10] Molecular graphics figures were created using PyMOL.[11]

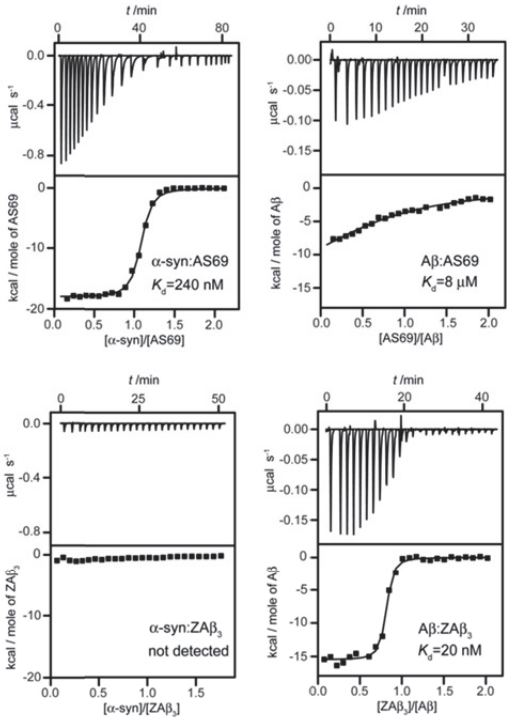

Figure S1. Generation of binding specificity for α-syn. The affinity of AS69 to α-syn was analyzed by ITC. AS69 was used as titrant in the cell at a concentration of 65 µM and α-syn at 680 µM as titrant in the syringe. For comparison, the affinity of AS69 to Aβ was determined, using Aβ as titrant in the cell at a concentration of 10 µM, and AS69 at 100 µM as titrant in the syringe. The affinities of $ZA\beta_3$ to α-syn and Aβ were analyzed under similar experimental conditions. ITC experiments were performed at 30 °C.

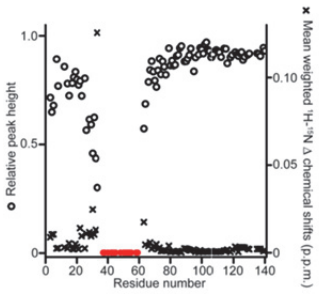

Figure S2. Effect of AS69 binding on different α-syn sequence regions. (^1H–^{15}N)-HSQC NMR spectra were recorded at 10 °C. At this temperature, resonances from nearly all residues in free α-syn are visible.[12] Upon addition of [NA]-AS69 to [U-^{15}N]-α-syn, the resonance signals of residues in the β-hairpin region of α-syn disappeared, indicative of intermediate exchange in the complex at this temperature (red circles). According to changes in the peak height (open circles) and in the chemical shifts (crosses), AS69 binding had some effect on the conformation of the N-terminal part of α-syn, especially on the very N-terminal residues up to Met-5 and the region α-syn(22-35) preceding the β-hairpin. The changes in chemical shifts were small, however, indicating that these regions remain disordered in the bound state. The central as well as the C-terminal region of α-syn were essentially unaffected.

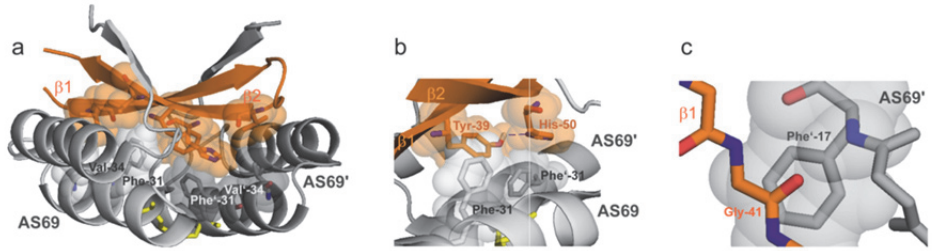

Figure S3. Effect of the mutations of the scaffold present in AS69. AS69 carries four amino acid substitutions in each homodimer subunit, i.e. G13D, V17F, I31F and L34V. a) The amino acids Phe-31 and Val-34 in both subunits are in contact with the interior face of the β-hairpin contributed by residues Val-37, Tyr-39, Val-48, His-50 and Val-52. Nonpolar side chains of α-syn with <60% solvent accessibility and Phe-31 and Val-34 of both AS69 subunits are displayed as sticks and spheres. The two AS69 subunits are shown in light and dark gray and are labeled AS69 or AS69′, respectively. The disulfide bond is shown in yellow. The β-hairpin of α-syn is shown in orange. b) The Phe-31 residues of both AS69 subunits are involved in aromatic-aromatic interactions with Tyr-39 and His-50 of α-syn. c) The V17F mutation in AS69 stabilizes the β-hairpin of α-syn by aromatic rescue of a glycine, i.e. Gly-41, in the β1 strand of α-syn. The side chain of Phe-17 in one AS69 subunit adopts the gauche$^+$ χ_1 rotamer and lays over the cross-strand Gly-41. For the G13D mutation located at the N-terminal end of the folded region of AS69 no specific interactions of the acidic side chain were discernible in the complex structure. However, this residue might be involved in electrostatic steering of binding,[13] e.g. by interacting with Lys-43, Lys-45, or Lys-58 of α-syn.

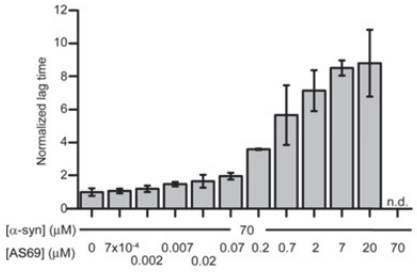

Figure S4. Inhibition of α-syn aggregation by substoichiometric concentrations of AS69. The lag-time of fibrillation kinetics monitored by thioflavin T in dependence of the concentration of AS69. The mean lag time determined from three experiments is given. Error bars represent the s.d. (n.d. = no fibrillation detectable).

Table S1. Constraint statistics of the α-syn:AS69 complex

Constraint type	Number
Distance constraints	
Unambiguous NOE constraints	3015
Intra-residue	930
Inter-residue	2085
Sequential ($\|i-j\|=1$)	598
Medium-range ($\|i-j\|\leq 5$)	595
Long-range ($\|i-j\|>5$)	410
Intermolecular	482
Hydrogen bonds	1
Ambiguous NOE constraints	319
Total dihedral angle restraints	196
ϕ/ψ	98

Table S2. Structure statistics of the α-syn:AS69 complex

Statistics	Value
Violations (mean and s.d.)	
Distance constraints (Å)	0.025 ± 0.0007
Dihedral angle constraints (°)	1.5 ± 0.08
Max. dihedral angle violation (°)	11
Max. distance constraint violation (Å)	0.35
Deviations from idealized geometry	
Bond lengths (Å)	0.0065 ± 0.0001
Bond angles (°)	0.75 ± 0.01
Impropers (°)	1.84 ± 0.04
Average pairwise r.m.s. deviation* (Å)	
Heavy	0.72 ± 0.08
Backbone	0.36 ± 0.05
Ramachandran statistics	
Core regions (%)	92.7 ± 0.6
Allowed regions (%)	6.3 ± 0.6
Generous regions (%)	1.1 ± 0
Disallowed regions (%)	0 ± 0

*Pairwise r.m.s. deviation was calculated among 10 refined structures

Supporting References

[1] C. Grönwall, A. Jonsson, S. Lindstrom, E. Gunneriusson, S. Stahl, N. Herne, *J. Biotechnol.* **2007**, *128*, 162-183.

[2] W. Hoyer, D. Cherny, V. Subramaniam, T. M. Jovin, *Biochemistry* **2004**, *43*, 16233-16242.

[3] B. Macao, W. Hoyer, A. Sandberg, A. C. Brorsson, C. M. Dobson, T. Härd, *BMC Biotechnol.* **2008**, *8*, 82.

[4] F. Delaglio, S. Grzesiek, G. W. Vuister, G. Zhu, J. Pfeifer, A. Bax, *J. Biomol. NMR* **1995**, *6*, 277-293.

[5] W. F. Vranken, W. Boucher, T. J. Stevens, R. H. Fogh, A. Pajon, M. Llinas, E. L. Ulrich, J. L. Markley, J. Ionides, E. D. Laue, *Proteins* **2005**, *59*, 687-696.

[6] Z. Solyom, M. Schwarten, L. Geist, R. Konrat, D. Willbold, B. Brutscher, *J. Biomol. NMR* **2013**, *55*, 311-321.

[7] J. G. Pelton, D. A. Torchia, N. D. Meadow, S. Roseman, *Protein Sci.* **1993**, *2*, 543-558.

[8] Y. Shen, F. Delaglio, G. Cornilescu, A. Bax, *J. Biomol. NMR* **2009**, *44*, 213-223.

[9] a) A. T. Brunger, *Nat. Protoc.* **2007**, *2*, 2728-2733; b) W. Rieping, M. Habeck, B. Bardiaux, A. Bernard, T. E. Malliavin, M. Nilges, *Bioinformatics* **2007**, *23*, 381-382.

[10] V. B. Chen, W. B. Arendall, 3rd, J. J. Headd, D. A. Keedy, R. M. Immormino, G. J. Kapral, L. W. Murray, J. S. Richardson, D. C. Richardson, *Acta Crystallogr. Sect. D. Biol. Crystallogr.* **2010**, *66*, 12-21.

[11] The PyMOL Molecular Graphics System, 1.2; Schrödinger, LLC.

[12] D. Eliezer, E. Kutluay, R. Bussell, Jr., G. Browne, *J. Mol. Biol.* **2001**, *307*, 1061-1073.

[13] D. Ganguly, S. Otieno, B. Waddell, L. Iconaru, R. W. Kriwacki, J. Chen, *J. Mol. Biol.* **2012**, *422*, 674-684.

Full Reference from Main Article

[1f] B. Winner, R. Jappelli, S. K. Maji, P. A. Desplats, L. Boyer, S. Aigner, C. Hetzer, T. Loher, M. Vilar, S. Campioni, C. Tzitzilonis, A. Soragni, S. Jessberger, H. Mira, A. Consiglio, E. Pham, E. Masliah, F. H. Gage, R. Riek, *Proc. Natl. Acad. Sci. USA* **2011**, *108*, 4194-4199.

Chapter 3: A β-Hairpin-Binding Protein to Three Different Disease-Related Amyloidogenic Proteins

Hamed Shaykhalishahi, Ewa A. Mirecka, Aziz Gauhar, Clara S. R. Grüning, Torleif Härd, Matthias Stoldt, and Wolfgang Hoyer

Status: published in *ChemBioChem 30 December 2014*

Impact factor: 3.08 (2014)

Own contribution to this work: 80%

Cloning, expression and purification of α-synuclein constructs; selection, subcloning, expression and purification of AS9, A10, A34, A60 and AS69 proteins; preparation of IAPP; isothermal titration calorimetry; surface plasmon resonance; aggregation studies; MTT assays for Aβ and IAPP targets; sample preparation for NMR measurements.

ChemPubSoc Europe

DOI: 10.1002/cbic.201402552

CHEMBIOCHEM Communications

A β-Hairpin-Binding Protein for Three Different Disease-Related Amyloidogenic Proteins

Hamed Shaykhalishahi,[a] Ewa A. Mirecka,[a] Aziz Gauhar,[a] Clara S. R. Grüning,[a] Dieter Willbold,[a, c] Torleif Härd,[b] Matthias Stoldt,[a, c] and Wolfgang Hoyer*[a, c]

Amyloidogenic proteins share a propensity to convert to the β-structure-rich amyloid state that is associated with the progression of several protein-misfolding disorders. Here we show that a single engineered β-hairpin-binding protein, the β-wrapin AS10, binds monomers of three different amyloidogenic proteins, that is, amyloid-β peptide, α-synuclein, and islet amyloid polypeptide, with sub-micromolar affinity. AS10 binding inhibits the aggregation and toxicity of all three proteins. The results demonstrate common conformational preferences and related binding sites in a subset of the amyloidogenic proteins. These commonalities enable the generation of multispecific monomer-binding agents.

The oligomerization and aggregation of proteins, ultimately resulting in fibrillar amyloid deposits, are pathological features of various diseases.[1] For example, senile plaques containing the amyloid-β peptide (Aβ), Lewy bodies consisting of α-synuclein (α-syn), and pancreatic islet amyloid composed of islet amyloid polypeptide (IAPP) are pathological features of Alzheimer's disease (AD), Parkinson's disease (PD), and type 2 diabetes, respectively.[2] The cross-β spine, built of stacked β-strands that are oriented perpendicular to the fibril axis, is the common core structure of the amyloid states of amyloidogenic proteins.[3] The individual polypeptide chains typically adopt β-strand–turn–β-strand motifs that align to form parallel, in-register β-sheets in β-sandwich, β-serpentine, or β-helical arrangements.[3] Structural similarities among different amyloidogenic proteins have also been recognized at the level of their oligomeric and protofibrillar states, evident for example, from the shared affinity for conformation-specific antibodies.[4]

In this work, we investigated whether the structural similarity of different amyloidogenic proteins extends to the coupled folding and binding reactions of the monomeric proteins. Common molecular-recognition motifs might be involved in the dysfunction of amyloidogenic proteins. Furthermore, they would allow for the generation of multispecific binding agents that could serve in diagnostic and therapeutic applications.

β-Wrapins are engineered binding proteins obtained from phage-display libraries based on the Aβ-binding affibody protein ZAβ$_3$. ZAβ$_3$ is a homodimer with a disulfide bond between the Cys28 residues of the subunits (Figure 1 A and C).[5] Monomeric Aβ adopts a β-hairpin conformation in complex with ZAβ$_3$ (Figure 1 A) that is reminiscent of the β-strand–turn–β-strand conformation found in Aβ amyloid fibrils.[6]

We have recently reported the selection of a binder to α-syn from a β-wrapin phage-display library obtained by random

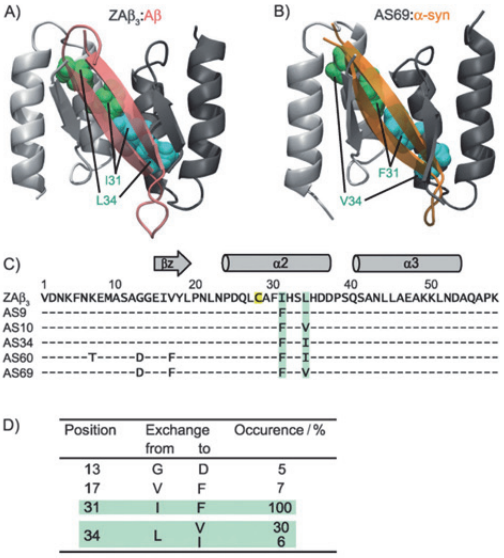

D)

Position	Exchange from	to	Occurence / %
13	G	D	5
17	V	F	7
31	I	F	100
34	L	V	30
		I	6

Figure 1. Amino acid positions in β-wrapins critical for interaction with amyloidogenic targets. Topologies of the A) Aβ:ZAβ$_3$ (PDB ID: 2OTK)[5b] and B) α-syn:AS69 (PDB ID: 4BXL)[7] complexes with homodimer subunits in light and dark gray. Residues 31 and 34, the two most frequently exchanged amino acids, are located at the interface between the homodimer subunits and the β-hairpins. C) Amino acid sequences of five representative β-wrapin variants selected against α-syn aligned to ZAβ$_3$. Residues 31 and 34 are highlighted in green, Cys28 in yellow. The positions of helical and β-sheet secondary structure in Aβ-bound ZAβ$_3$ are indicated by cylinders and arrow, respectively. D) Most frequent amino acid exchanges in ZAβ$_3$ occurring in 90 clones selected to bind α-synuclein. Residues 31 and 34 are highlighted.

[a] H. Shaykhalishahi, Dr. E. A. Mirecka, A. Gauhar, Dr. C. S. R. Grüning, Prof. Dr. D. Willbold, Dr. M. Stoldt, Dr. W. Hoyer
Institute of Physical Biology, Heinrich-Heine-Universität Düsseldorf
40204 Düsseldorf (Germany)
E-mail: wolfgang.hoyer@uni-duesseldorf.de

[b] Prof. Dr. T. Härd
Department of Chemistry and Biotechnology
Swedish University of Agricultural Sciences (SLU)
Box 7015, 750 07 Uppsala (Sweden)

[c] Prof. Dr. D. Willbold, Dr. M. Stoldt, Dr. W. Hoyer
Institute of Structural Biochemistry (ICS-6), Research Centre Jülich
52425 Jülich (Germany)

Supporting information for this article is available on the WWW under http://dx.doi.org/10.1002/cbic.201402552.

ChemPubSoc Europe

CHEMBIOCHEM Communications

mutagenesis of ZAβ$_3$.[7] The phage-display library contained 7×10^7 transformants with an average of approximately two exchanges per ZAβ$_3$ subunit. To avoid selecting binders to the highly charged C-terminal domain, the C-terminally truncated construct α-syn(1–108) was used as a target.[7] After four selection rounds, the sequences of 90 individual β-wrapin clones were determined. We have previously studied the interaction of one of the clones, AS69, with α-syn.[7] Like ZAβ$_3$, AS69 stabilizes a β-hairpin conformer of its target and consequently inhibits its α-syn aggregation and toxicity.

Here we chose four additional clones from the selection against α-syn(1–108), that is, AS9, AS10, AS34, and AS60, which have between one and four of the most frequent amino acid exchanges (Figure 1C and D) for affinity determination towards α-syn and Aβ (Figure 2A and B, and Table 1). Isothermal titration calorimetry (ITC) demonstrated that one of these β-wrapins, AS10, exhibited nanomolar affinity for both α-syn and Aβ (Aβ(1–40) with an N-terminal methionine[8] was used in this study). Size-exclusion chromatography confirmed that AS10 bound monomers of α-syn and Aβ (Figure S1). In order to test if AS10 also exhibits affinity for further amyloidogenic proteins, a potential interaction with IAPP was investigated. To avoid problems caused by precipitation of the highly aggregation-prone IAPP during the ITC experiment, the affinity was determined by surface plasmon resonance (SPR) in this case. Monomeric, N-terminally biotinylated IAPP was immobilized on a streptavidin SA chip. The association of AS10 was monitored for 90 s, followed by 600 s dissociation time (Figure 2C). The SPR data could be fit to a two-state conformational change model to yield a K_d value of 910 nM.

Table 1. Affinities of β-wrapins and ZAβ$_3$ for α-synuclein and Aβ determined by ITC.

β-Wrapin	Exchange in ZAβ$_3$ at position					K_d [nM]	
	7	13	17	31	34	α-syn	Aβ
ZAβ$_3$[a]	–	–	–	–	–	n.d.[b]	20
AS9	–	–	–	F	–	2500	500
AS10	–	–	–	F	V	380	150
AS34	–	–	–	F	I	1200	190
AS60	T	D	F	F	I	200	n.d.[b]
AS69[a]	–	D	F	F	V	240	5000

[a] Affinities for ZAβ$_3$ and AS69 reported in Mirecka et al.[7] [b] n.d. = not detected.

We performed ^{1}H,^{15}N HSQC NMR spectroscopy on ^{15}N-labeled AS10 ([U-^{15}N]-AS10) to investigate its binding to Aβ, α-syn, and IAPP. In the presence of the amyloidogenic target proteins, the resonance dispersion greatly increased as a consequence of coupled folding and binding, and four amide proton resonances appeared in the glycine region (stemming from Gly13 and Gly14 in the two AS10 subunits) as well as amide proton resonances in the downfield region of the spectrum with shift values typical for β-sheet conformation (Figures 2D and S2). This has been observed before for the interaction of ZAβ$_3$ with Aβ[5b] (Figure 2D) and for the interaction of β-wrapin AS69 with α-syn.[7] These findings indicate that all three amyloidogenic targets adopt a β-hairpin conformation in complex with AS10, analogous to the interactions of Aβ and α-syn with ZAβ$_3$ and AS69, respectively.

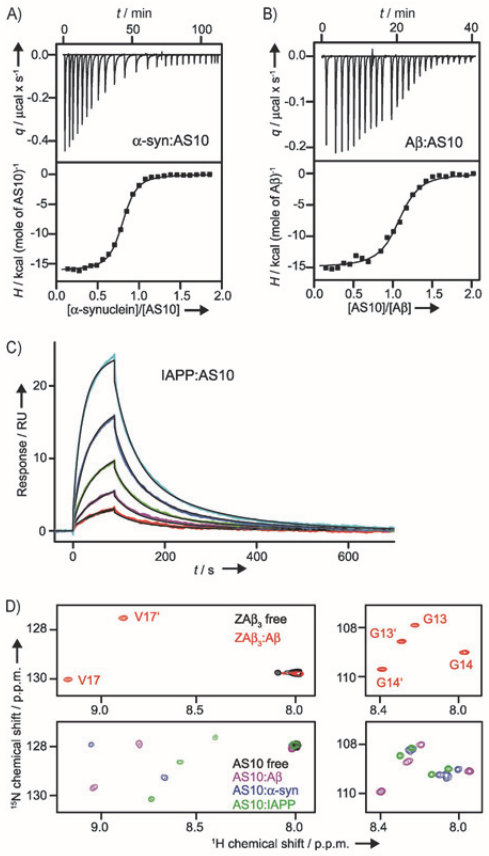

Figure 2. Sub-micromolar binding of AS10 to three different amyloidogenic targets. The K_d values of AS10 for A) α-syn and B) Aβ were 380 and 150 nM, respectively, as determined by ITC. C) SPR analysis of binding of 2 μM (——), 1 μM (——), 500 nM (——), 250 nM (——), and 125 nM (——) AS10 to IAPP according to a two-state conformational change model gave a K_d of 910 nM, with association and dissociation rate constants of $k_{a1} = 1.44 \times 10^4\ M^{-1}\ s^{-1}$, $k_{d1} = 1.94 \times 10^{-2}\ s^{-1}$, $k_{a2} = 3.38 \times 10^{-3}\ s^{-1}$, and $k_{d2} = 7.00 \times 10^{-3}\ s^{-1}$. D) Downfield (left) and glycine (right) regions of the (^{1}H,^{15}N) HSQC NMR spectra of [U-^{15}N]-AS10 in the absence or presence of [NA]-Aβ, [NA]-α-syn, or [NA]-IAPP (bottom), compared to the corresponding spectra of [U-^{15}N]-ZAβ$_3$ in the absence or presence of [NA]-Aβ[5b] (top). Assignment to the two ZAβ$_3$ subunits is indicated by presence or absence of prime symbols.

AS10 has two amino acid substitutions compared to ZAβ$_3$, namely Ile31Phe and Leu34Val (Figure 1C). These were the two most frequent amino acid exchanges in the selected binders to α-syn, occurring in 100 or 30%, respectively, of the 90 sequenced clones (Figure 1D), thus indicating a critical role for these exchanges for the β-wrapin–α-syn interaction. According to high-resolution structures of ZAβ$_3$ bound to Aβ[5b] and of

ChemPubSoc Europe

CHEMBIOCHEM Communications

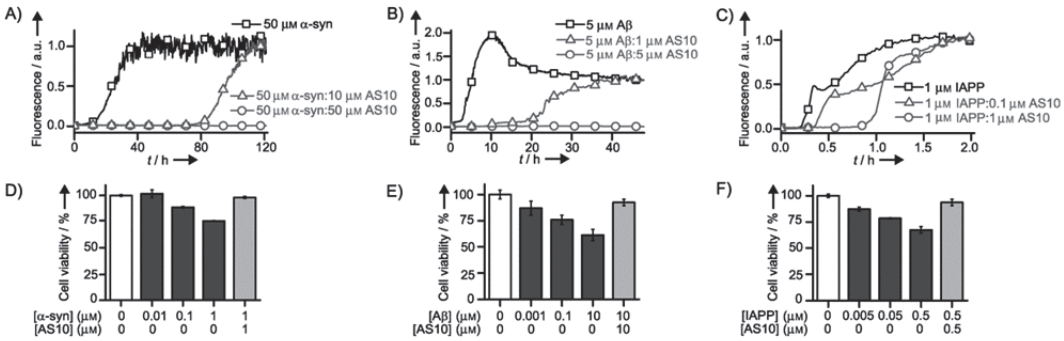

Figure 3. AS10 inhibits amyloid formation and toxicity of α-syn (left), Aβ (center), and IAPP (right). Top: Amyloid formation was followed by thioflavin T fluorescence. Bottom: Toxicity to SH-SY5Y cells was assessed by an MTT assay, applying protein solutions aged in the absence (dark gray bars) and presence (light gray bars) of AS10; white bars: control.

AS69 bound to α-syn,[7] these residues are located at the interface between the homodimer subunits and the β-hairpins, which is evidently a critical region for the stability of the complexes (Figure 1 A and B).

The effect of AS10 on amyloid formation was studied by thioflavin T fluorescence (Figure 3 A–C). AS10 inhibited the aggregation of Aβ, α-syn, and IAPP. Substoichiometric concentrations of the β-wrapin were sufficient to achieve a significant delay in amyloid formation. The effect of AS10 on the toxicity of the three amyloidogenic proteins was investigated in SH-SY5Y neuroblastoma cells (Figure 3 D–F). Fibrillar samples of aged Aβ, α-syn, or IAPP caused concentration-dependent decreases in cell viability. Addition of AS10 at the beginning of the ageing reactions rescued the cell viability.

We tested for potential interactions of AS10 with further amyloidogenic proteins by $^{1}H,^{15}N$ HSQC NMR spectroscopy, employing the four-repeat-domain tau protein construct K18K280/AA[9] and the Y145Stop variant of human prion protein (huPrP(23–144)).[10] Addition of AS10 to K18K280/AA or to huPrP(23-144) did not affect the NMR spectra, thus demonstrating the absence of binding (Figure S3).

This study establishes that the monomers of a subset of the disease-related amyloidogenic proteins can be bound with sub-micromolar affinity by a single engineered binding protein. Upon binding, the amyloidogenic proteins form β-hairpin motifs. In the case of Aβ and α-syn, the β-hairpins were shown to contain sequence regions that are critical for amyloid formation, namely Aβ(17–36)[5b] and α-syn(37–54).[7] These regions are enriched in hydrophobic amino acids with β-sheet propensity and, furthermore, they contain aromatic amino acids, these are features that might prime them for β-hairpin formation and for interaction with the β-wrapin scaffold. Several computer simulations revealed a propensity of amyloidogenic proteins to transiently populate β-hairpin conformations and implicated the β-hairpins in the formation of intermolecular contacts.[11] The data presented here provide experimental evidence for the preference for formation of β-hairpin motifs within at least a subset of amyloidogenic proteins.

Our results emphasize the adaptability of small, engineered binding proteins to intrinsically disordered, amyloidogenic target proteins. Binding is coupled to local folding of the targets. Coupled folding and binding is associated with an entropic cost for the disorder-to-order transition that frequently results in complexes of high specificity and relatively low affinity.[12] It is thus interesting to note that the β-wrapin AS10 binds three different amyloidogenic proteins with sub-micromolar affinity. This indicates that Aβ, α-syn, and IAPP share important properties that are not only reflected in the shared ability to form amyloid fibrils, but also in the common adoption of a β-hairpin conformation in complex with β-wrapins. This supports the view that by exploiting such commonalities general anti-amyloid therapeutic approaches could be contrived.

Experimental Section

Experimental details are given in the Supporting Information.

Acknowledgements

This work was supported by the Ministerium für Innovation, Wissenschaft und Forschung des Landes Nordrhein–Westfalen.

Keywords: amyloids · intrinsically disordered proteins · molecular recognition · protein aggregation · protein engineering

[1] T. P. Knowles, M. Vendruscolo, C. M. Dobson, *Nat. Rev. Mol. Cell Biol.* **2014**, *15*, 384–396.
[2] a) Y. Huang, L. Mucke, *Cell* **2012**, *148*, 1204–1222; b) H. A. Lashuel, C. R. Overk, A. Oueslati, E. Masliah, *Nat. Rev. Neurosci.* **2013**, *14*, 38–48; c) P. Westermark, A. Andersson, G. T. Westermark, *Physiol. Rev.* **2011**, *91*, 795–826.
[3] D. Eisenberg, M. Jucker, *Cell* **2012**, *148*, 1188–1203.
[4] R. Kayed, E. Head, J. L. Thompson, T. M. McIntire, S. C. Milton, C. W. Cotman, C. G. Glabe, *Science* **2003**, *300*, 486–489.
[5] a) C. Grönwall, A. Jonsson, S. Lindström, E. Gunneriusson, S. Ståhl, N. Herne, *J. Biotechnol.* **2007**, *128*, 162–183; b) W. Hoyer, C. Grönwall, A.

ChemPubSoc Europe

CHEMBIOCHEM Communications

Jonsson, S. Ståhl, T. Härd, *Proc. Natl. Acad. Sci. USA* **2008**, *105*, 5099–5104.

[6] a) T. Lührs, C. Ritter, M. Adrian, D. Riek-Loher, B. Bohrmann, H. Dobeli, D. Schubert, R. Riek, *Proc. Natl. Acad. Sci. USA* **2005**, *102*, 17342–17347; b) A. T. Petkova, W. M. Yau, R. Tycko, *Biochemistry* **2006**, *45*, 498–512.

[7] E. A. Mirecka, H. Shaykhalishahi, A. Gauhar, S. Akgül, J. Lecher, D. Willbold, M. Stoldt, W. Hoyer, *Angew. Chem. Int. Ed.* **2014**, *53*, 4227–4230; *Angew. Chem.* **2014**, *126*, 4311–4314.

[8] B. Macao, W. Hoyer, A. Sandberg, A. C. Brorsson, C. M. Dobson, T. Härd, *BMC Biotechnol.* **2008**, *8*, 82.

[9] C. S. Grüning, E. A. Mirecka, A. N. Klein, E. Mandelkow, D. Willbold, S. F. Marino, M. Stoldt, W. Hoyer, *J. Biol. Chem.* **2014**, *289*, 23209–23218.

[10] T. Kitamoto, R. Iizuka, J. Tateishi, *Biochem. Biophys. Res. Commun.* **1993**, *192*, 525–531.

[11] a) I. Daidone, F. Simona, D. Roccatano, R. A. Broglia, G. Tiana, G. Colombo, A. Di Nola, *Proteins Struct. Funct. Bioinf.* **2004**, *57*, 198–204; b) N. F. Dupuis, C. Wu, J. E. Shea, M. T. Bowers, *J. Am. Chem. Soc.* **2009**, *131*, 18283–18292; c) A. C. Gill, *PLoS One* **2014**, *9*, e87354; d) M. Grabenauer, C. Wu, P. Soto, J. E. Shea, M. T. Bowers, *J. Am. Chem. Soc.* **2010**, *132*, 532–539; e) S. Mitternacht, I. Staneva, T. Härd, A. Irbäck, *J. Mol. Biol.* **2011**, *410*, 357–367; f) A. S. Reddy, L. Wang, S. Singh, Y. L. Ling, L. Buchanan, M. T. Zanni, J. L. Skinner, J. J. de Pablo, *Biophys. J.* **2010**, *99*, 2208–2216; g) D. J. Rosenman, C. R. Connors, W. Chen, C. Wang, A. E. Garcia, *J. Mol. Biol.* **2013**, *425*, 3338–3359.

[12] H. J. Dyson, P. E. Wright, *Nat. Rev. Mol. Cell Biol.* **2005**, *6*, 197–208.

Received: September 20, 2014
Published online on December 30, 2014

CHEMBIOCHEM

Supporting Information

A β-Hairpin-Binding Protein for Three Different Disease-Related Amyloidogenic Proteins

Hamed Shaykhalishahi,[a] Ewa A. Mirecka,[a] Aziz Gauhar,[a] Clara S. R. Grüning,[a] Dieter Willbold,[a, c] Torleif Härd,[b] Matthias Stoldt,[a, c] and Wolfgang Hoyer*[a, c]

cbic_201402552_sm_miscellaneous_information.pdf

Supporting Information

Table of contents

Supporting Experimental Section

Phage Display. Library generation and selections were performed as described.[1] Briefly, a β-wrapin library based on a pComb3HSS vector backbone (provided by C. F. Barbas, The Scripps Research Institute, La Jolla, USA) containing the $ZA\beta_3$ gene was generated by error-prone PCR. The library consisted of 7×10^7 transformants. After four selection rounds against biotinylated α-syn(1-108), DNA from 90 single colonies was sequenced.

Protein Preparation. β-Wrapins,[1] $ZA\beta_3$,[1] α-syn,[1] Aβ(1-40) with an N-terminal methionine,[2] and tau K18ΔK280/AA[3] were prepared as previously described. Synthetic IAPP amidated at the C-terminus (Merck Millipore) was dissolved in 6 M guanidine hydrochloride (GdnHCl), 50 mM NaCl, 20 mM sodium phosphate, pH 6.0, and eluted at a flow rate of 0.5 ml/min from a Superdex 75 10/300 GL column (GE Healthcare) equilibrated in 20 mM sodium phosphate, pH 6.0.

huPrP(23-144) with an N-terminal 6xHis tag and a TEV-protease recognition site (ENLYFQG) was expressed from a pET-302 vector in *E. coli* BL21 DE3 and purified adopting previously published methods.[4] Briefly, following cell lysis, the pellet containing inclusion bodies was resuspended in 6 M guanidine hydrochloride, 100 mM sodium phosphate, 10 mM Tris-HCl, pH 8.0. After centrifugation, the protein was refolded in 100 mM sodium phosphate, 10 mM Tris-HCl, pH 8.0, and purified by elution from a Ni-NTA (His-Select, Sigma) gravity-flow chromatography column with 300 mM imidazole in the same buffer. The protein was digested with TEV-protease (20 µg per mg of protein) over night and purified using reverse phase high-pressure liquid chromatography (RP-HPLC) on a Zorbax 300SB-C3 column employing a gradient of 10-80 % (vol/vol) acetonitrile in water containing 0.1% (vol/vol) TFA for 15 min at a flow rate of 4 ml/min and at 80 °C, followed by lyophilization.

ITC. ITC was performed in 20 mM sodium phosphate, 50 mM NaCl, pH 7.4, at 30 °C on a Microcal iTC200 calorimeter (GE Healthcare). Affinities to α-syn were determined with β-wrapins/ZAβ$_3$ as titrant in the cell at a concentration of ~60 μM, and α-syn at approximately 10-fold higher concentration as titrant in the syringe. Affinities to Aβ were obtained with Aβ as titrant in the cell at a concentration of ~10 μM, and β-wrapins/ZAβ$_3$ at approximately 10-fold higher concentration as titrant in the syringe. Heats of post-saturation injections were averaged and subtracted from each injection to correct for heats of dilution and mixing. Dissociation constants were obtained from a nonlinear least-squares fit to a 1:1 binding model using MicroCal Origin.

SPR. Synthetic IAPP, N-terminally modified with biotin and an aminohexanoyl spacer and amidated at the C-terminus (Bachem), was dissolved in 20 mM sodium acetate, 50 mM NaCl, pH 4.0, and immobilized on a series S sensor chip SA (GE Healthcare) to ~1300 response units (RU) on a BIAcore T200 (GE Healthcare). The running buffer was 10 mM HEPES, pH 7.4, 150 mM NaCl, 3 mM EDTA, and 0.005% (v/v) Tween 20 surfactant. Measurements were performed at a flow rate of 30 μl/min and 25 °C. The data were fitted using a two-state 1:1 binding reaction model, consisting of an initial complex formation step with association rate constant k_{a1} and dissociation rate constant k_{d1} and a subsequent conformational change in the complex with forward and reverse rate constants k_{a2} and k_{d2}. The overall equilibrium dissociation constant K_d was calculated using the equation: $K_d=k_{d1}*k_{d2}/(k_{a1}(k_{d2}+k_{a2}))$. The signals of an uncoated reference cell and the signals generated by injection of running buffer were subtracted from the sensorgrams.

NMR Spectroscopy. NMR spectra were acquired on a 900 MHz VNMRS spectrometer (Varian) equipped with a cryogenically cooled Z-axis pulse-field-gradient triple resonance probe. The temperature was 25 °C except for the tau K18ΔK280/AA samples which were analyzed at 5 °C. The [*NA*]-component was added in slight excess relative to the [*U*-^{15}N]-component. The buffers were: 20 mM sodium phosphate, 50 mM NaCl, pH 7.4 (Aβ, α-syn, and IAPP samples); 20 mM sodium phosphate, 50 mM NaCl, pH 7.0 (tau K18ΔK280/AA samples); 15 mM sodium phosphate, 50 mM NaCl, pH 5.8 (huPrP(23-144) samples). NMR data were processed using NMRPipe[5] and analyzed with CcpNmr.[6]

Amyloid Formation. Fibrillation was performed in round-bottom 96-well black plate (Nunc) in an Infinite M1000 plate reader (Tecan). α-Syn fibrillation was done at 37 °C in 20 mM NaPi buffer, 50 mM NaCl, pH 6.0, under orbital shaking with 1 glass bead per microplate well. Aβ fibrillation was done at 37 °C in 20 mM NaPi buffer, 50 mM NaCl, pH 7.4, under orbital shaking with 1 glass bead per microplate well. IAPP fibrillation was done at 30 °C in 20 mM NaPi buffer, 50 mM NaCl, pH 6.0, under quiescent conditions. Amyloid formation was followed by Thioflavin T fluorescence at 480 nm

Toxicity Assay. The viability of SH-SY5Y neuroblastoma cells was assessed with an MTT assay (Cell Proliferation Kit I, Roche Diagnostics) as described before.[1] Protein samples were aged under amyloid formation conditions as described in the section above for 44 h (Aβ), 24 h (α-syn), or 30 min (IAPP) at a protein concentration of 50 μM (Aβ), 100 μM (α-syn), or 50 μM (IAPP), respectively, and diluted into the cell culture medium to the final concentrations given in Figure 3 D-F.

Size Exclusion Chromatography. Size exclusion chromatography was performed at 25°C by injecting 200 μl of 60 μM protein solutions in 20 mM NaPi, 50 mM NaCl, pH 7.4, onto a Superdex 10/300 column connected to an Äkta Purifier System (GE Healthcare). Molecular weight calibration was achieved with conalbumin, ovalbumin, carbonic anhydrase, ribonuclease A, and aprotinin as globular protein standards.

Supporting Figures

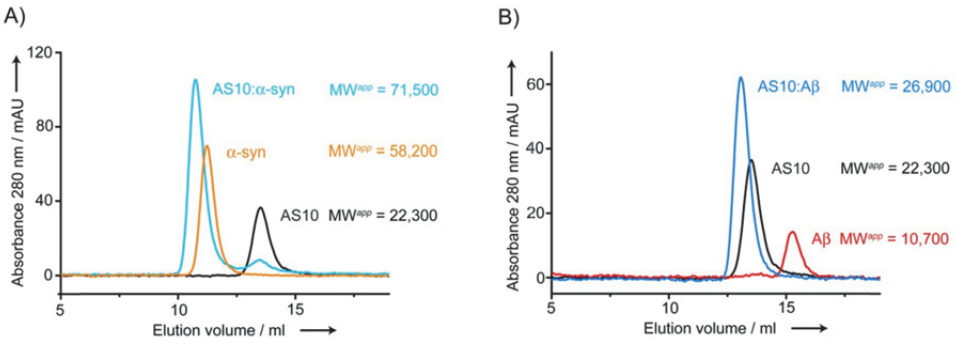

Figure S1. AS10 binds monomers of α-syn and Aβ. Size exclusion chromatography of the AS10:α-syn (A) and AS10:Aβ (B) complexes and their free components on a Superdex 75 10/300 column at a protein concentration of 60 μM. The apparent molecular weight (MW) of all three proteins in their free states is higher than their actual MW (MW(AS10) = 15,100; MW (α-syn) = 14,500; MW (Met-$Aβ_{1-40}$) = 4,500) as a consequence of their (partially) disordered character.[7] The apparent MW of the complexes is lower than the sum of the apparent MWs of the components, demonstrating that (i) AS10 binds monomers of the amyloidogenic proteins and (ii) compaction occurs upon complex formation due to partial folding coupled to binding. Monomer binding is in agreement with the 1:1 stoichiometry observed by ITC (Figure 2 A and B) and with the similarity of the NMR spectra of bound AS10 to those of $ZAβ_3$ (Figure 2 D and Figure S2) and AS69[1] in their complexes with monomeric Aβ or α-syn, respectively.

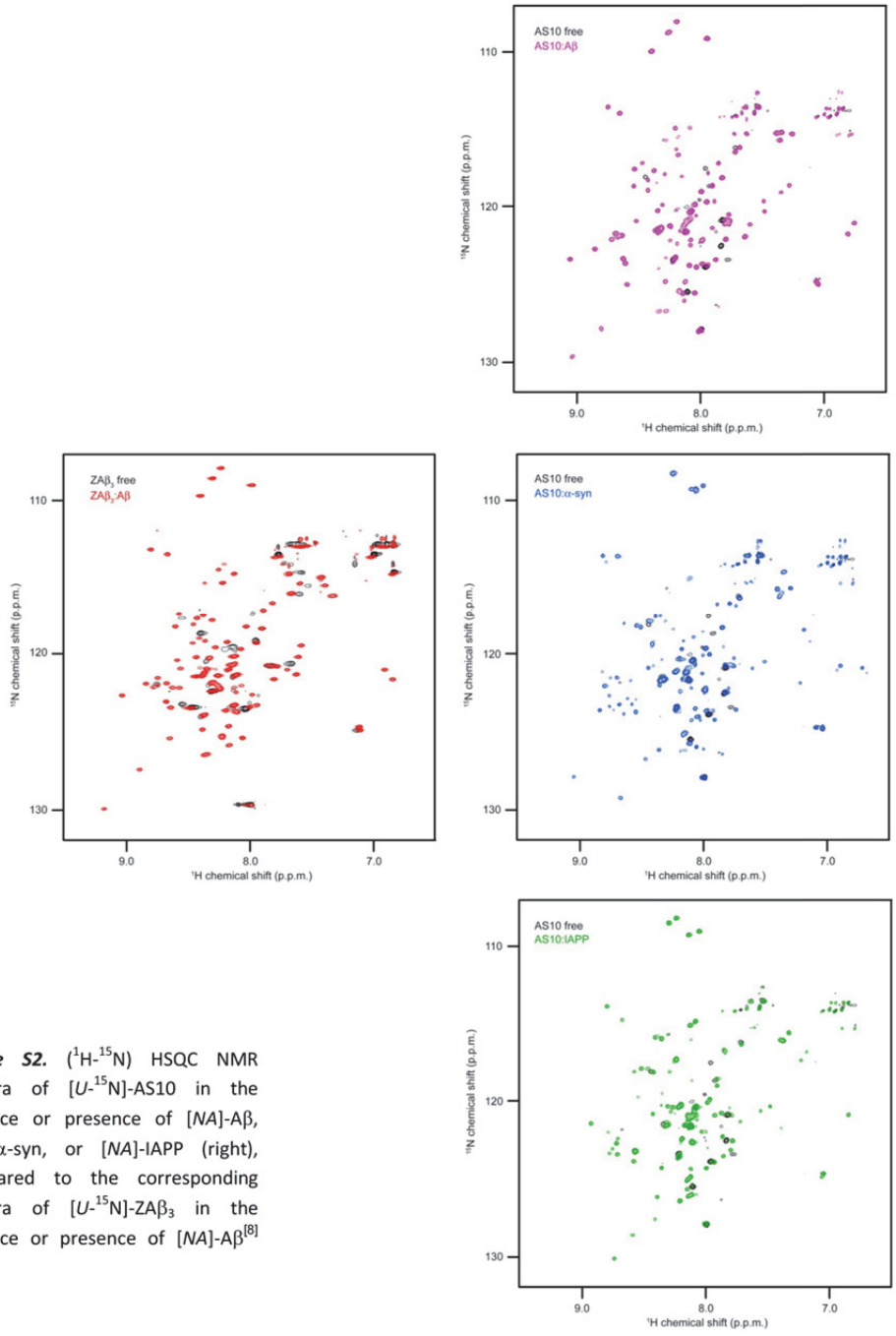

Figure S2. (^{1}H-^{15}N) HSQC NMR spectra of [*U*-^{15}N]-AS10 in the absence or presence of [*NA*]-Aβ, [*NA*]-α-syn, or [*NA*]-IAPP (right), compared to the corresponding spectra of [*U*-^{15}N]-ZAβ$_3$ in the absence or presence of [*NA*]-Aβ[8] (left).

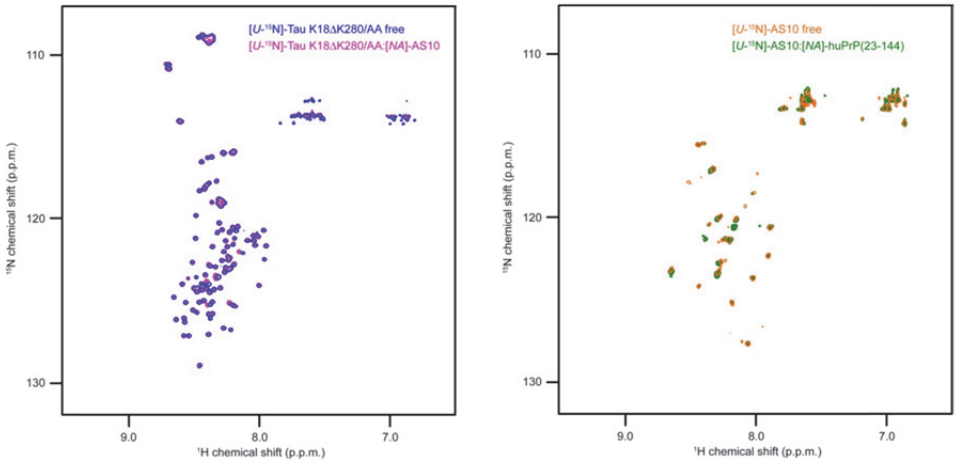

Figure S3. Left, (^{1}H-^{15}N) HSQC NMR spectra of [*U*-^{15}N]-Tau K18ΔK280/AA in the absence or presence of [*NA*]-AS10. Buffer, 20 mM sodium phosphate, 50 mM NaCl, pH 7.0. Right, (^{1}H-^{15}N) HSQC NMR spectra of [*U*-^{15}N]-AS10 in the absence or presence of [*NA*]-huPrP(23-144). Buffer, 15 mM sodium phosphate, 50 mM NaCl, pH 5.8.

References

[1] E. A. Mirecka, H. Shaykhalishahi, A. Gauhar, S. Akgül, J. Lecher, D. Willbold, M. Stoldt, W. Hoyer, *Angew. Chem. Int. Ed. Engl.* **2014**, *53*, 4227-4230.

[2] B. Macao, W. Hoyer, A. Sandberg, A. C. Brorsson, C. M. Dobson, T. Härd, *BMC Biotechnol.* **2008**, *8*, 82.

[3] C. S. Grüning, E. A. Mirecka, A. N. Klein, E. Mandelkow, D. Willbold, S. F. Marino, M. Stoldt, W. Hoyer, *J. Biol. Chem.* **2014**, *289*, 23209-23218.

[4] a) R. A. Moore, C. Herzog, J. Errett, D. A. Kocisko, K. M. Arnold, S. F. Hayes, S. A. Priola, *Protein Sci.* **2006**, *15*, 609-619; b) R. Zahn, C. von Schroetter, K. Wüthrich, *FEBS Lett.* **1997**, *417*, 400-404.

[5] F. Delaglio, S. Grzesiek, G. W. Vuister, G. Zhu, J. Pfeifer, A. Bax, *J. Biomol. NMR* **1995**, *6*, 277-293.

[6] W. F. Vranken, W. Boucher, T. J. Stevens, R. H. Fogh, A. Pajon, M. Llinas, E. L. Ulrich, J. L. Markley, J. Ionides, E. D. Laue, *Proteins* **2005**, *59*, 687-696.

[7] a) B. Fauvet, M. K. Mbefo, M. B. Fares, C. Desobry, S. Michael, M. T. Ardah, E. Tsika, P. Coune, M. Prudent, N. Lion, D. Eliezer, D. J. Moore, B. Schneider, P. Aebischer, O. M. El-Agnaf, E. Masliah, H. A. Lashuel, *J. Biol. Chem.* **2012**, *287*, 15345-15364; b) W. Hoyer, T. Härd, *J. Mol. Biol.* **2008**, *378*, 398-411.

[8] W. Hoyer, C. Grönwall, A. Jonsson, S. Ståhl, T. Härd, *Proc. Natl Acad. Sci. USA* **2008**, *105*, 5099-5104.

Chapter 4: Subunit linkages in an engineered binding protein to α-synuclein

Aziz Gauhar, Hamed Shaykhalishahi, Lothar Gremer, Ewa A. Mirecka, and Wolfgang Hoyer

Status: published in *PEDS (Protein Engineering, Design and Selection) 20 October 2014*

Impact factor: 2.53 (2014)

Own contribution to this work: 30%

Expression and purification of α-synuclein; expression and purification of AS69; kinetic study of disulfide bond formation in monomeric and head-to-tail AS69 constructs.

PEDS Advance Access published October 20, 2014

Protein Engineering, Design & Selection pp. 1–7, 2014
doi:10.1093/protein/gzu047

Impact of subunit linkages in an engineered homodimeric binding protein to α-synuclein

Aziz Gauhar[1], Hamed Shaykhalishahi[1], Lothar Gremer[1,2], Ewa A.Mirecka[1] and Wolfgang Hoyer[1,2,3]

[1]Institute of Physical Biology, Heinrich-Heine-Universität, Universitätsstraße 1, 40225 Düsseldorf, Germany and [2]Institute of Structural Biochemistry (ICS-6), Research Centre Jülich, 52425 Jülich, Germany

[3]To whom correspondence should be addressed. E-mail: wolfgang.hoyer@uni-duesseldorf.de

Received June 25, 2014; revised September 21, 2014; accepted September 24, 2014

Edited by Fabrizio Chiti

Aggregation of the protein α-synuclein (α-syn) has been implicated in Parkinson's disease and other neurodegenerative disorders, collectively referred to as synucleinopathies. The β-wrapin AS69 is a small engineered binding protein to α-syn that stabilizes a β-hairpin conformation of monomeric α-syn and inhibits α-syn aggregation at substoichiometric concentrations. AS69 is a homodimer whose subunits are linked via a disulfide bridge between their single cysteine residues, Cys-28. Here we show that expression of a functional dimer as a single polypeptide chain is achievable by head-to-tail linkage of AS69 subunits. Choice of a suitable linker is essential for construction of head-to-tail dimers that exhibit undiminished α-syn affinity compared with the solely disulfide-linked dimer. We characterize AS69-GS3, a head-to-tail dimer with a glycine-serine-rich linker, under oxidized and reduced conditions in order to evaluate the impact of the Cys28-disulfide bond on structure, stability and α-syn binding. Formation of the disulfide bond causes compaction of AS69-GS3, increases its thermostability, and is a prerequisite for high-affinity binding to α-syn. Comparison of AS69-GS3 and AS69 demonstrates that head-to-tail linkage promotes α-syn binding by affording accelerated disulfide bond formation.

Keywords: alternative scaffold/amyloid/disulfide bond/α-synuclein/β-wrapin

Introduction

Protein aggregates are a feature of several diseases, including many neurodegenerative diseases. For example, senile plaques consisting of the amyloid-β peptide (Aβ) are a neuropathological feature of Alzheimer's disease (Querfurth and LaFerla, 2010), while Lewy bodies containing α-synuclein (α-syn) as the main protein component are a characteristic of Parkinson's disease, dementia with Lewy bodies and other synucleinopathies (Lashuel *et al.*, 2013). The development of protein aggregation inhibitors constitutes a promising therapeutic approach (Härd and Lendel, 2012). Several classes of molecules have been explored to counteract the deleterious effects of fibrils and of the particularly toxic oligomeric assemblies of α-syn. Small molecules interfering with α-syn aggregation, e.g. various polyphenols, generally act by complex mechanisms, including direct binding to the intrinsically disordered protein, oxidation, covalent modification and stabilization of non-toxic α-syn oligomers (Li *et al.*, 2004; Masuda *et al.*, 2006; Ehrnhoefer *et al.*, 2008; Meng *et al.*, 2009; Zhou *et al.*, 2009). The propensity to self-associate into chemical aggregates is an essential property of aggregation-inhibiting compounds (Feng *et al.*, 2008; Lendel *et al.*, 2009; Lamberto *et al.*, 2011). Different hot spots for small molecule interactions were identified in the α-syn sequence, in the N-terminal region as well as in the central non-Aβ component (NAC) region and in the C-terminal region (Norris *et al.*, 2005; Herrera *et al.*, 2008; Lamberto *et al.*, 2009; Lendel *et al.*, 2009). Aggregation-inhibiting peptides with the potential to add to α-syn aggregates and to block any further aggregate growth were designed by modification of short amino acid stretches from the aggregation-prone NAC region, either by fusion of solubilizing amino acid residues or by N-methylation (El-Agnaf *et al.*, 2004; Madine *et al.*, 2008). Antibody-based approaches are particularly promising for the therapy of neurodegenerative diseases (Valera and Masliah, 2013). The predominantly intracellular localization of α-syn suggests the application of intrabodies, and anti-α-syn scFv antibodies indeed inhibit aggregation and toxicity upon transfection in cell culture models (Zhou *et al.*, 2004; Lynch *et al.*, 2008). However, recent evidence demonstrates that accumulation of α-syn oligomers in the plasma membrane and their propagation from cell-to-cell play crucial roles in the synucleinopathies (Lee *et al.*, 2014). Therefore, extracellular targeting of α-syn is a viable approach for immunotherapy of synucleinopathies. Both active and passive immunization against α-syn proved successful in mouse models (Masliah *et al.*, 2005, 2011). Passive immunization with the antibody 9E4 recognizing a C-terminal epitope resulted in reduced α-syn accumulation, reduced neurodegeneration, and reduced motor deficits (Masliah *et al.*, 2011). α-Syn immunotherapy appears to be effective through a combination of mechanisms, including the binding of membrane-bound α-syn oligomers, followed by receptor-mediated endocytosis and degradation by autophagy, as well as the blocking of the propagation of misfolded α-syn (Valera and Masliah, 2013; Tran *et al.*, 2014). One active and one passive immunization study are currently tested clinically, i.e. the vaccine AFFITOPE PD01 (Schneeberger *et al.*, 2012) and PRX002, a humanized version of 9E4.

The Affibody molecule $ZA\beta_3$ is a potent inhibitor of Aβ aggregation, obtained by phage display of a scaffold derived from staphylococcal protein A (Grönwall *et al.*, 2007). The small size of $ZA\beta_3$ (two subunits of ~60 amino acids each) has facilitated the detailed analysis of its interaction with Aβ (Hoyer *et al.*, 2008; Hoyer and Härd, 2008). $ZA\beta_3$ wraps the aggregation-prone sequence stretches of Aβ by forming a hydrophobic tunnel upon coupled folding and binding. Bound Aβ adopts a β-hairpin conformation, with those sequence regions forming an intramolecular β-sheet that otherwise build the core of the intermolecular β-sheets in amyloid fibrils (Hoyer *et al.*, 2008). The amyloid-like conformation of $ZA\beta_3$-bound Aβ prompted us to exploit $ZA\beta_3$ as a scaffold for the generation

of binders to other amyloidogenic targets. We generated ZAβ$_3$-based phage display libraries from which ligands are selected that we term β-wrapins (β-wrap proteins), referring to the observation that ZAβ$_3$ wraps around its target which adopts a β-structure in the complex. AS69 is a β-wrapin selected to bind to α-syn, exhibiting an affinity of 240 nM (Mirecka *et al.*, 2014). In complex with AS69, α-syn forms a β-hairpin in the sequence region of amino acids 37–54, which contains most of the reported disease-related mutations (Fig. 1A) (Mirecka *et al.*, 2014). Concomitantly, α-syn aggregation is inhibited, with substantial increases in the lag time of aggregation even at low substoichiometric concentrations of AS69 (Mirecka *et al.*, 2014).

Like ZAβ$_3$, AS69 is a homodimer covalently linked by a disulfide bridge between the subunits' single cysteine residues, Cys-28 (Fig. 1A). The disulfide bond connects the helices α1 of both subunits and is located close to the interface with the β-hairpin of α-syn. In addition to the disulfide linkage, two

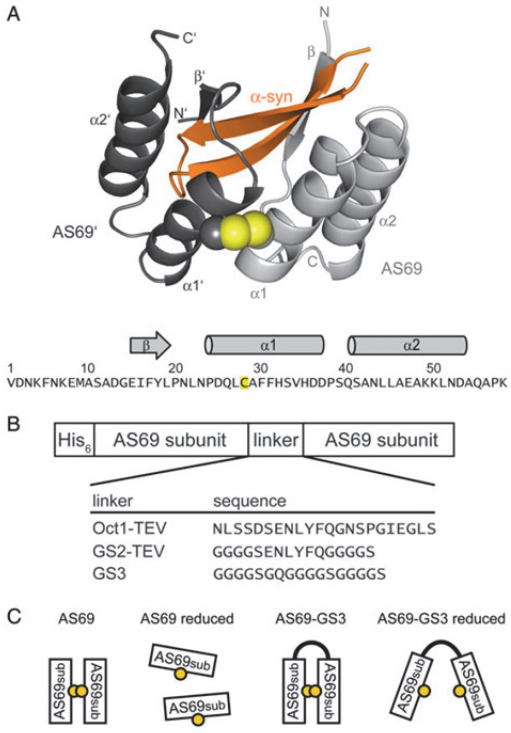

Fig. 1. Structure and subunit linkages of β-wrapin AS69. (A) Ribbon drawing of AS69 (gray) bound to α-syn (orange), pdb entry 4BXL. The two AS69 subunits are shown in light and dark gray and are labeled AS69 and AS69′, respectively. The folded core of the complex is shown, comprising residues 13–58 of both AS69 subunits and residues 35–56 of α-syn. The disordered N-termini of the AS69 subunits are not displayed. The Cys-28 disulfide bond is shown in yellow. The amino acid sequence of AS69 is displayed and the positions of α-helical and β-sheet secondary structures in α-syn-bound AS69 are indicated by cylinders and arrow, respectively. (B) Head-to-tail fusion constructs of two AS69 subunits with alternative linker sequences. (C) Scheme of the AS69 subunit linkage configurations investigated in this study. Boxes represent AS69 subunits, yellow circles represent Cys-28 residues, and thick lines indicate head-to-tail linkage.

β-wrapin subunits can be fused on the nucleic acid level to yield head-to-tail linked dimers. Head-to-tail linkage of ZAβ$_3$ subunits proved to be advantageous for treatment of a *Drosophila melanogaster* model of Alzheimer's disease (Luheshi *et al.*, 2010). Expression of a head-to-tail variant of ZAβ$_3$ inhibited the toxicity of wild-type Aβ42 and of the arctic mutant Aβ42(E22G) almost completely, while expression of individual ZAβ$_3$ subunits was only partially effective. In order to evaluate the effect of AS69 on α-syn pathology in cell culture and animal models of synucleinopathies, it would thus be desirable to likewise employ a single-chain AS69 dimer. Such a construct would also be a preferable starting point for combinatorial protein engineering for affinity maturation of AS69, since it would allow independent optimization of the subunits (Lindberg *et al.*, 2013).

Here we investigate the linker requirements for head-to-tail fusion of AS69 subunits. We generated AS69-GS3, a single-chain construct containing a glycine-serine-rich linker that exhibits the same affinity for α-syn as solely disulfide-linked AS69, and employed it to evaluate the impact of the Cys-28 disulfide bond on AS69 and its interaction with α-syn. Finally, we examined the effect of head-to-tail linkage on the kinetics of disulfide formation.

Materials and methods

Protein preparation

Genes encoding the head-to-tail constructs AS69-Oct1-TEV, AS69-GS2-TEV, as well as a direct head-to-tail fusion of two AS69 subunits, were obtained from Life Technologies. The gene encoding AS69-GS3 was generated from the AS69 gene by introduction of the linker sequence by PCR using specifically designed primers. Here, the first subunit was amplified employing the T7 promoter, 5′-TAA TAC GAC TCA CTA TAG GG, and the reverse primer 5′-A TAT GCC ACC CTG GCC ACT GCC ACC GCC ACC TTT CGG CGC CTG AGC, thus adding one copy of (G_4S) to the first subunit. Amplification of the second subunit along with addition of two copies of (G_4S) was achieved using the forward primer 5′-A TAT GGC CAG GGT GGC GGT GGC AGT GGT GGC GGT GGC AGT GTA GAT AAC AAA TTC, and T7 terminator, 5′-GCT AGT TAT TGC TCA GCG G. Genes were subjected to digestion using the appropriate restriction enzymes, i.e. EcoRI, AvrII and BglI (New England Biolabs), followed by ligation into the pET-302/NT-His expression vector and subsequent transformation into electrocompetent *Escherichia coli* JM109 cells. Sequence congruence of all constructs was verified by DNA sequencing (MWG Biotech). AS69 and the head-to-tail constructs were expressed from the pET-302/NT-His vector and purified as described previously (Mirecka *et al.*, 2014). In short, following expression and cell lysis, lysates were cleared by centrifugation and proceeded for purification on a HisTrap FF affinity column (GE Healthcare), followed by further purification on a HiLoad 16/60 Superdex 75 size exclusion chromatography column (GE Healthcare). Purity of the peak fractions was confirmed by application on 16.5% Tris-Tricine SDS–PAGE (Bio-Rad) and visualization by Coomassie Blue staining. Expression and purification of α-synuclein were performed as previously described (Mirecka *et al.*, 2014).

Isothermal titration calorimetry

Isothermal titration calorimetry (ITC) was performed on a Microcal iTC200 calorimeter (GE Healthcare) at 30°C. The

buffer was 20 mM sodium phosphate, 50 mM NaCl, pH 7.4. The titrant in the syringe was at ~10-fold higher concentration as the titrant in the cell, which was applied at a concentration in the range of 35–180 μM. For the experiment investigating the α-syn affinity of AS69-GS3 under reducing conditions, 5 mM DTT was added to the protein samples. The heat of post-saturation injections was averaged and subtracted from each injection to correct for heats of dilution and mixing. Data were processed using MicroCal Origin software provided with the calorimeter. Apparent dissociation constants K_d^{app} were obtained from a nonlinear least-squares fit to a 1 : 1 binding model. AS69 and its head-to-tail variants show partial thermal unfolding (see Fig. 6) at the temperature of the ITC experiment. For those constructs with experimentally determined thermal denaturation profiles, the K_d^{app} values were therefore corrected for the contribution from the coupled folding equilibrium (Dincbas-Renqvist *et al.*, 2004), yielding the K_d values given in Table I.

Aggregation assay

Aggregation of α-syn was monitored by thioflavin T (ThT) fluorescence (LeVine, 1999). Aggregation reactions contained 50 μM of α-syn and 40 μM ThT in 20 mM sodium phosphate, 50 mM NaCl, pH 6.0, 0.04% Na-azide, in a final volume of 150 μl. Aggregation was performed at 37°C with continuous orbital shaking (300 rpm) in a round-bottom 96-well black plate (Nunc) containing a 2 mm glass bead in each well. ThT fluorescence was excited at 440 nm and measured at 480 nm on an Infinite M1000 plate reader (Tecan). The signal of a buffer sample containing ThT was subtracted for background correction.

Circular dichroism spectroscopy

Far-UV circular dichroism (CD) spectra were measured on a JASCO J-815 spectropolarimeter in a 0.5 mm Quartz cuvette (Hellma) using protein samples at a concentration of 17.5 μM. The buffer was 20 mM sodium phosphate, 50 mM NaCl, pH 7.4. For measurements under reducing conditions, Tris-(2-carboxyethyl)-phosphine (TCEP) (Thermo Scientific) was added at a concentration of 10 mM. Melting curves were recorded at 222 nm with a heating rate of 1°C min $^{-1}$. Melting temperatures were derived from fits of the melting curves to a two-state unfolding model (Pace *et al.*, 1998).

Analytical size exclusion chromatography

Analytical size exclusion chromatography (SEC) was performed on a Superdex 75 10/300 GL column (GE Healthcare) connected to an ÄKTA Purifier system (GE Healthcare) at a temperature of 20°C and a flow rate of 0.5 ml min $^{-1}$. Proteins were detected by absorbance at 280 nm. Samples of 0.1 ml at a concentration of 180 μM (AS69) or 160 μM (AS69-GS3) were injected and eluted with 20 mM sodium phosphate, 50 mM NaCl, pH 7.4. For SEC experiments under reducing conditions, the protein samples were reduced by incubation with 10 mM TCEP for 1 h at 20°C, and 5 mM dithiothreitol (DTT) was added to the elution buffer. Molecular weight calibration was achieved with conalbumin, ovalbumin, carbonic anhydrase, ribonuclease A and aprotinin as globular protein standards.

Analytical RP-HPLC

Separation and quantification of the oxidized and reduced fractions of AS69 and AS69-GS3 were achieved by injecting 20 μl of protein solutions at a concentration of 115 μM (subunit concentration 230 μM) onto an analytical Zorbax 300SB-C8 RP-HPLC column (5 μm, 4.8 × 250 mm, Agilent) connected to an Agilent 1260 Infinity system at a column temperature of 80°C and a flow rate of 1 ml/min. The analysis was performed using a gradient of 30–36% (vol/vol) acetonitrile, 0.1% (vol/vol) TFA, in water within 20 min, followed by an isocratic step at 36% (vol/vol) acetonitrile, 0.1% (vol/vol) TFA, in water for 3 min. Ultra-violet absorption at 214 nm was used for protein detection and relative quantification of the oxidized and reduced fractions of AS69 and AS69-GS3. Reversed phase-high performance liquid chromatography (RP-HPLC) of AS69 and AS69-GS3 in the absence and presence of 10 mM TCEP was performed to determine the elution volumes of the oxidized and reduced proteins. To follow the kinetics of disulfide bond formation, AS69 and AS69-GS3 were reduced by incubation with 10 mM TCEP for 30 min at 25°C. TCEP was removed by size exclusion chromatography on Sephadex G-25 (two HiTrap Desalting 5 ml columns (GE Healthcare) connected in series to an ÄKTA Purifier system) using 20 mM sodium phosphate, 50 mM NaCl, pH 7.4, as buffer system at a flow rate of 1.5 ml min $^{-1}$. Protein containing fractions were combined and immediately used for analysis of reoxidation kinetics ($t = 0$ min). The reoxidation reaction was performed by incubation at 25°C in closed reaction tubes without agitation. Aliquots were withdrawn at different time points and analyzed for the amount of oxidized and reduced states by RP-HPLC as described above.

Kinetics of disulfide bond formation

The kinetic data of reoxidation of AS69-GS3 were fitted as a single exponential in compliance with an intramolecular reaction, yielding the first-order rate constant $k_{AS69\text{-}GS3}$. AS69 reoxidation involves dimerization and was fitted to the dimerization rate law, providing the second-order rate constant k_{AS69}:

$$\frac{1}{[AS69_{red}]_t} = k_{AS69}t + \frac{1}{[AS69_{red}]_{t-0}}$$

The effective concentration of subunits in the disulfide formation reaction of AS69-GS3 was calculated from the above rate constants as $2k_{AS69-GS3}/k_{AS69}$ according to Robinson and Sauer (1996).

Results

Linker sequence is critical to retain α-syn affinity in head-to-tail AS69 dimers

In the case of $ZA\beta_3$, direct fusion of two subunits without introduction of an extra linker sequence was feasible for retaining a functional dimer (Hoyer and Härd, 2008; Luheshi *et al.*, 2010; Lindberg *et al.*, 2013). The N-terminal ~13 residues of $ZA\beta_3$ remain disordered in the complex with Aβ and can therefore serve as a linker. Likewise, the N-terminus of α-syn-bound AS69 is disordered (Mirecka *et al.*, 2014). Direct head-to-tail linkage of AS69 subunits, however, resulted in a complete loss of α-syn binding according to ITC (Fig. 2A, Table I). Therefore, we introduced different linker sequences (Fig. 1B) and tested their ability

to restore the affinity for α-syn. Introduction of a 15-amino acid variant of the disordered, flexible linker of the Oct-1 POU domain (van Leeuwen *et al.*, 1997) with an additional TEV protease cleavage site resulted in the head-to-tail construct AS69-Oct1-TEV. Titration of AS69-Oct1-TEV with α-syn gave very weak, slowly decaying binding heat indicative of very slow association kinetics, demonstrating that the head-to-tail linkage interferes with binding (data not shown). Glycine-serine-rich sequences such as $(Gly_4\text{-}Ser)_3$ are frequently used as flexible linkers, particularly to link antibody domains in a single-chain Fv format (Huston *et al.*, 1988). We tested two glycine-serine-rich linkers, with and without an additional TEV protease cleavage site. In both constructs, AS69-GS2-TEV and AS69-GS3, the α-syn affinity of the solely disulfide-linked AS69 was recovered (Fig. 2B, Table I).

To test whether the head-to-tail linkage of AS69 interferes with its aggregation-inhibitory action, α-syn aggregation was followed in the presence and absence of AS69-GS3 (Fig. 3). The increased fluorescence of the dye ThT upon binding to the amyloid cross-β structure was used as an indicator of α-syn aggregation (LeVine, 1999). Stoichiometric amounts of AS69-GS3 completely inhibited α-syn aggregation, while substoichiometric amounts led to significant increases in the aggregation lag-time (Fig. 3), matching the data previously obtained for AS69 (Mirecka *et al.*, 2014).

The Cys-28 disulfide causes compaction and increased thermostability of AS69-GS3 and is essential for α-syn binding

We studied the properties of AS69 and AS69-GS3 before and after reduction of the disulfide bond, in order to evaluate the impact of the head-to-tail and disulfide linkages on structure, stability and α-syn binding of AS69. The investigated AS69 configurations are schematically depicted in Fig. 1C. High-affinity binding of α-syn required the presence of the Cys-28 disulfide linkage, which is evidenced by an ~1000-fold lower affinity of AS69-GS3 as a consequence of disulfide bond cleavage upon reduction (Table I).

The secondary structure contents of AS69 and AS69-GS3 in their oxidized and reduced states were analyzed by CD spectroscopy (Fig. 4). The CD spectra of AS69 and AS69-GS3 show minima at 208 and 222 nm, in agreement with largely α-helical conformation. Upon disulfide bond reduction, a slight decrease in the 222:208 nm ellipticity ratio is observed for both, AS69 and AS69-GS3, in line with partial unfolding. SEC was performed for comparison of the hydrodynamic

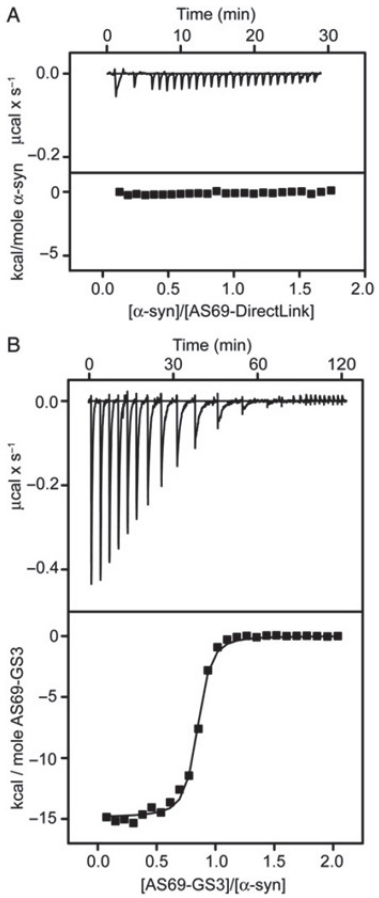

Fig. 2. Impact of the linker on the α-syn affinity of head-to-tail AS69 constructs determined by ITC. (A) No heat of binding were detected when 465 µM α-syn was titrated into a 54 µM solution of a head-to-tail construct in which two AS69 subunits are directly fused without an extra linker. (B) Titration of 716 µM AS69-GS3 into 75 µM α-syn, yielding an apparent affinity of $K_d^{app} = 250$ nM.

Table I. Affinity for α-syn of AS69 variants with different dimer linkages determined by ITC at 30°C

Head-to-tail linkage	Cys-28 disulfide	K_d^{app} (µM)	K_d (µM)[a]
None	Oxidized	0.24	0.18
Direct head-to-tail linkage	Oxidized	n.d.[b]	
Oct1-TEV	Oxidized	n.d.[c]	
GS2-TEV	Oxidized	0.14	
GS3	Oxidized	0.25	0.21
GS3	Reduced	280	200

[a]Corrected for coupled AS69 folding equilibrium.
[b]n.d., not detected.
[c]n.d., not determined, weak heat signal with a time profile indicative of very slow association kinetics.

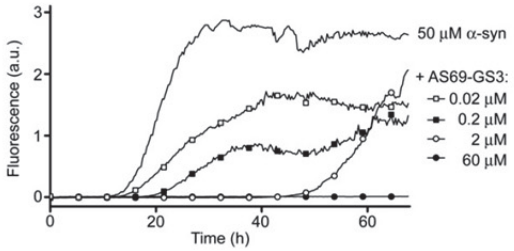

Fig. 3. Inhibition of α-syn aggregation by AS69-GS3. Kinetics of α-syn aggregation in the absence and presence of the indicated concentrations of AS69-GS3 monitored by ThT fluorescence.

volumes of the different β-wrapin configurations (Fig. 5). According to calibration with globular standard proteins, AS69 and AS69-GS3 eluted as proteins with apparent masses of 24 or 27 kDa, respectively, although their real molecular weight (MW) is ~15 kDa. The high apparent MW reflects the presence of disorder in the N-termini, as previously observed for ZAβ_3 (Hoyer and Härd, 2008). Upon disulfide bond reduction, elution of AS69 is strongly retarded, demonstrating the separation of the homodimer into its subunits. In contrast, AS69-GS3 elutes earlier from SEC after disulfide bond reduction, at an apparent MW of 32 kDa. The increased hydrodynamic volume of reduced AS69-GS3 suggests that the interface between the subunits' α1-helices is not fully established if the disulfide bond is not formed.

Thermal melting profiles were obtained by CD at 222 nm for AS69 and AS69-GS3 in their free and α-syn-bound states and were analyzed by a two-state unfolding model (Fig. 6). Disulfide bond reduction led to a decrease in the melting temperatures of AS69 and AS69-GS3 by 11 and 8K, respectively, revealing a strong impact of the Cys-28 disulfide linkage on thermostability. Comparison of melting profiles of AS69-GS3 and AS69 showed that the head-to-tail linkage also enhanced thermostability, with an increase in melting temperatures of ~5K (Fig. 6). An additional increase in the melting temperature of 13K is observed upon complex formation with α-syn (Fig. 6), which was dependent on formation of the Cys-28 disulfide bond, in agreement with the ITC data (Fig. 2, Table I).

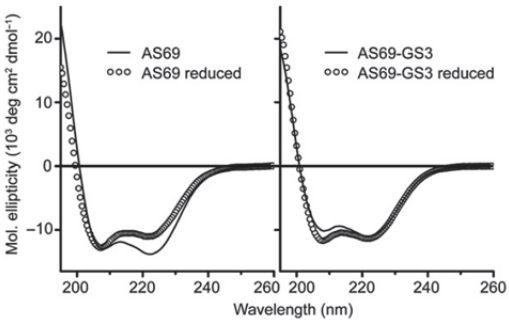

Fig. 4. Far-UV CD spectra of AS69 and AS69-GS3 at 20°C before and after reduction of the Cys-28 disulfide bond.

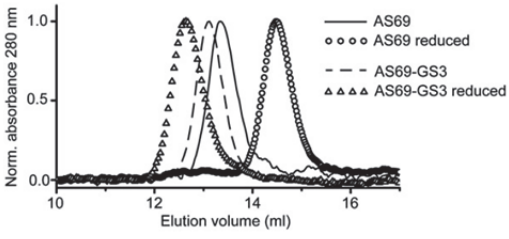

Fig. 5. SEC of AS69 and AS69-GS3 at 20°C before and after reduction of the Cys-28 disulfide bond.

Head-to-tail linkage affords accelerated disulfide bond formation

The kinetics of formation of the Cys-28 disulfide bond was monitored starting from reduced AS69 or reduced AS69-GS3, both at a subunit concentration of 230 μM (Fig. 7). The fractions of oxidized and reduced molecules were separated by HPLC and quantified by their absorbance (Fig. 7A). Disulfide bond formation in AS69-GS3 was significantly accelerated compared with AS69, even at the high protein concentrations used in this experiment, which foster the intermolecular dimerization reaction of AS69 (Fig. 7B). The first-order rate constant obtained for intramolecular disulfide bond formation in AS69-GS3 was $k_{AS69\text{-}GS3} = 1.56\ (\pm 0.07)\ 10^{-4}\ s^{-1}$. The second-order rate constant determined for intermolecular disulfide bond formation in AS69 was $k_{AS69} = 7.7\ (\pm 0.5)\ 10^{-2}\ M^{-1}\ s^{-1}$. The effective concentration of subunits in the disulfide formation reaction of AS69-GS3 can be calculated from the above rate constants (Robinson and Sauer, 1996) and is 4.1 ± 0.5 mM.

Discussion

In the present study, we investigated the requirements for subunit linkages of the β-wrapin AS69, an engineered binding protein to α-syn. While the head-to-tail linkage of AS69 subunits can generate functional single-chain binders to α-syn, the

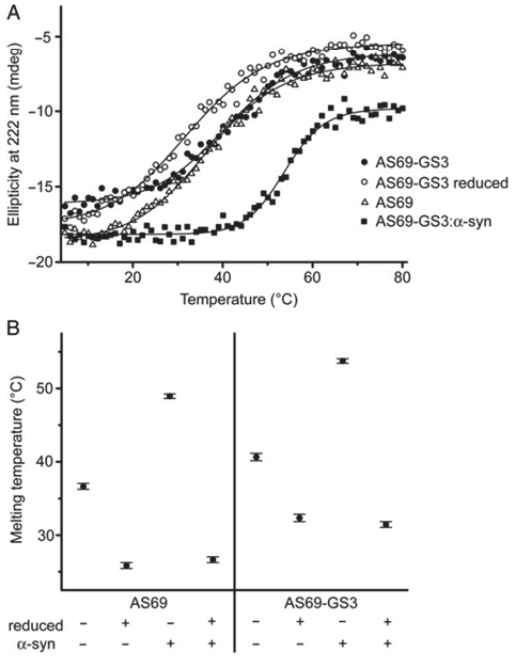

Fig. 6. Thermal stability of free and α-syn-bound AS69 and AS69-GS3 before and after reduction of the Cys-28 disulfide bond. (A) Thermal denaturation monitored by CD at 222 nm using a concentration of 17.5 μM of all proteins. Lines represent fits to a two-state transition model. (B) Melting temperatures for the different proteins and conditions obtained from the fits to the two-state transition model.

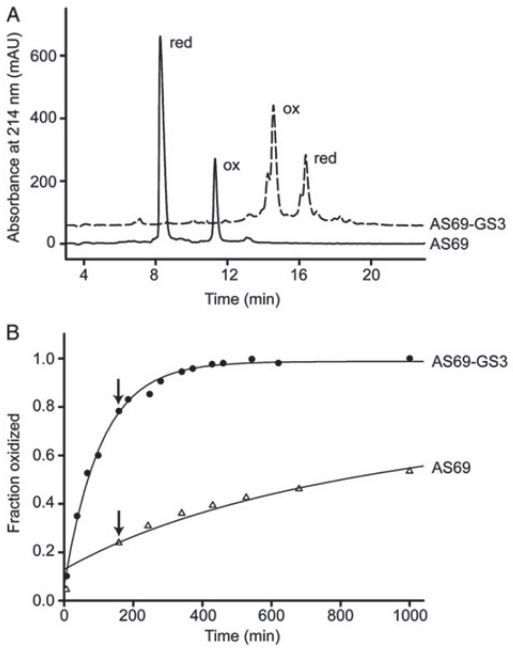

Fig. 7. Head-to-tail linkage leads to accelerated formation of the Cys-28 disulfide bond. The kinetics of disulfide bond formation was monitored starting from reduced AS69 and AS69-GS3, respectively. (A) The oxidized and reduced fractions were separated and quantified by HPLC, exemplified for the time point of 158 min, indicated by arrows in (B). (B) Time traces of disulfide bond formation. The lines represent fits to first-order reaction kinetics in the case of AS69-GS3 (intramolecular disulfide bond formation) and to second-order dimerization kinetics in the case of AS69 (intermolecular disulfide bond formation).

affinity is sensitive to the identity of the linker sequence. In contrast to $ZA\beta_3$ (Hoyer and Härd, 2008; Luheshi *et al.*, 2010; Lindberg *et al.*, 2013), direct fusion of two AS69 results in the loss of affinity for the target. On the other hand, head-to-tail constructs with glycine-serine linkers, commonly employed in the construction of single-chain antibody fragments (Huston *et al.*, 1988), recover the α-syn affinity of solely disulfide-linked AS69.

The presence of the Cys-28 disulfide bond is a prerequisite for high-affinity binding to α-syn. This can be explained by its potential to fix the contact between the subunits' α1-helices, which in turn establishes the interaction surface for α-syn binding (Fig. 1A). In line with this, Cys-28 disulfide bond formation causes compaction and increased stability of AS69 as demonstrated by SEC and thermal melting experiments. The critical importance of the Cys-28 disulfide bond also for the $ZA\beta_3$: Aβ interaction is highlighted by the conserved occurrence of Cys-28 in combinatorial engineering of Affibody molecules to Aβ (Grönwall *et al.*, 2007; Lindberg *et al.*, 2013).

Head-to-tail linkage via a glycine-serine linker in the construct AS69-GS3 leads to increased protein stability, similar to the observations reported before for a single-chain variant of the Arc repressor dimer of phage P22 (Robinson and Sauer, 1996, 1998). In addition, head-to-tail linkage promotes α-syn binding by entailing accelerated disulfide formation, providing an effective subunit concentration of 4.1 ± 0.5 mM for the disulfide formation reaction. This value is in good agreement with the effective subunit concentration in a single-chain variant of the Arc repressor dimer of phage P22, containing a 15-residue, glycine-rich linker (4.5 ± 1.8 mM, calculated from the bimolecular and unimolecular refolding reactions) (Robinson and Sauer, 1996).

AS69 exhibits a unique mode of interaction with α-syn (Mirecka *et al.*, 2014). It sequesters a sequence region that is critical for α-syn dysfunction, judging from the clustering of disease-related mutations. Monomeric α-syn is stabilized at low substoichiometric concentrations of AS69, indicating that AS69 interferes with the nucleation of aggregation. The β-wrapin thus offers a distinct therapeutic approach to the synucleinopathies. The small size of the β-wrapin might support its uptake into the brain and limits the costs of production. AS69-GS3 is an advantageous construct to evaluate the therapeutic potential of β-wrapin interference with α-syn assembly in cell culture and animal models of synucleinopathies. AS69-GS3 can moreover be employed for affinity maturation of β-wrapins to α-syn as it is compatible with the independent adaption of its subunits to the target.

Acknowledgements

This work was supported by the Ministerium für Innovation, Wissenschaft und Forschung des Landes Nordrhein-Westfalen.

References

Dincbas-Renqvist,V., Lendel,C., Dogan,J., Wahlberg,E. and Härd,T. (2004) *J. Am. Chem. Soc.*, **126**, 11220–11230.
Ehrnhoefer,D.E., Bieschke,J., Boeddrich,A., Herbst,M., Masino,L., Lurz,R., Engemann,S., Pastore,A. and Wanker,E.E. (2008) *Nat. Struct. Mol. Biol.*, **15**, 558–566.
El-Agnaf,O.M., Paleologou,K.E., Greer,B., *et al.* (2004) *FASEB J.*, **18**, 1315–1317.
Feng,B.Y., Toyama,B.H., Wille,H., Colby,D.W., Collins,S.R., May,B.C., Prusiner,S.B., Weissman,J. and Shoichet,B.K. (2008) *Nat. Chem. Biol.*, **4**, 197–199.
Grönwall,C., Jonsson,A., Lindström,S., Gunneriusson,E., Ståhl,S. and Herne,N. (2007) *J. Biotechnol.*, **128**, 162–183.
Härd,T. and Lendel,C. (2012) *J. Mol. Biol.*, **421**, 441–465.
Herrera,F.E., Chesi,A., Paleologou,K.E., Schmid,A., Munoz,A., Vendruscolo,M., Gustincich,S., Lashuel,H.A. and Carloni,P. (2008) *PLoS One*, **3**, e3394.
Hoyer,W. and Härd,T. (2008) *J. Mol. Biol.*, **378**, 398–411.
Hoyer,W., Grönwall,C., Jonsson,A., Ståhl,S. and Härd,T. (2008) *Proc. Natl Acad. Sci. USA*, **105**, 5099–5104.
Huston,J.S., Levinson,D., Mudgett-Hunter,M., *et al.* (1988) *Proc. Natl Acad. Sci. USA*, **85**, 5879–5883.
Lamberto,G.R., Binolfi,A., Orcellet,M.L., Bertoncini,C.W., Zweckstetter,M., Griesinger,C. and Fernandez,C.O. (2009) *Proc. Natl Acad. Sci. USA*, **106**, 21057–21062.
Lamberto,G.R., Torres-Monserrat,V., Bertoncini,C.W., Salvatella,X., Zweckstetter,M., Griesinger,C. and Fernandez,C.O. (2011) *J. Biol. Chem.*, **286**, 32036–32044.
Lashuel,H.A., Overk,C.R., Oueslati,A. and Masliah,E. (2013) *Nat. Rev. Neurosci.*, **14**, 38–48.
Lee,H.J., Bae,E.J. and Lee,S.J. (2014) *Nat. Rev. Neurol.*, **10**, 92–98.
Lendel,C., Bertoncini,C.W., Cremades,N., Waudby,C.A., Vendruscolo,M., Dobson,C.M., Schenk,D., Christodoulou,J. and Toth,G. (2009) *Biochemistry*, **48**, 8322–8334.
LeVine,H., III (1999) *Methods Enzymol.*, **309**, 274–284.
Li,J., Zhu,M., Rajamani,S., Uversky,V.N. and Fink,A.L. (2004) *Chem. Biol.*, **11**, 1513–1521.
Lindberg,H., Johansson,A., Härd,T., Ståhl,S. and Löfblom,J. (2013) *Biotechnol. J.*, **8**, 139–145.
Luheshi,L.M., Hoyer,W., de Barros,T.P., *et al.* (2010) *PLoS Biol.*, **8**, e1000334.

Lynch,S.M., Zhou,C. and Messer,A. (2008) *J. Mol. Biol.*, **377**, 136–147.
Madine,J., Doig,A.J. and Middleton,D.A. (2008) *J. Am. Chem. Soc.*, **130**, 7873–7881.
Masliah,E., Rockenstein,E., Adame,A., *et al.* (2005) *Neuron*, **46**, 857–868.
Masliah,E., Rockenstein,E., Mante,M., *et al.* (2011) *PLoS One*, **6**, e19338.
Masuda,M., Suzuki,N., Taniguchi,S., Oikawa,T., Nonaka,T., Iwatsubo,T., Hisanaga,S., Goedert,M. and Hasegawa,M. (2006) *Biochemistry*, **45**, 6085–6094.
Meng,X., Munishkina,L.A., Fink,A.L. and Uversky,V.N. (2009) *Biochemistry*, **48**, 8206–8224.
Mirecka,E.A., Shaykhalishahi,H., Gauhar,A., Akgül,S., Lecher,J., Willbold,D., Stoldt,M. and Hoyer,W. (2014) *Angew. Chem. Int. Ed.*, **53**, 4227–4230.
Norris,E.H., Giasson,B.I., Hodara,R., Xu,S., Trojanowski,J.Q., Ischiropoulos,H. and Lee,V.M. (2005) *J. Biol. Chem.*, **280**, 21212–21219.
Pace,C.N., Hebert,E.J., Shaw,K.L., *et al.* (1998) *J. Mol. Biol.*, **279**, 271–286.
Querfurth,H.W. and LaFerla,F.M. (2010) *N. Engl. J. Med.*, **362**, 329–344.
Robinson,C.R. and Sauer,R.T. (1996) *Biochemistry*, **35**, 13878–13884.
Robinson,C.R. and Sauer,R.T. (1998) *Proc. Natl Acad. Sci. USA*, **95**, 5929–5934.
Schneeberger,A., Mandler,M., Mattner,F. and Schmidt,W. (2012) *Parkinsonism Relat. Disord.*, **18**, S11–S13.
Tran,H.T., Chung,C.H., Iba,M., Zhang,B., Trojanowski,J.Q., Luk,K.C. and Lee,V.M. (2014) *Cell Rep.*, **7**, 2054–2065.
Valera,E. and Masliah,E. (2013) *Pharmacol. Ther.*, **138**, 311–322.
van Leeuwen,H.C., Strating,M.J., Rensen,M., de Laat,W. and van der Vliet,P.C. (1997) *EMBO J.*, **16**, 2043–2053.
Zhou,C., Emadi,S., Sierks,M.R. and Messer,A. (2004) *Mol. Ther.*, **10**, 1023–1031.
Zhou,W., Gallagher,A., Hong,D.P., Long,C., Fink,A.L. and Uversky,V.N. (2009) *J. Mol. Biol.*, **388**, 597–610.

Chapter 5: Contact between the β1 and β2 segments of α-synuclein entails inhibition of amyloid formation

Hamed Shaykhalishahi, Aziz Gauhar, Michael M. Wördehoff, Clara Grüning, Antonia N. Klein, Oliver Bannach, Eva Birkmann, Matthias Stoldt, Dieter Willbold, Torleif Härd, Wolfgang Hoyer

Status: published in *Angewandte Chemie* 26 June 2015

Impact factor: 11.2 (2014)

Own contribution to this work: 80%

Design, cloning, expression and purification of truncated and full length α-synCC construct; dot blotting, purification of truncated and wild-type α-synuclein; aggregation studies; MTT assays for Aβ and IAPP targets; preparation of protein samples for EM and NMR measurements, SEC analytical runs.

Angewandte International Edition Chemie

Protein Aggregation

International Edition: DOI: 10.1002/anie.201503018
German Edition: DOI: 10.1002/ange.201503018

Contact between the β1 and β2 Segments of α-Synuclein that Inhibits Amyloid Formation**

*Hamed Shaykhalishahi, Aziz Gauhar, Michael M. Wördehoff, Clara S. R. Grüning, Antonia N. Klein, Oliver Bannach, Matthias Stoldt, Dieter Willbold, Torleif Härd, and Wolfgang Hoyer**

Abstract: *Conversion of the intrinsically disordered protein α-synuclein (α-syn) into amyloid aggregates is a key process in Parkinson's disease. The sequence region 35–59 contains β-strand segments β1 and β2 of α-syn amyloid fibril models and most disease-related mutations. β1 and β2 frequently engage in transient interactions in monomeric α-syn. The consequences of β1–β2 contacts are evaluated by disulfide engineering, biophysical techniques, and cell viability assays. The double-cysteine mutant α-synCC, with a disulfide linking β1 and β2, is aggregation-incompetent and inhibits aggregation and toxicity of wild-type α-syn. We show that α-syn delays the aggregation of amyloid-β peptide and islet amyloid polypeptide involved in Alzheimer's disease and type 2 diabetes, an effect enhanced in the α-synCC mutant. Tertiary interactions in the β1–β2 region of α-syn interfere with the nucleation of amyloid formation, suggesting promotion of such interactions as a potential therapeutic approach.*

Protein aggregation and the toxicity of the resulting aggregates are fundamental to the pathogenesis of several human degenerative diseases. For example, aggregates consisting of α-synuclein (α-syn), the amyloid-β peptide (Aβ), or islet amyloid polypeptide (IAPP) are pathological features of Parkinson's disease (PD), Alzheimer's disease (AD), and type 2 diabetes, respectively.[1] α-Syn is a cytoplasmic protein of 140 amino acids, which predominantly exists as an intrinsically disordered protein (IDP) in the cell.[2] The conformational ensemble of the IDP contains a substantial fraction of conformers that exhibit long-range intramolecular interactions, which may promote or inhibit aggregation.[3]

According to paramagnetic relaxation-enhancement NMR spectroscopy and molecular simulations, contacts between the β1 and β2 sequence segments are among the most prevalent tertiary interactions in monomeric α-syn.[3c] The designations β1 and β2 refer to two of the approximately five β-strands of α-syn molecules in the amyloid fibril state.[4] The β1–β2 region comprises amino acids 35–59, lies outside of the hydrophobic, fibrillation-triggering NAC region,[5] and is the most N-terminal sequence region of α-syn incorporated in the fibril core of most of the fibril polymorphs described to date.[4,6] Several lines of evidence support a critical role of the β1–β2 region for α-syn aggregation and pathogenesis: First, it harbors most of the disease-related mutations, which alter the oligomerization and fibrillation propensity of α-syn.[7] Second, it is part of the core of α-syn oligomers, exhibiting particularly high resistance to H/D exchange.[8] Third, it regulates α-syn strain type and seeding efficiency.[9] Fourth, we have recently shown that sequestration of the β1–β2 region by the engineered binding protein β-wrapin AS69 potently inhibits α-syn aggregation.[10] In complex with AS69, α-syn locally adopts a β-hairpin conformation with β-strands comprising residues 37–43 and 48–54, reminiscent of the β1 and β2 strands of fibrillar α-syn.[10] The tertiary contacts between the β-strands of the AS69-bound β-hairpin agree well with the β1–β2 contact map of free monomeric α-syn.[3c]

Considering the importance of the β1–β2 region for α-syn aggregation, β1–β2 tertiary contacts might be crucial regulators of aggregation. Herein we investigate the effect of contact between β1 and β2 on amyloid formation. A stable contact was established by introduction of an intramolecular disulfide bond in the double cysteine mutant G41C/V48C, called α-synCC. The C41–C48 disulfide bond is compatible with the β-hairpin conformation of AS69-bound α-syn (Figure 1a). The two exchanges G41C and V48C are located in the β1 and β2 strand, respectively, diagonally opposite of each other. The Cα–Cα distance of G41 and V48 in the α-syn:AS69 complex is 6.1 Å, which is within the Cα–Cα distance range of cysteine disulfide bonds in X-ray structures (average: 5.6 Å).[11] The steric demands of two disulfide-bonded cysteine residues (sum of residue volumes 207 Å^3) are similar to those of the original glycine–valine combination (sum of residue volumes 203 Å^3).[12] To analyze the conformation of α-synCC, the (^{1}H–^{15}N) HSQC NMR spectrum of [U-^{15}N]-α-synCC was compared to that of [U-^{15}N]-wt α-syn (Figure 1b). The limited resonance dispersion of wt α-syn was retained for α-synCC, demonstrating that the engineered

[*] Dr. H. Shaykhalishahi, Dr. A. Gauhar, M. M. Wördehoff, Dr. C. S. R. Grüning, Dr. O. Bannach, Dr. M. Stoldt, Prof. Dr. D. Willbold, Dr. W. Hoyer
Institut für Physikalische Biologie
Heinrich-Heine-Universität Düsseldorf
40204 Düsseldorf (Germany)
E-mail: Wolfgang.Hoyer@uni-duesseldorf.de
A. N. Klein, Dr. O. Bannach, Dr. M. Stoldt, Prof. Dr. D. Willbold, Dr. W. Hoyer
Strukturbiochemie (ICS-6), Forschungszentrum Jülich
52425 Jülich (Germany)
Prof. Dr. T. Härd
Department of Chemistry and Biotechnology
Swedish University of Agricultural Sciences (SLU)
750 07 Uppsala (Sweden)

[**] This work was supported by the Ministerium für Innovation, Wissenschaft und Forschung des Landes Nordrhein-Westfalen.

Supporting information for this article is available on the WWW under http://dx.doi.org/10.1002/anie.201503018.

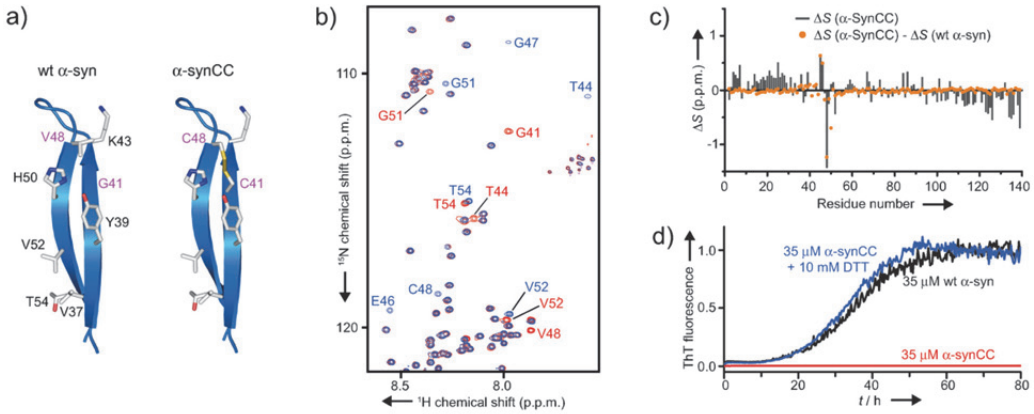

Figure 1. Protein engineering and characterization of α-synCC. a) Left: β-Hairpin conformation of the β1–β2 region of α-syn bound to β-wrapin AS69 (PDB: 4bxl). The side chains at the front face are shown as sticks. Right: Model of a β-hairpin conformation of α-synCC, in which residues 41 and 48 of wt α-syn have been exchanged to cysteines. b) Section of overlaid (^{1}H–^{15}N)-HSQC NMR spectra of [U-^{15}N]-wt α-syn (red) and [U-^{15}N]-α-synCC (blue) at 10°C. Assignments of peaks affected by the double cysteine exchange are indicated. c) Averaged Cα and C′ secondary chemical shifts of α-synCC and difference in secondary chemical shifts between α-synCC and wt α-syn. d) ThT time course of fibrillation of oxidized and reduced α-synCC compared to wt α-syn.

disulfide does not induce folding into a stable conformation. α-synCC showed insignificant secondary chemical shifts, further indicating that it is an IDP like wt α-syn (Figure 1c). Noticeable differences in chemical shifts of α-synCC and wt α-syn were only observed for the amino acid residues adjacent to the two mutation sites; however, secondary chemical shifts did not support formation of any stable secondary structure in this region (Figure 1c). Oxidized α-synCC did not form fibrils after prolonged incubation in a fibrillation assay monitored by thioflavin T (ThT) fluorescence (Figure 1d). Breakage of the β1–β2 disulfide bond with the reducing agent dithiothreitol (DTT), however, resulted in aggregation kinetics similar to those of wt α-syn (Figure 1d). Formation of the β1–β2 disulfide bond thus renders α-synCC non-fibrillogenic, indicating that β1–β2 contacts entail conformations belonging to the pool of autoinhibitory conformations.[3a] Size-exclusion chromatography (SEC) confirmed that oxidized α-synCC did not form stable oligomers upon incubation but remained monomeric (Supporting Information, Figure S1). This is in contrast to AβCC, a double cysteine mutant of Aβ engineered following an analogous strategy (Figure S2), which was previously shown to form stable, neurotoxic oligomers.[13] This difference might be a consequence of the lower hydrophobicity of the hairpin region of α-synCC compared to the hairpin region of AβCC, with GRAVY (grand average of hydropathy)[14] values of 0.48 for α-synCC(37–54) and 1.27 for AβCC(17–36).

α-synCC inhibited the aggregation of wt α-syn both at equivalent and at substoichiometric concentrations (Figure 2a). The inhibitory effect at substoichiometric ratios indicates that α-synCC interferes with nucleation and/or elongation of wt α-syn fibrils. The inhibitory effect is a consequence of the β1–β2 disulfide linkage as it was abolished by disulfide reduction by DTT (Figure 2a). To test if α-synCC inhibits elongation of wt α-syn fibrils, seeded fibrillation reactions of wt α-syn were performed in the absence and presence of α-synCC and monitored either in a fluorescence microplate reader (Figure S3) or by total internal reflection fluorescence microscopy (TIRFM) (Figure 2d). Ultrasonicated wt α-syn fibrils were used as seeds. Addition of α-synCC entailed a concentration-dependent inhibition of seeded wt α-syn aggregation (Figure S3). Wt α-syn fibril seeds were imaged by TIRFM as particles with several fibrillation sites, resulting in a fibril network after quiescent incubation with wt α-syn monomers (Figure 2d).[15] In contrast, fibril networks were not formed when α-synCC was incubated with wt α-syn fibril seeds, in agreement with the finding that α-synCC is non-fibrillogenic (Figure 2d). Incubation of wt α-syn monomers with wt α-syn fibril seeds did not lead to the formation of fibril networks when α-synCC was present (Figure 2d). The inhibitory effect of α-synCC on wt α-syn fibril elongation was dependent on the β1–β2 disulfide linkage as it was abrogated by disulfide reduction by DTT (Figure 2d). Thus, the seeded fibrillation experiments indicate that α-synCC interacts with fibril ends. Wt α-syn samples that were aged under aggregation-promoting conditions reduced the viability of human SH-SY5Y neuroblastoma cells, as assessed by an MTT (3-(4,5-dimethylthiazol-2-yl)-2,5-diphenyltetrazolium bromide) assay (Figure 2e). However, when ageing of wt α-syn was performed in the presence of α-synCC, the cell viability was rescued.

Different protein aggregation disorders, associated with amyloidogenic proteins of non-homologous sequences, frequently overlap clinically and pathologically, suggesting a mutual interference of the aggregation reactions of the involved proteins.[9,16] While Aβ plaques are often found in PD patients, α-syn Lewy bodies are found in most of the AD cases.[17] Similarly, IAPP oligomers and plaques were identified in the brains of diabetic AD patients.[18] We investigated potential heterotypic interactions of α-synCC with other

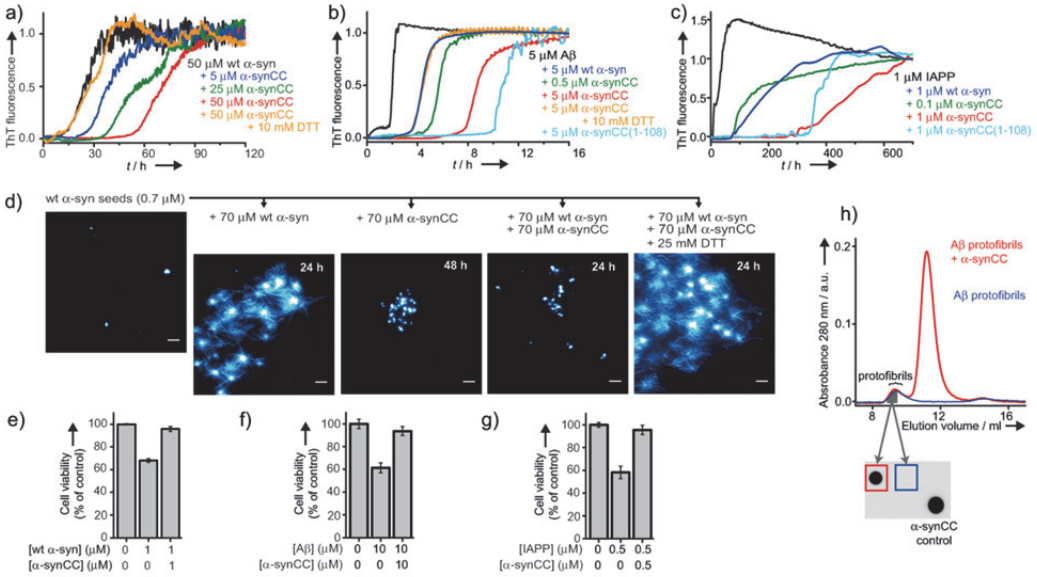

Figure 2. α-SynCC inhibits aggregation and toxicity of wt α-syn, Aβ and IAPP. a)–c) ThT time course of fibrillation of wt α-syn (a), Aβ (b), and IAPP (c) in the absence and presence of α-synCC. d) TIRF microscopy of fibrillation of α-synCC and wt α-syn in the presence of wt α-syn fibril seeds under quiescent condition. Scale bar: 5 μm. e)–g) MTT assays to evaluate the toxicity of wt α-syn (e), Aβ (f), and IAPP (g) aged in the absence and presence of α-synCC to SH-SY5Y neuroblastoma cells. The data are representative of experiments carried out in triplicate (mean ± s.d.), expressed as percentage relative to the untreated cells (control). h) α-SynCC interacts with Aβ protofibrils. SEC chromatograms of purified Aβ protofibril samples re-injected onto the column after 10 min incubation at room temperature in the absence (blue) or presence (red) of a twofold excess (calculated in monomer units) of α-synCC. Aβ protofibrils elute close to the void volume (ca. 8.5 mL), while the elution peak at circa 11.5 mL corresponds to α-synCC. Dot blot analysis of the protofibrils fractions using the anti-α-syn antibody 211 is shown below the chromatogram. Fresh α-synCC served as positive control. Aβ(1-40) (b,f) or Aβ(1-42) (h) with an N-terminal methionine[19] was used.

amyloidogenic proteins by testing its effects on the fibrillation of Aβ and IAPP. The effects of α-synCC were compared to those exerted by wt α-syn. Wt α-syn and α-synCC both inhibited fibrillation of Aβ and IAPP, with more potent inhibition exhibited by α-synCC (Figure 2b,c). The lag-time of fibrillation of 5 μM Aβ increased 2- and 4-fold upon addition of an equimolar amount of wt α-syn and α-synCC, respectively (Figure 2b). Reduction of the disulfide bond in α-synCC decreased the inhibitory effect of α-synCC to the level of wt α-syn, demonstrating that the β1–β2 disulfide linkage is responsible for the higher inhibitory potential of α-synCC (Figure 2b).The lag-time of fibrillation of a 1 μM solution of IAPP increased by 10- and 40-fold in the presence of an equimolar amount of wt α-syn and α-synCC, respectively (Figure 2c). A 1:10 ratio of α-synCC:Aβ or α-synCC:IAPP was sufficient to achieve a significant prolongation of the fibrillation lag time, supporting an impact of α-synCC on the nucleation and/or elongation of Aβ and IAPP fibrils (Figure 2b,c). A chaperone-like activity of α-syn was observed before in thermally induced and chemically induced protein aggregation assays.[20] The acidic C-terminal tail was critical for this activity by serving as a solubilizing domain. A C-terminally truncated variant of α-synCC, α-synCC(1-108), however, caused similar increases in the fibrillation lag times of Aβ and IAPP as full-length α-synCC (Figure 2b,c). β1–β2-mediated aggregation inhibition does therefore not depend on the acidic C-terminal of α-syn and must act through a different mechanism than the previously reported chaperone-like function. To complement the ThT fluorescence data, Aβ aggregation was analyzed by SEC and transmission electron microscopy (TEM), demonstrating that α-synCC inhibited the formation of oligomers and fibrils (Figure S4). Ageing of solutions of Aβ and IAPP under aggregation-promoting conditions resulted in cytotoxicity in an MTT assay on SH-SY5Y neuroblastoma cells (Figure 2f,g). However, when the cells were treated with Aβ and IAPP samples aged in the presence of α-synCC they displayed a viability similar to that of untreated cells (Figure 2f,g).

To identify the molecular species interacting with α-synCC, binding of α-synCC to monomers of wt α-syn, Aβ, or IAPP, and to Aβ protofibrils, metastable neurotoxic oligomers, was tested. Biotinylated monomers of the target proteins were coated on streptavidin SA sensor chips. No response indicative of binding was detected for any of the three target proteins when α-synCC was passed as analyte over the sensor surfaces (data not shown). Freshly prepared Aβ protofibrils were incubated for 10 min with or without α-synCC. The incubated samples were analyzed by reinjection onto the SEC column, isolation of the protofibril fraction, and dot blot using the anti-α-syn antibody 211 (Figure 2h). The Aβ protofibrils sample pre-incubated with α-synCC showed immunoreactivity, indicating binding of α-synCC to Aβ protofibrils.

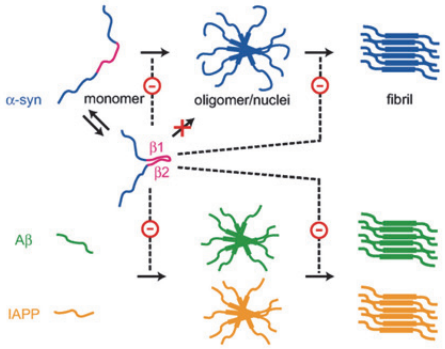

Figure 3. Representation of the inhibitory effect of tertiary contacts in the β1–β2 region of α-syn on the aggregation of amyloidogenic IDPs. Conformations of α-syn featuring β1–β2 contacts are incompetent to form oligomers and fibrils. Furthermore, they inhibit fibril nucleation and elongation of α-syn, Aβ, and IAPP.

The present study shows that α-synCC with established disulfide bond actively interferes with the aggregation of amyloidogenic proteins (Figure 3). How does the β1–β2 contact lead to inhibition of protein aggregation? Considering the amino acid sequence, formation of β1–β2 contacts is likely accompanied by population of conformers with clusters of hydrophobic and aromatic amino acids, including, for example, Tyr-39 and His-50. These conformers might not be compatible with the fibrillation reaction, but prone to interact with other species on the aggregation pathway that also exhibit hydrophobic patches, such as oligomeric nuclei and fibril ends, eventually precluding further assembly of these species.

This work supports the view that the β1–β2 region is an important regulatory element of α-syn aggregation. Tertiary interactions between β1 and β2 interfere with aggregation and steer the capacity of α-syn to engage in heterointeractions with other amyloidogenic IDPs. In the search for inhibitors of amyloid formation,[21] promotion of β1–β2 contacts therefore constitutes a potential approach.

Keywords: aggregation · intrinsically disordered proteins · protein engineering · protein folding · protein–protein interactions

How to cite: *Angew. Chem. Int. Ed.* **2015**, *54*, 8837–8840
Angew. Chem. **2015**, *127*, 8962–8966

[1] a) T. P. Knowles, M. Vendruscolo, C. M. Dobson, *Nat. Rev. Mol. Cell Biol.* **2014**, *15*, 384–396; b) M. G. Spillantini, M. L. Schmidt, V. M. Lee, J. Q. Trojanowski, R. Jakes, M. Goedert, *Nature* **1997**, *388*, 839–840.

[2] a) J. Burré, S. Vivona, J. Diao, M. Sharma, A. T. Brunger, T. C. Südhof, *Nature* **2013**, *498*, E4–6; b) B. Fauvet, M. K. Mbefo, M. B. Fares, C. Desobry, S. Michael, M. T. Ardah, E. Tsika, P. Coune, M. Prudent, N. Lion, et al., *J. Biol. Chem.* **2012**, *287*, 15345–15364.

[3] a) C. W. Bertoncini, Y. S. Jung, C. O. Fernandez, W. Hoyer, C. Griesinger, T. M. Jovin, M. Zweckstetter, *Proc. Natl. Acad. Sci. USA* **2005**, *102*, 1430–1435; b) M. M. Dedmon, K. Lindorff-Larsen, J. Christodoulou, M. Vendruscolo, C. M. Dobson, *J. Am. Chem. Soc.* **2005**, *127*, 476–477; c) S. Esteban-Martín, J. Silvestre-Ryan, C. W. Bertoncini, X. Salvatella, *Biophys. J.* **2013**, *105*, 1192–1198; d) J. C. Lee, R. Langen, P. A. Hummel, H. B. Gray, J. R. Winkler, *Proc. Natl. Acad. Sci. USA* **2004**, *101*, 16466–16471; e) A. Nath, M. Sammalkorpi, D. C. DeWitt, A. J. Trexler, S. Elbaum-Garfinkle, C. S. O'Hern, E. Rhoades, *Biophys. J.* **2012**, *103*, 1940–1949; f) O. Ullman, C. K. Fisher, C. M. Stultz, *J. Am. Chem. Soc.* **2011**, *133*, 19536–19546.

[4] M. Vilar, H. T. Chou, T. Luhrs, S. K. Maji, D. Riek-Loher, R. Verel, G. Manning, H. Stahlberg, R. Riek, *Proc. Natl. Acad. Sci. USA* **2008**, *105*, 8637–8642.

[5] E. A. Waxman, J. R. Mazzulli, B. I. Giasson, *Biochemistry* **2009**, *48*, 9427–9436.

[6] a) M. Chen, M. Margittai, J. Chen, R. Langen, *J. Biol. Chem.* **2007**, *282*, 24970–24979; b) H. Heise, W. Hoyer, S. Becker, O. C. Andronesi, D. Riedel, M. Baldus, *Proc. Natl. Acad. Sci. USA* **2005**, *102*, 15871–15876; c) G. Comellas, L. R. Lemkau, A. J. Nieuwkoop, K. D. Kloepper, D. T. Ladror, R. Ebisu, W. S. Woods, A. S. Lipton, J. M. George, C. M. Rienstra, *J. Mol. Biol.* **2011**, *411*, 881–895.

[7] D. Ghosh, S. Sahay, P. Ranjan, S. Salot, G. M. Mohite, P. K. Singh, S. Dwivedi, E. Carvalho, R. Banerjee, A. Kumar, et al., *Biochemistry* **2014**, *53*, 6419–6421.

[8] W. Paslawski, S. Mysling, K. Thomsen, T. J. Jorgensen, D. E. Otzen, *Angew. Chem. Int. Ed.* **2014**, *53*, 7560–7563; *Angew. Chem.* **2014**, *126*, 7690–7693.

[9] J. L. Guo, D. J. Covell, J. P. Daniels, M. Iba, A. Stieber, B. Zhang, D. M. Riddle, L. K. Kwong, Y. Xu, J. Q. Trojanowski, et al., *Cell* **2013**, *154*, 103–117.

[10] E. A. Mirecka, H. Shaykhalishahi, A. Gauhar, S. Akgül, J. Lecher, D. Willbold, M. Stoldt, W. Hoyer, *Angew. Chem. Int. Ed.* **2014**, *53*, 4227–4230; *Angew. Chem.* **2014**, *126*, 4311–4314.

[11] B. Schmidt, L. Ho, P. J. Hogg, *Biochemistry* **2006**, *45*, 7429–7433.

[12] Y. Harpaz, M. Gerstein, C. Chothia, *Structure* **1994**, *2*, 641–649.

[13] a) C. Lendel, M. Bjerring, A. Dubnovitsky, R. T. Kelly, A. Filippov, O. N. Antzutkin, N. C. Nielsen, T. Härd, *Angew. Chem. Int. Ed.* **2014**, *53*, 12756–12760; *Angew. Chem.* **2014**, *126*, 12970–12974; b) A. Sandberg, L. M. Luheshi, S. Sollvander, T. Pereira de Barros, B. Macao, T. P. Knowles, H. Biverstal, C. Lendel, F. Ekholm-Petterson, A. Dubnovitsky, et al., *Proc. Natl. Acad. Sci. USA* **2010**, *107*, 15595–15600.

[14] J. Kyte, R. F. Doolittle, *J. Mol. Biol.* **1982**, *157*, 105–132.

[15] M. M. Wördehoff, O. Bannach, H. Shaykhalishahi, A. Kulawik, S. Schiefer, D. Willbold, W. Hoyer, E. Birkmann, *J. Mol. Biol.* **2015**, *427*, 1428–1435.

[16] E. Andreetto, L. M. Yan, M. Tatarek-Nossol, A. Velkova, R. Frank, A. Kapurniotu, *Angew. Chem. Int. Ed.* **2010**, *49*, 3081–3085; *Angew. Chem.* **2010**, *122*, 3146–3151.

[17] A. Serrano-Pozo, M. P. Frosch, E. Masliah, B. T. Hyman, *Cold Spring Harbor Perspect. Med.* **2011**, *1*, a006189.

[18] K. Jackson, G. A. Barisone, E. Diaz, L. W. Jin, C. DeCarli, F. Despa, *Ann. Neurol.* **2013**, *74*, 517–526.

[19] B. Macao, W. Hoyer, A. Sandberg, A. C. Brorsson, C. M. Dobson, T. Härd, *BMC Biotechnol.* **2008**, *8*, 82.

[20] a) S. M. Park, H. Y. Jung, T. D. Kim, J. H. Park, C. H. Yang, J. Kim, *J. Biol. Chem.* **2002**, *277*, 28512–28520; b) J. M. Souza, B. I. Giasson, V. M. Lee, H. Ischiropoulos, *FEBS Lett.* **2000**, *474*, 116–119.

[21] T. Härd, C. Lendel, *J. Mol. Biol.* **2012**, *421*, 441–465.

Received: April 1, 2015
Published online: June 26, 2015

Angewandte Chemie
Eine Zeitschrift der Gesellschaft Deutscher Chemiker

Supporting Information

Contact between the β1 and β2 Segments of α-Synuclein that Inhibits Amyloid Formation**

*Hamed Shaykhalishahi, Aziz Gauhar, Michael M. Wördehoff, Clara S. R. Grüning, Antonia N. Klein, Oliver Bannach, Matthias Stoldt, Dieter Willbold, Torleif Härd, and Wolfgang Hoyer**

anie_201503018_sm_miscellaneous_information.pdf

Table of contents

Supporting Experimental Section

Protein preparation. Wt α-syn and α-syn(1-108) were expressed and purified as described.[1] To generate α-synCC and α-synCC(1-108) constructs, the Gly-41 and Val-48 residues of wt α-syn and α-syn(1-108) were exchanged to cysteines using a site-directed mutagenesis approach. In order to ensure formation of the intramolecular disulfide bond, the purified α-synCC proteins were dialyzed against 100 mM Tri-HCl, pH 8.4, containing 2 μM CuSO4.[2] Oxidized α-synCC was further purified by activated thiol sepharose 4B medium (GE Healthcare). For NMR experiments, both wt α-syn and α-synCC were expressed in M9 minimal medium supplemented with ^{15}N-NH_4Cl (1 g/l) and $^{13}C_6$-glucose (2 g/l) and purified as described for the unlabeled protein.

Aβ40 and Aβ42 were produced with an N-terminal methionine by recombinant co-expression with ZAβ3.[3] The N-terminal methionine is required for translation initiation in the employed expression system. Aβ with and without N-terminal methionine are highly similar in terms of structure and aggregation properties.[3-4]

Synthetic human IAPP (EMD Millipore), amidated at the C-terminus to correspond to the form with full biological activity,[5] was dissolved in 20 mM NaPi, 50 mM NaCl, pH 6.0, containing 6 M Guanidine HCl to dissolve pre-existing aggregates. The monomeric fraction was collected after SEC on a Superdex 75 10/300 GL column (GE Healthcare) in 20 mM NaPi, 50 mM NaCl, pH 6.0.

NMR spectroscopy. NMR data were collected at 10 °C using a 900 MHz spectrometer (Varian) equipped with a cryogenically cooled Z-axis pulse-field-gradient triple resonance probe. (^{1}H-^{15}N)-HSQC (heteronuclear single quantum coherence) measurements were performed on samples of ca. 250 μM [U-^{15}N]-wt α-syn or [U-^{15}N]-α-synCC in 20 mM NaPi, 50 mM NaCl, pH 7.4. Backbone assignments were obtained with BEST-TROSY experiments[6] and standard triple resonance heteronuclear NMR techniques using samples of the [U-^{13}C,^{15}N]-labeled proteins. NMR data were processed using NMRPipe[7] and analyzed with CcpNmr.[8] Averaged Cα and C' secondary chemical shifts were calculated as ΔS = (3 x ΔS(Ca) + 4 x ΔS(C'))/7 applying random coil shifts according to Kjaergaard et al.[9]

Microplate aggregation assay. Fibrillation was performed in black round-bottom 96-well plates (Nunc) in an Infinite M1000 plate reader (Tecan). α-Syn fibrillation was done at 37 °C in 20 mM NaPi, 50 mM NaCl, pH 6.0, under orbital shaking with 1 glass bead (2 mm) per microplate well. Aβ fibrillation was done at 30 °C (Figure 2b,f) or 37 °C (Figure S4) in 20 mM NaPi, 50 mM NaCl, pH 7.4, under orbital shaking with 1 glass bead per microplate well. Aβ(1-40) with an N-terminal methionine[3] was used in the fibrillation experiments. IAPP fibrillation was done at 30 °C in 20 mM NaPi, 50 mM NaCl, pH 6.0, under quiescent conditions. All samples contained 40 μM ThT and 0.04% NaN_3. The plates were sealed with polyolefin tape (Nunc) before incubation. Amyloid formation was followed by ThT fluorescence at 480 nm (excitation 440 nm). Seeded-growth fibrillation of α-syn was performed under the same conditions as applied for *de novo* fibrillation, but in the presence of 20% (w/w) α-syn seeds. Seeds were prepared by ultrasonication of preformed α-syn fibrils for 15 min in an ultrasound water bath.

Size exclusion chromatography. SEC runs were performed on a Superdex 75 10/300 GL column connected to an Äkta Purifier system (GE Healthcare) at a flow rate of 0.8 ml/min.

TIRF microscopy. Wt α-syn and α-synCC were incubated in 20 mM MES, 10 mM $MgCl_2$, pH 6.0, at 37 °C in PCR tubes in the presence of α-syn seeds, prepared by ultrasonication of preformed α-syn fibrils for 15 minutes

in an ultrasound water bath. After 0 h, 24 h, and 48 h, 2 µl samples were withdrawn and dried on a cleaned glass coverslip (Menzel-Gläser coverslips #1, 25 x 60 mm, 0.13-0.16 mm thickness, hydrolytic class 1, Gerhard Menzel GmbH, Braunschweig, Germany). Directly prior to imaging, 5 µl of 5 µM Thioflavin T in dH2O were pipetted onto the dried spots. TIRFM was performed on a Leica AF6000LX inverted microscope equipped with a HCX PL APO 100x 1.47 oil objective and a Hamamatsu C9100-02-LNK00 EM-CCD camera (objective-style TIRFM). A 405 nm laser diode was used for the excitation of ThT. Excitation light was filtered from the fluorescence signal by a 450/50 bandpass filter. Exposure times and EM gain were set to 100 ms and 800-1200 for preview and 1-2 s and 200-500 for the final images. Images were processed with ImageJ software (available at http://rsb.info.nih.gov/ij; developed by Wayne Rasband, National Institutes of Health, Bethesda, MD) with respect to brightness and contrast settings, cropping of images, and application of lookup table hot cyan.

Transmission electron microscopy. Samples from an Aβ aggregation assay were diluted to an Aβ concentration of 5 µM, and 20 µl were applied to formvar/carbon coated copper grids (S162, Plano), followed by incubation for 3 min. The grids were washed three times with H_2O and once with 2% aqueous uranyl acetate, followed by 1 min incubation with 2% aqueous uranyl acetate for negative staining. The grids were dried overnight. The samples were examined with a Libra 120 electron microscope (Zeiss) operating at 120 kV.

Toxicity assay. The viability of SH-SY5Y neuroblastoma cells was assessed with an MTT assay (Cell Proliferation Kit I, Roche Diagnostics) as described before.[1] Protein samples were aged under the conditions of the microplate aggregate assay described above for 48 h (α-syn), 4 h (Aβ), or 1 h (IAPP) at a protein concentration of 50 µM (α-syn), 96 µM (Aβ), or 50 µM (IAPP), respectively, and diluted into the cell culture medium to the final concentrations of 1 µM (α-syn), 10 µM (Aβ) and 0.5 µM (IAPP). The cell cultures were further incubated for 24 h before the MTT assay was carried out.

Aβ protofibril interaction. Aβ42 protofibrils were prepared as described before.[10] 480 µl of freshly SEC-purified Aβ protofibrils (52 µM monomer concentration) in 20 mM NaPi buffer, pH 7.0, were mixed with 200 µl of 283 µM α-synCC or with 200 µl of buffer and incubated at room temperature for 10 min. Following re-injection of the samples onto a Superdex 75 10/300 column, Aβ protofibril fractions were collected for further analysis by dot blotting. The anti-α-syn antibody 211 (Santa Cruz Biotechnology) recognizing a C-terminal epitope was used at a concentration of 0.5 µg/ml to detect α-synCC. A HRP-conjugated goat anti-rabbit IgG antibody was applied to detect bound antibody 211 on a CCD camera, using SuperSignal West Pico chemiluminescent substrate (Thermo Scientific).

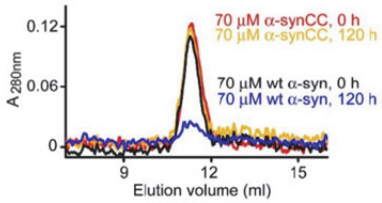

Figure S1. SEC analysis of aggregation of α-synCC and wt α-syn. Protein samples subjected to an aggregation assay for the indicated times were loaded onto a Superdex 75 10/300 GL column (void volume ~8.5 ml). For wt α-syn, the elution peak was greatly reduced after 120 h incubation due to the formation of amyloid fibrils which do not enter the column bed.

Figure S2. The positions of the exchanges to cysteine (yellow) in α-synCC are identical to those in AβCC[11] in relation to the β-hairpin. Backbone hydrogen bonding across the strands is indicated with black dots.

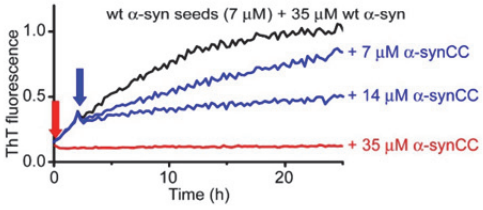

Figure S3. ThT time course of fibrillation of wt α-syn in the presence of preformed wt α-syn fibril seeds, with addition of α-synCC at the time points indicated by arrows.

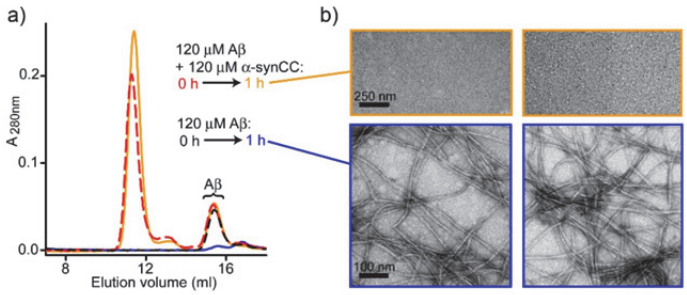

Figure S4. a) SEC analysis of Aβ aggregation in absence and presence of α-synCC. Protein samples were subjected to an aggregation assay for the indicated times and loaded on a Superdex 75 10/300 GL column (void volume ~8.5 ml). In the absence of α-synCC, the elution peak of Aβ was strongly reduced after 1 h incubation (blue trace) due to the formation of amyloid fibrils which do not enter the column bed. b) Two representative TEM images of each of the 1 h incubation samples analyzed in a).

Supporting References

[1] E. A. Mirecka, H. Shaykhalishahi, A. Gauhar, S. Akgül, J. Lecher, D. Willbold, M. Stoldt, W. Hoyer, *Angew. Chem. Int. Ed.* **2014**, *53*, 4227-4230; *Angew. Chem.* **2014**, *126*, 4311-4314.

[2] C. Jiang, J. Y. Chang, *Biochemistry* **2007**, *46*, 602-609.

[3] B. Macao, W. Hoyer, A. Sandberg, A. C. Brorsson, C. M. Dobson, T. Härd, *BMC Biotechnol.* **2008**, *8*, 82.

[4] D. M. Walsh, E. Thulin, A. M. Minogue, N. Gustavsson, E. Pang, D. B. Teplow, S. Linse, *FEBS J.* **2009**, *276*, 1266-1281.

[5] A. N. Roberts, B. Leighton, J. A. Todd, D. Cockburn, P. N. Schofield, R. Sutton, S. Holt, Y. Boyd, A. J. Day, E. A. Foot, et al., *Proc. Natl Acad. Sci. USA* **1989**, *86*, 9662-9666.

[6] Z. Solyom, M. Schwarten, L. Geist, R. Konrat, D. Willbold, B. Brutscher, *J. Biomol. NMR* **2013**, *55*, 311-321.

[7] F. Delaglio, S. Grzesiek, G. W. Vuister, G. Zhu, J. Pfeifer, A. Bax, *J. Biomol. NMR* **1995**, *6*, 277-293.

[8] W. F. Vranken, W. Boucher, T. J. Stevens, R. H. Fogh, A. Pajon, M. Llinas, E. L. Ulrich, J. L. Markley, J. Ionides, E. D. Laue, *Proteins* **2005**, *59*, 687-696.

[9] a) M. Kjaergaard, S. Brander, F. M. Poulsen, *J. Biomol. NMR* **2011**, *49*, 139-149; b) M. Kjaergaard, F. M. Poulsen, *J. Biomol. NMR* **2011**, *50*, 157-165.

[10] C. S. Grüning, S. Klinker, M. Wolff, M. Schneider, K. Toksöz, A. N. Klein, L. Nagel-Steger, D. Willbold, W. Hoyer, *J. Biol. Chem.* **2013**, *288*, 37104-37111.

[11] A. Sandberg, L. M. Luheshi, S. Sollvander, T. Pereira de Barros, B. Macao, T. P. Knowles, H. Biverstal, C. Lendel, F. Ekholm-Petterson, A. Dubnovitsky, et al., *Proc. Natl Acad. Sci. USA* **2010**, *107*, 15595-15600.

Full References from Main Article

[2b] B. Fauvet, M. K. Mbefo, M. B. Fares, C. Desobry, S. Michael, M. T. Ardah, E. Tsika, P. Coune, M. Prudent, N. Lion, D. Eliezer, D. J. Moore, B. Schneider, P. Aebischer, O. M. El-Agnaf, E. Masliah, H. A. Lashuel, *J. Biol. Chem.* **2012**, *287*, 15345-15364.

[7] D. Ghosh, S. Sahay, P. Ranjan, S. Salot, G. M. Mohite, P. K. Singh, S. Dwivedi, E. Carvalho, R. Banerjee, A. Kumar, S. K. Maji, *Biochemistry* **2014**, *53*, 6419-6421.

[9] J. L. Guo, D. J. Covell, J. P. Daniels, M. Iba, A. Stieber, B. Zhang, D. M. Riddle, L. K. Kwong, Y. Xu, J. Q. Trojanowski, V. M. Lee, *Cell* **2013**, *154*, 103-117.

[13b] A. Sandberg, L. M. Luheshi, S. Sollvander, T. Pereira de Barros, B. Macao, T. P. Knowles, H. Biverstal, C. Lendel, F. Ekholm-Petterson, A. Dubnovitsky, L. Lannfelt, C. M. Dobson, T. Härd, *Proc. Natl Acad. Sci. USA* **2010**, *107*, 15595-15600.

Chapter 6: Discussion

6.1 Engineered binding proteins as study tool for amyloid research

In amyloid diseases, abnormal misfolding of a certain protein into β-rich intermediate structures leads to formation of toxic oligomeric and fibrillar species [3, 6, 19]. Understanding the mechanism of fibril formation, particularly the identification and characterization of involved intermediate structures, is the main of focus of current research with primary aim to provide valuable knowledge for development of novel therapeutics and diagnostic tools. Deposition of α-synuclein aggregates in form of LBs is the main pathological hallmark of PD [41]. Furthermore, discovery of several familial PD-linked α-synuclein mutations propose α-synuclein aggregation as the main pathological event in PD pathogenesis [52]. Despite extensive research on α-synuclein aggregation, the exact mechanism remains unclear. An increasing body of literature indicates the potential of engineered binding proteins for diagnostic and therapeutic applications [210, 211]. Moreover, engineered binding proteins can be used as study tools in protein aggregation research. Selection and biophysical characterization of an engineered binding protein, the affibody ZAβ$_3$, resulted in the identification of a critical region in Aβ [212]. ZAβ$_3$ is a cysteine-linked homodimer and NMR studies demonstrate the sequestration of a β-hairpin structure of Aβ inside the hydrophobic cavity of ZAβ$_3$. The identified β-hairpin structure is formed by two β-strands whose sequence positions strongly resemble the position of β-strands present in the fibril core [20]. Furthermore, intramolecular disulfide bond-assisted stabilization of the identified β-hairpin motif causes formation of stable toxic oligomer and, thus, provides further proof of the importance of the Aβ β-hairpin forming ion exposed by ZAβ$_3$ [170]. Accordingly, development of affibody protein binders for ıer aggregation-prone proteins or peptides

could be regarded as a valuable tool for clarifying the mechanism of aggregation. In the present thesis, we primarily set out to select binders against α-synuclein. ZAβ$_3$ was employed as the scaffold for generation of the combinatorial β-wrapin library using error-prone PCR.

6.2 Selection and characterization of β-wrapin binders

Chapter 2 and chapter 3 describe the selection and characterization of engineered binding proteins against α-synuclein. To select β-wrapins specific for α-synuclein, the ZAβ$_3$-derived β-wrapin scaffold library was screened using phage display technology. A C-terminally truncated construct of α-synuclein, α-syn$_{1\text{-}108}$, was used as the target protein, in order to prevent the possibility of selection of unwanted binding proteins for the highly charged C-terminal region which is unstructured in fibril core [160, 161]. To select high affinity binders, four phage display (biopanning) rounds were performed, accompanied by a gradual decrease in the concentration of α-synuclein and an increase in washing stringency. In the first round, incubation of α-synuclein with the β-wrapin library was carried out overnight at 4°C, whereas in subsequent rounds it was performed at room temperature for 1 hour. After selection, sequence analysis indicated the maintenance of Cys-28 in all 90 randomly selected clones, indicating the importance of homodimerization for high affinity β-wrapins to α-synuclein. Moreover, characterization of five representative clones (AS9, AS10, AS34, AS60 and AS69) by ITC demonstrated that the selected β-wrapin clones bind to monomeric α-synuclein with 1:1 stoichiometry. Therefore, it is concluded that one dimer molecule of the selected β-wrapin binds to one molecule of α-synuclein, reminiscent of ZAβ$_3$ interacting with Aβ. In addition to maintenance of Cys-28, the Ile31Phe substitution appears to be critical for β-wrapin interactions with α-synuclein because all selected clones carried this exchange and, moreover, this single substitution in AS9 clone is sufficient to gain an affinity to α-synuclein and loose the affinity to Aβ, compared with ZAβ3. Substitution of Leu-34 by either valine or isoleucine was

the second most frequent amino acid exchange. In comparison with AS9, one additional Leu34Val mutation in AS10 clone results in adopting a nanomolar affinity to both Aβ and α-synuclein. Additionally, few other mutations were detected in N-terminal part of selected β-wrapin proteins. Occurrence of three additional mutations, V17F, G13D and K7T, in AS60 and AS69 results in a further loss of affinity to Aβ and an increase in affinity to α-synuclein. AS69 and AS10 clones are further described in chapter 1 and chapter 2, respectively.

6.2.1 AS69: a specific β-wrapin binder for α-synuclein

AS69 is a homodimeric β-wrapin protein which specifically binds to α-synuclein with nanomolar affinity. To map the binding epitope of AS69 on the α-synuclein sequence, [$^{1}H^{15}N$] HSQC NMR measurements were performed. consistent with typical HSQC spectra for IDPs, the α-synuclein HSQC spectrum represents a narrow dispersion of cross peaks in the ^{1}H dimension [218]. The number of cross peaks in spectrum acquired at 10°C is higher than that recorded at 30°C, with only few cross peaks stemming from the C-terminus. In consistent with this observation, Mcnulty et al. have previously shown that an increase in temperature results in disappearance of cross peaks due to the reversible conformational exchange in N-terminal 100 residues [219]. Comparison of the HSQC spectra of free ^{15}N-labeled α-synuclein and ^{15}N-labeled α-synuclein in complex with unlabeled AS69 indicates the disappearance of chemical shift cross peaks at 10°C but reappearance of cross peaks at 30°C, indicating the partial folding of α-synuclein upon interaction with AS69. The assignment of cross peaks affected by AS69 revealed the α-synuclein residues 37-54 as the binding region.

Further structural analysis of the AS69:α-synuclein complex demonstrated that the binding region adopts a β-hairpin motif inside the hydrophobic tunnel-like cavity of AS69, formed by 2 β-strands and four α-helices of dimeric AS69. Despite the four amino acid exchanges, the structure of AS69:α-synuclein complex highly resembles that of the ZAβ$_3$:Aβ complex [212]. The α-synuclein β-hairpin wrapped by AS69 is composed of two β-strands, β1 (^{37}VLYVGSK^{43}) and β2

(^{48}VVHGVAT^{54}), connected by a short linker (^{44}TKEG^{47}). Three features of the β1-β2-region might be preferred by the β-wrapin scaffold. First, the β-strands have the suitable length to fit into the binding site provided by the β-wrapin scaffold. Second, they are connected by a short linker, T^{44}KEG^{47}. This linker is of type I β-turn potentials >1 for all of the 4 amino acids at their respective positions in the turn and thus has a preference for turn formation [220]. Third, this region contains two aromatic acids, Tyr-39 and His-50 located at the center of one β-hairpin face with their side chains hydrogen-bonded by the hydroxy proton of Tyr-39 and the N^{δ}-nitrogen of His-50. Moreover, one of the exchanged residues, Phe-31 of both AS69 subunits is involved in aromatic-aromatic interactions with Tyr39 and His-50 residues within β-hairpin region. Notably, aromatic amino acids are also present in the Aβ-hairpin and overrepresented at protein interfaces, where they significantly contribute to the binding energy [221].

In the case of Aβ, the sequence position of the two β-strands bound to ZAβ$_3$ is strongly similar to those of Aβ within amyloid fibrils [20]. In contrast to Aβ, one α-synuclein monomer does not contribute two but approximately five β-strands to the fibril core (figure 4), which fold into a parallel, in-register superpleated cross-β structure [160-163]. The sequence positions of the two β-strands established in AS69-bound α-synuclein are in a good agreement with the N-terminal β-strands β1 and β2 identified by Vilar et al (figure 10) [162]. Long-range interactions between the side chains of Tyr-39 in β1 and His-50 in β2, previously detected in α-synuclein amyloid fibrils [222], also exist in the α-synuclein structure bound to AS69. The NAC region including the β3 to β5 segments, the most hydrophobic stretch with high β-sheet propensity [223] is however not affected by AS69 binding, demonstrating the specificity of the interaction of AS69 with the β1-β2-region.

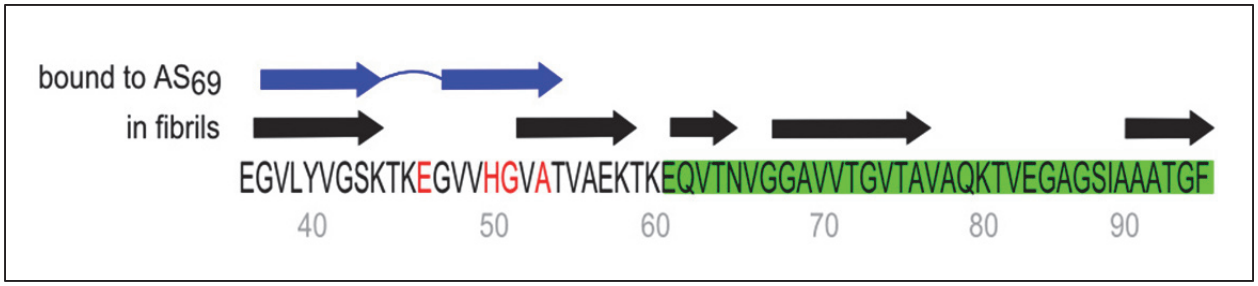

Figure 9: Sequence position of β-hairpin bound to AS69. The β-strands wrapped by AS69 (blue arrows) are compared to β-strands in fibril (black arrows) identified by Vilar et al. [162]. The NAC region is highlighted in green. Position of PD-related mutations is shown in red.

Due to the lack of persistent secondary structure, tertiary interactions restrict the conformational ensemble in the monomeric state of natively unfolded proteins, which can be detected by NMR approaches, e.g. paramagnetic relaxation enhancement, PRE [224]. Remarkably, analysis of soluble monomeric α-synuclein using PRE method has stablished the intramolecular interaction between β1 and β2 strands as one of the main transient fibril-like contacts [225]. Moreover, employing a combination of solution and solid-state NMR, Kim et al. have identified a nascent β-structure in β1-β2 region as one of the structural correlations between unfolded and fibrillar α-synuclein [226]. These data suggest that β-hairpin structure bound to AS69 is also present in conformational ensembles of monomeric α-synuclein. This also supports the hypothesis suggesting that interaction of IDPs with their partners is not merely via induced-fit mechanism but also could be exerted by conformational selection [227, 228]. In this context it is noteworthy that contacts between the β1 and β2 strands within the β-hairpin may establish the clustering of hydrophobic residues, potentially promoting interactions between α-synuclein monomers and formation of early oligomers stabilized mainly by hydrophobic interactions [229]. The presence of β-hairpin conformation within α-synuclein oligomers is in line with FTIR spectroscopy data detecting antiparallel β-sheet structure in α-synuclein oligomers, in contrast to the parallel β-sheet structure observed for fibrils [230].

The critical role of the β1-β2 region in PD pathogenesis is highlighted by the fact that it includes four out of five disease-related point mutations discovered to date. H50Q, G51D and A53T mutations are localized within the C-terminal β-strand (β2) of the α-synuclein β-hairpin, whereas the E46K mutation exists in in the connecting β-turn. Interestingly, A53T and E46K mutations have been shown to promote oligomerization and fibril formation [140]. Additionally, the most severe dopaminergic loss has been observed in animal with accelerated oligomerization of α-synuclein induced by mutations in residues preceding (E35K) and succeeding (E57K) the β-hairpin region [225]. These data support a link between the local structure formation in the β-hairpin region, oligomerization, and disease pathogenesis. Furthermore, several designed mutations within the β-hairpin region have been shown to promote (e.g. K45V, E46V [231]) or prevent (e.g. V37P, Y39A, V48P, V49P [232, 233]) fibrillation of α-synuclein. The β1-β2 region is furthermore an interaction site for small molecule aggregation inhibitors, with Tyr-39 serving as a key anchoring residue [233, 234].

As the most hydrophobic region requisite for fibril formation, NAC region has been constantly regarded as the potential target for drug design and screening [235]. However, the present study indicates that α-synuclein aggregation can also be inhibited by targeting the β1-β2 region. Based on our NMR and aggregation results and considering the overall features of amyloid assemblies presented in the literature, we suggest a model for AS69-mediated inhibition of α-synuclein. At stoichiometric concentration, AS69 protein readily binds to α-synuclein and wraps the β-hairpin structure formed by β1-β2 region, and thereby completely inhibits the fibrillation process and toxicity. Consistent with the aggregation results, our SEC analysis added further evidence for the sequestration of monomeric α-synuclein bound to AS69. Our aggregation experiments demonstrate that addition of AS69 at different time points results in arrestment of fibril growth, indicating the possible interaction of AS69 with fibril ends. In addition, sub-stoichiometric concentration of AS69 is able to prolong the lag time of aggregation. The lag time of aggregation reflects the time required for formation of nuclei.

Thus, the sub-stoichiometric effect of AS69 on duration of the lag time could be explained by possible interactions of AS69 or AS69:α-synuclein complex with β-hairpin-containing intermediates and thereby a depletion of primary nuclei for fibril growth. Moreover, the formation of nuclei on the surface of fibrils has been reported as a secondary nucleation event in the fibrillation process of several amyloidogenic proteins such as Aβ, IAPP and insulin [28-30]. Therefore, the sub-stoichiometric effect of AS69 could be also exerted by possible interference with secondary nucleation catalyzed by fibrils.

In cells, several proteins have been demonstrated as binding partners for α-synuclein [146, 153, 236]. Our in vitro observations on α-synuclein:AS69 interaction could mimic the interaction of some cellular protein partners which regulate α-synuclein aggregation upon binding to the identified binding β1-β2 region. Out of the set of protein cellular partners, phospholipase Cβ1 (PLCβ1) exhibits one of the strongest binding affinities to α-synuclein [236] and its expression is high in neuronal cells, similar to α-synuclein. Moreover, cellular loss of PLCβ1 promotes α-synuclein aggregation [237]. Interestingly, PLCβ1 binds to α-synuclein residues 45-53 residing in the C-terminal region of β-hairpin identified by AS69. Similar to the effect of AS69, interaction of PLCβ1 with this region results in inhibition of aggregation and moreover, release of this interaction diminishes the inhibitory effect of PLCβ1. Guo et al. have proposed the oxidative stress condition, resulting in down-regulation of PLCβ1, as the promoting factor for α-synuclein aggregation [237], suggesting a link between oxidative stress and α-synuclein aggregation. Furthermore, it is tempting to hypothesize that α-synuclein aggregation linked to PD-related mutations and overexpression of α-synuclein could be due to the release of tight regulating interactions with cellular protein partners.

In conclusion, we have successfully engineered a β-wrapin scaffold to interact with α-synuclein. More importantly, our structural and biophysical study using AS69 provided new insights into

conformational features of α-synuclein defining a β-hairpin epitope as an important element controlling α-synuclein aggregation.

6.2.1.1 Outlook

The present data cannot clarify the mechanism behind the sub-stoichiometric inhibition by AS69. Our study here describes the AS69 interaction with monomeric α-synuclein. Potential interactions with oligomeric and fibrillar α-synuclein remain to be elucidated. Furthermore, the role of the described α-synuclein β-hairpin may be further elucidated by introduction of a stabilizing disulfide bond (see chapter 5), as it was successfully done for the Aβ β-hairpin [170]. Finally, it is of interest to check the inhibitory effect of AS69 in *in vivo* models.

6.2.2 AS10: a β-wrapin binder for α-synuclein, Aβ and IAPP

As earlier discussed in section 6-2, the Ile31Phe mutation was present in all wrapin binders selected against α-synuclein. With respect to the loss of binding affinity for Aβ in AS9, with only the Ile31Phe mutation compared with ZAβ3, it can be concluded that presence of Ile at position 31 is required for the maintenance of high affinity of β-wrapin scaffold to Aβ, whereas an Ile to Phe substitution yields an improved affinity to α-synuclein. However, the presence of a second substitution in AS10, Le34Val, results in an increase in the binding affinity to both Aβ (K_d decreases from 500 nM to 150 nM) and α-synuclein (K_d decreases from 2500 nM to 380 nM). Moreover, our binding study using Biacore indicates that AS10 also binds to IAPP, with a Kd value of 910 nM. Therefore, chapter 3 deals with AS10 as a β-wrapin protein which interacts with three distinct amyloidogenic proteins.

The high resolution structure of $ZA\beta_3$ and AS69 bound to Aβ and α-synuclein, respectively, confirms the sequestration of a β-hairpin structure formed by amyloidogenic proteins inside the dimeric β-wrapin proteins [212, 238]. Moreover, structural analysis indicates that both

substituted residues in AS10, Phe-31 and Val-34, are positioned in the interface flanked by the β-hairpin and the two subunits of the β-wrapin, which is clearly a critical region for stability of the β-wrapin: target complexes. We employed [$^{1}H^{15}N$] HSQC NMR spectroscopy in order to shed more light on the interaction of AS10 with α-synuclein, Aβ and IAPP. Similar to the ZAβ$_3$: Aβ interaction [212], addition of AS10 to all three targets resulted in a great dispersion of resonances indicating coupled folding and binding. In addition, four amide proton resonances are appeared in glycine region, originating from Gly-13 and Gly-14 of each subunit of AS10, along with amide proton resonances in the downfield region of spectrum with the typical shift values for formation of β-sheet structure. These data establish the formation of β-hairpin structure in all three amyloidogenic proteins upon binding to AS10, resembling the interaction ZAβ$_3$ and AS69 with Aβ and α-synuclein, respectively. Furthermore, [$^{1}H^{15}N$] HSQC analysis of AS10 addition to the four-repeat-domain construct of tau protein, K18ΔK280/AA [239], and Y145Stop variant of human prion protein, huPrP$_{23\text{-}144}$ [240], indicated no binding effect which rules out the commonality of AS10 interactions with all amyloidogenic proteins.

Our present data obtained by ThT and MTT assay indicate the inhibitory effect of AS10 on the fibrillation process and toxicity of α-synuclein, Aβ and IAPP. In addition, similar to AS69, AS10 affects the aggregation rate of all three targets at sub-stoichiometric concentrations, indicating the possible interference with primary or secondary nucleation events.

Several computer simulations have indicated the high tendency of amyloidogenic proteins to transiently adopt β-hairpin conformation and involvement of the β-hairpins in the formation of intramolecular contacts [241-247]. Our study highlights the adaptability of small engineered binding proteins to natively unfolded, amyloidogenic target proteins. In case of unfolded proteins, binding goes along with local folding of the targets. Coupled folding and binding is of an entropic cost for the disorder-to-order transition, which normally yields complexes of high specificity and relatively low affinity [248]. It is therefore of interest that AS10 binds to three

distinct amyloidogenic proteins with a high affinity. This indicates that Aβ, α-synuclein, and IAPP share key features which not only contribute to their ability for amyloid fibril formation, but also the common adoption of a β-hairpin conformation in complex with β-wrapins.

6.2.2.1 Outlook

Regarding the binding effect of the β-wrapin AS10 on three distinct natively disordered amyloidogenic proteins, it is of interest to check this property on other amyloidogenic proteins and thereby to identify proteins which adopt β-hairpin conformations. Evaluation of the interaction of AS10 with oligomeric and fibrillar forms of different amyloidogenic protein partners would be also of interest.

6.3 AS69-GS3: a head-to-tail construct of AS69

In chapter 3, to specify the impact of the Cys-28 disulfide bond, we generated a head to tail construct of AS69, AS69-GS3. AS69-GS3 features a glycine-serine rich linker like those commonly used in the generation of scFvs [249]. The comparative characterization of the stabilities and binding features of AS69 and AS69-GS3 reveal an important impact of Cys-28. In case of ZAβ_3, direct fusion of subunits was sufficient for recovery of high affinity to Aβ [214]. In constrast, Cys-28 linkage is critical for the maintenance of AS69-GS3 binding affinity to α-synuclein. The Cys-28 linkage fixes the contact between the subunits' helices 1 and thereby establishes the surface required for interaction with α-synuclein. In addition, our SEC and thermal melting results indicate an increase in compaction and stability of AS69 structure upon formation of Cys-28 linkage. The important role of this linkage is further supported by the conservative selection of Cys-28 in affibody molecules selections for Aβ and moreover, maintenance of this residue in all binders selected against α-synuclein [250, 251].

Head-to-tail linkage of the two subunits of the homodimeric protein of Arc repressor via glycine-serine linkage has been reported to increase the stability of this protein [252, 253]. Head-to-tail dimerization in AS69 not only increases the protein stability but also accelerates the rate of disulfide bond formation. In this case, the effective subunit concentration for disulfide bond formation (4.1 (± 0.5) mM) is in a good agreement with that determined for the folding reaction of head-to-tail linked Arc repressor dimers of phage P22 (4.5 (± 1.8) mM) [252].

6.3.1 Outlook

AS69-GS3 is a useful construct for evaluation of the effect of α-synuclein (37-54) region in cell culture and animal models. Furthermore, AS69-GS3 can be further used as the scaffold for development of β-wrapins with higher affinity to α-synuclein.

6.4 Stabilization of contacts between the β1 and β2 segments of α-synuclein

We previously showed that AS69 completely impedes fibril formation upon binding to a β-hairpin forming amino acid region 37-54 in α-synuclein [238]. In a separate study, the accommodation of an intramolecular disulfide bond on the certain position of Aβ sequence was enough to stabilize the toxic oligomers [170]. In this work, we engineered α-synCC with an intramolecular disulfide bond in order to elucidate the role of β1-β2 contacts on the α-synuclein aggregation. We observed that stabilization of contacts between β1-β2 makes α-synCC unable to form both fibrils and oligomers. In contrast, AβCC forms stable oligomers, which might be due to the higher hydrophobicity of Aβ compared to α-synuclein. We obtained several evidence demonstrating that α-synCC interacts with oligomeric and fibrillar species. First, lag time of wild-type-α-synuclein, IAPP and Aβ fibrillation process is prolonged in the presence of substoichiometric concentrations of α-synCC, suggesting the possible interactions with aggregation nuclei. Second, addition of α-synCC to the aggregation reaction of wild-type-

α-synuclein blocks fibril elongation, proposing the interaction with fibril ends. Third, we here observed that α-synCC binds to Aβ protofibrils, evidenced by dot blotting. Taken together, we suggest that the tertiary interactions cause an increase in population of conformers with clustering of aromatic and hydrophobic amino acids, including Tyr-39 and His-50. Long range interactions between Tyr-39 (in β1 strand) and H50 (in β2 strand) present in fibril core [222] and β-hairpin conformation in complex with AS69 wrapin [238] might also be involved in tertiary contacts between β1 and β2 in monomeric α-synuclein. As the only histidine residue existing in α-synuclein, His-50 protects against aggregation at physiological pH and its disease-related mutation, H50Q, accelerates the aggregation [54, 139, 254]. Regarding the fact that stabilization of the regulating β1-β2 contact by an intramolecular disulfide bond in α-synCC inhibits the aggregation, perturbation of this contact, for example in H50Q, might be responsible for the acceleration of aggregation process [254].

Evidence provided by deletion mutants have shown that C-terminal served as 'solubilizing domain' is required for chaperon activity of α-syn [65, 107, 255]. Here we observed that C-terminally truncated α-synCC is as efficient as full length α-synCC in inhibition of fibrillation of Aβ and IAPP, indicating that inhibitory effect of α-synCC is independent of C-terminal interactions previously reported. The present research also highlights that different intrinsically disordered and amyloidogenic proteins have a strong propensity to undergo hetero-interactions [256, 257].

The β1-β-2 region is an important regulating element for α-synuclein aggregation [258]. Contacts between β1 and β2 strongly influence the aggregation tendency. Promotion of these contacts could be regards as therapeutic approaches.

6.4.1 Outlook

Evaluation the effect of α-synCC on other amyloidogenic proteins is of interesting. In order to identify the minimum sequence region required for the inhibitory effect of α-synCC, generation of truncated constructs may be considered. Additional NMR studies could help to further understand the impact of β1-β2 contacts on the protein-protein interactions involved in the aggregation process.

References

1. Lodish H, B.A., Zipursky SL, *Molecular Cell Biology. .* New York: W. H. Freeman, 2000. **4th edition**.
2. Crick, F.H., *On protein synthesis.* Symp Soc Exp Biol, 1958. **12**: p. 138-63.
3. Dobson, C.M., *Protein folding and misfolding.* Nature, 2003. **426**(6968): p. 884-90.
4. Uversky, V.N., J.R. Gillespie, and A.L. Fink, *Why are "natively unfolded" proteins unstructured under physiologic conditions?* Proteins, 2000. **41**(3): p. 415-27.
5. Goldberg, A.L., *Protein degradation and protection against misfolded or damaged proteins.* Nature, 2003. **426**(6968): p. 895-9.
6. Chiti, F. and C.M. Dobson, *Protein misfolding, functional amyloid, and human disease.* Annu Rev Biochem, 2006. **75**: p. 333-66.
7. Hartl, F.U., A. Bracher, and M. Hayer-Hartl, *Molecular chaperones in protein folding and proteostasis.* Nature, 2011. **475**(7356): p. 324-32.
8. Eisenberg, D. and M. Jucker, *The amyloid state of proteins in human diseases.* Cell, 2012. **148**(6): p. 1188-203.
9. Calero, M. and M. Gasset, *Fourier transform infrared and circular dichroism spectroscopies for amyloid studies.* Methods Mol Biol, 2005. **299**: p. 129-51.
10. Sunde, M., et al., *Common core structure of amyloid fibrils by synchrotron X-ray diffraction.* J Mol Biol, 1997. **273**(3): p. 729-39.
11. Sipe, J.D. and A.S. Cohen, *Review: history of the amyloid fibril.* J Struct Biol, 2000. **130**(2-3): p. 88-98.
12. Jimenez, J.L., et al., *Cryo-electron microscopy structure of an SH3 amyloid fibril and model of the molecular packing.* EMBO J, 1999. **18**(4): p. 815-21.
13. Hoyer, W., et al., *Dependence of alpha-synuclein aggregate morphology on solution conditions.* J Mol Biol, 2002. **322**(2): p. 383-93.
14. Khurana, R., et al., *A general model for amyloid fibril assembly based on morphological studies using atomic force microscopy.* Biophys J, 2003. **85**(2): p. 1135-44.
15. Jansen, R., W. Dzwolak, and R. Winter, *Amyloidogenic self-assembly of insulin aggregates probed by high resolution atomic force microscopy.* Biophys J, 2005. **88**(2): p. 1344-53.
16. Segers-Nolten, I., et al., *Quantitative characterization of protein nanostructures using atomic force microscopy.* Conf Proc IEEE Eng Med Biol Soc, 2007. **2007**: p. 6609-12.
17. Eanes, E.D. and G.G. Glenner, *X-ray diffraction studies on amyloid filaments.* J Histochem Cytochem, 1968. **16**(11): p. 673-7.
18. Fitzpatrick, A.W., et al., *Atomic structure and hierarchical assembly of a cross-beta amyloid fibril.* Proc Natl Acad Sci U S A, 2013. **110**(14): p. 5468-73.
19. Nelson, R., et al., *Structure of the cross-beta spine of amyloid-like fibrils.* Nature, 2005. **435**(7043): p. 773-8.
20. Luhrs, T., et al., *3D structure of Alzheimer's amyloid-beta(1-42) fibrils.* Proc Natl Acad Sci U S A, 2005. **102**(48): p. 17342-7.
21. Khurana, R., et al., *Is Congo red an amyloid-specific dye?* J Biol Chem, 2001. **276**(25): p. 22715-21.

22. Krebs, M.R., E.H. Bromley, and A.M. Donald, *The binding of thioflavin-T to amyloid fibrils: localisation and implications.* J Struct Biol, 2005. **149**(1): p. 30-7.
23. Macao, B., et al., *Recombinant amyloid beta-peptide production by coexpression with an affibody ligand.* BMC Biotechnol, 2008. **8**: p. 82.
24. Colletier, J.P., et al., *Molecular basis for amyloid-beta polymorphism.* Proc Natl Acad Sci U S A, 2011. **108**(41): p. 16938-43.
25. Makin, O.S., et al., *Molecular basis for amyloid fibril formation and stability.* Proc Natl Acad Sci U S A, 2005. **102**(2): p. 315-20.
26. Wood, S.J., et al., *alpha-synuclein fibrillogenesis is nucleation-dependent. Implications for the pathogenesis of Parkinson's disease.* J Biol Chem, 1999. **274**(28): p. 19509-12.
27. Krebs, M.R., et al., *Formation and seeding of amyloid fibrils from wild-type hen lysozyme and a peptide fragment from the beta-domain.* J Mol Biol, 2000. **300**(3): p. 541-9.
28. Padrick, S.B. and A.D. Miranker, *Islet amyloid: phase partitioning and secondary nucleation are central to the mechanism of fibrillogenesis.* Biochemistry, 2002. **41**(14): p. 4694-703.
29. Biancalana, M. and S. Koide, *Molecular mechanism of Thioflavin-T binding to amyloid fibrils.* Biochim Biophys Acta, 2010. **1804**(7): p. 1405-12.
30. Knowles, T.P., et al., *An analytical solution to the kinetics of breakable filament assembly.* Science, 2009. **326**(5959): p. 1533-7.
31. Librizzi, F. and C. Rischel, *The kinetic behavior of insulin fibrillation is determined by heterogeneous nucleation pathways.* Protein Sci, 2005. **14**(12): p. 3129-34.
32. Cohen, S.I., et al., *Nucleated polymerization with secondary pathways. I. Time evolution of the principal moments.* J Chem Phys, 2011. **135**(6): p. 065105.
33. Thies, W., L. Bleiler, and A. Alzheimer's, *2013 Alzheimer's disease facts and figures.* Alzheimers Dement, 2013. **9**(2): p. 208-45.
34. Armstrong, R.A., *The molecular biology of senile plaques and neurofibrillary tangles in Alzheimer's disease.* Folia Neuropathol, 2009. **47**(4): p. 289-99.
35. Head, E. and I.T. Lott, *Down syndrome and beta-amyloid deposition.* Curr Opin Neurol, 2004. **17**(2): p. 95-100.
36. Pillay, K. and P. Govender, *Amylin uncovered: a review on the polypeptide responsible for type II diabetes.* Biomed Res Int, 2013. **2013**: p. 826706.
37. Abedini, A. and A.M. Schmidt, *Mechanisms of islet amyloidosis toxicity in type 2 diabetes.* FEBS Lett, 2013. **587**(8): p. 1119-27.
38. Parkinson, J., *An essay on the shaking palsy. 1817.* J Neuropsychiatry Clin Neurosci, 2002. **14**(2): p. 223-36; discussion 222.
39. Holdorff, B., A.M. Rodrigues e Silva, and R. Dodel, *Centenary of Lewy bodies (1912-2012).* J Neural Transm, 2013. **120**(4): p. 509-16.
40. Goedert, M., *Alpha-synuclein and neurodegenerative diseases.* Nat Rev Neurosci, 2001. **2**(7): p. 492-501.
41. Beyer, K., M. Domingo-Sabat, and A. Ariza, *Molecular pathology of Lewy body diseases.* Int J Mol Sci, 2009. **10**(3): p. 724-45.
42. Gurlo, T., et al., *Evidence for proteotoxicity in beta cells in type 2 diabetes: toxic islet amyloid polypeptide oligomers form intracellularly in the secretory pathway.* Am J Pathol, 2010. **176**(2): p. 861-9.

43. Maroteaux, L., J.T. Campanelli, and R.H. Scheller, *Synuclein: a neuron-specific protein localized to the nucleus and presynaptic nerve terminal.* J Neurosci, 1988. **8**(8): p. 2804-15.
44. Maroteaux, L. and R.H. Scheller, *The rat brain synucleins; family of proteins transiently associated with neuronal membrane.* Brain Res Mol Brain Res, 1991. **11**(3-4): p. 335-43.
45. Ueda, K., et al., *Molecular cloning of cDNA encoding an unrecognized component of amyloid in Alzheimer disease.* Proc Natl Acad Sci U S A, 1993. **90**(23): p. 11282-6.
46. Weinreb, P.H., et al., *NACP, a protein implicated in Alzheimer's disease and learning, is natively unfolded.* Biochemistry, 1996. **35**(43): p. 13709-15.
47. Iwai, A., et al., *Non-A beta component of Alzheimer's disease amyloid (NAC) is amyloidogenic.* Biochemistry, 1995. **34**(32): p. 10139-45.
48. Hashimoto, M., et al., *Human recombinant NACP/alpha-synuclein is aggregated and fibrillated in vitro: relevance for Lewy body disease.* Brain Res, 1998. **799**(2): p. 301-6.
49. Bodles, A.M., et al., *Identification of the region of non-Abeta component (NAC) of Alzheimer's disease amyloid responsible for its aggregation and toxicity.* J Neurochem, 2001. **78**(2): p. 384-95.
50. Chen, X., et al., *The human NACP/alpha-synuclein gene: chromosome assignment to 4q21.3-q22 and TaqI RFLP analysis.* Genomics, 1995. **26**(2): p. 425-7.
51. Polymeropoulos, M.H., et al., *Mutation in the alpha-synuclein gene identified in families with Parkinson's disease.* Science, 1997. **276**(5321): p. 2045-7.
52. Parsian, A. and J.S. Perlmutter, *Point Mutations in the alpha-Synuclein Gene.* Methods Mol Med, 2001. **62**: p. 3-11.
53. Zarranz, J.J., et al., *The new mutation, E46K, of alpha-synuclein causes Parkinson and Lewy body dementia.* Ann Neurol, 2004. **55**(2): p. 164-73.
54. Appel-Cresswell, S., et al., *Alpha-synuclein p.H50Q, a novel pathogenic mutation for Parkinson's disease.* Mov Disord, 2013. **28**(6): p. 811-3.
55. Lesage, S., et al., *G51D alpha-synuclein mutation causes a novel parkinsonian-pyramidal syndrome.* Ann Neurol, 2013. **73**(4): p. 459-71.
56. Pasanen, P., et al., *A novel alpha-synuclein mutation A53E associated with atypical multiple system atrophy and Parkinson's disease-type pathology.* Neurobiol Aging, 2014. **35**(9): p. 2180 e1-5.
57. Farrer, M., et al., *Comparison of kindreds with parkinsonism and alpha-synuclein genomic multiplications.* Ann Neurol, 2004. **55**(2): p. 174-9.
58. Maraganore, D.M., et al., *Collaborative analysis of alpha-synuclein gene promoter variability and Parkinson disease.* JAMA, 2006. **296**(6): p. 661-70.
59. Spillantini, M.G., et al., *Alpha-synuclein in Lewy bodies.* Nature, 1997. **388**(6645): p. 839-40.
60. Spillantini, M.G., et al., *alpha-Synuclein in filamentous inclusions of Lewy bodies from Parkinson's disease and dementia with lewy bodies.* Proc Natl Acad Sci U S A, 1998. **95**(11): p. 6469-73.
61. Baba, M., et al., *Aggregation of alpha-synuclein in Lewy bodies of sporadic Parkinson's disease and dementia with Lewy bodies.* Am J Pathol, 1998. **152**(4): p. 879-84.
62. Greten-Harrison, B., et al., *alphabetagamma-Synuclein triple knockout mice reveal age-dependent neuronal dysfunction.* Proc Natl Acad Sci U S A, 2010. **107**(45): p. 19573-8.
63. Davidson, W.S., et al., *Stabilization of alpha-synuclein secondary structure upon binding to synthetic membranes.* J Biol Chem, 1998. **273**(16): p. 9443-9.

64. Giasson, B.I., et al., *A hydrophobic stretch of 12 amino acid residues in the middle of alpha-synuclein is essential for filament assembly.* J Biol Chem, 2001. **276**(4): p. 2380-6.
65. Hoyer, W., et al., *Impact of the acidic C-terminal region comprising amino acids 109-140 on alpha-synuclein aggregation in vitro.* Biochemistry, 2004. **43**(51): p. 16233-42.
66. Dedmon, M.M., et al., *Mapping long-range interactions in alpha-synuclein using spin-label NMR and ensemble molecular dynamics simulations.* J Am Chem Soc, 2005. **127**(2): p. 476-7.
67. Bertoncini, C.W., et al., *Release of long-range tertiary interactions potentiates aggregation of natively unstructured alpha-synuclein.* Proc Natl Acad Sci U S A, 2005. **102**(5): p. 1430-5.
68. Kim, T.D., S.R. Paik, and C.H. Yang, *Structural and functional implications of C-terminal regions of alpha-synuclein.* Biochemistry, 2002. **41**(46): p. 13782-90.
69. Bussell, R., Jr. and D. Eliezer, *A structural and functional role for 11-mer repeats in alpha-synuclein and other exchangeable lipid binding proteins.* J Mol Biol, 2003. **329**(4): p. 763-78.
70. Ulmer, T.S., et al., *Structure and dynamics of micelle-bound human alpha-synuclein.* J Biol Chem, 2005. **280**(10): p. 9595-603.
71. Jao, C.C., et al., *Structure of membrane-bound alpha-synuclein from site-directed spin labeling and computational refinement.* Proc Natl Acad Sci U S A, 2008. **105**(50): p. 19666-71.
72. Lokappa, S.B. and T.S. Ulmer, *Alpha-synuclein populates both elongated and broken helix states on small unilamellar vesicles.* J Biol Chem, 2011. **286**(24): p. 21450-7.
73. Madine, J., A.J. Doig, and D.A. Middleton, *A study of the regional effects of alpha-synuclein on the organization and stability of phospholipid bilayers.* Biochemistry, 2006. **45**(18): p. 5783-92.
74. Kamp, F. and K. Beyer, *Binding of alpha-synuclein affects the lipid packing in bilayers of small vesicles.* J Biol Chem, 2006. **281**(14): p. 9251-9.
75. Varkey, J., et al., *Membrane curvature induction and tubulation are common features of synucleins and apolipoproteins.* J Biol Chem, 2010. **285**(42): p. 32486-93.
76. Lee, H.J., C. Choi, and S.J. Lee, *Membrane-bound alpha-synuclein has a high aggregation propensity and the ability to seed the aggregation of the cytosolic form.* J Biol Chem, 2002. **277**(1): p. 671-8.
77. Zhu, M. and A.L. Fink, *Lipid binding inhibits alpha-synuclein fibril formation.* J Biol Chem, 2003. **278**(19): p. 16873-7.
78. Abedini, A. and D.P. Raleigh, *A critical assessment of the role of helical intermediates in amyloid formation by natively unfolded proteins and polypeptides.* Protein Eng Des Sel, 2009. **22**(8): p. 453-9.
79. Ramakrishnan, M., P.H. Jensen, and D. Marsh, *Association of alpha-synuclein and mutants with lipid membranes: spin-label ESR and polarized IR.* Biochemistry, 2006. **45**(10): p. 3386-95.
80. Pall, H.S., et al., *Raised cerebrospinal-fluid copper concentration in Parkinson's disease.* Lancet, 1987. **2**(8553): p. 238-41.
81. Riederer, P., et al., *Transition metals, ferritin, glutathione, and ascorbic acid in parkinsonian brains.* J Neurochem, 1989. **52**(2): p. 515-20.
82. Dexter, D.T., et al., *Alterations in the levels of iron, ferritin and other trace metals in Parkinson's disease and other neurodegenerative diseases affecting the basal ganglia.* Brain, 1991. **114 (Pt 4)**: p. 1953-75.
83. Youdim, M.B., D. Ben-Shachar, and P. Riederer, *Iron in brain function and dysfunction with emphasis on Parkinson's disease.* Eur Neurol, 1991. **31 Suppl 1**: p. 34-40.

84. Binolfi, A., et al., *Site-specific interactions of Cu(II) with alpha and beta-synuclein: bridging the molecular gap between metal binding and aggregation.* J Am Chem Soc, 2008. **130**(35): p. 11801-12.
85. Peng, Y., et al., *Binding of alpha-synuclein with Fe(III) and with Fe(II) and biological implications of the resultant complexes.* J Inorg Biochem, 2010. **104**(4): p. 365-70.
86. Binolfi, A., et al., *Interaction of alpha-synuclein with divalent metal ions reveals key differences: a link between structure, binding specificity and fibrillation enhancement.* J Am Chem Soc, 2006. **128**(30): p. 9893-901.
87. Dudzik, C.G., E.D. Walter, and G.L. Millhauser, *Coordination features and affinity of the Cu(2)+ site in the alpha-synuclein protein of Parkinson's disease.* Biochemistry, 2011. **50**(11): p. 1771-7.
88. Lucas, H.R., et al., *Evidence for copper-dioxygen reactivity during alpha-synuclein fibril formation.* J Am Chem Soc, 2010. **132**(19): p. 6636-7.
89. Davies, P., D. Moualla, and D.R. Brown, *Alpha-synuclein is a cellular ferrireductase.* PLoS One, 2011. **6**(1): p. e15814.
90. Tabner, B.J., et al., *Formation of hydrogen peroxide and hydroxyl radicals from A(beta) and alpha-synuclein as a possible mechanism of cell death in Alzheimer's disease and Parkinson's disease.* Free Radic Biol Med, 2002. **32**(11): p. 1076-83.
91. Uversky, V.N., J. Li, and A.L. Fink, *Metal-triggered structural transformations, aggregation, and fibrillation of human alpha-synuclein. A possible molecular NK between Parkinson's disease and heavy metal exposure.* J Biol Chem, 2001. **276**(47): p. 44284-96.
92. Uversky, V.N., J. Li, and A.L. Fink, *Evidence for a partially folded intermediate in alpha-synuclein fibril formation.* J Biol Chem, 2001. **276**(14): p. 10737-44.
93. Bartels, T., J.G. Choi, and D.J. Selkoe, *alpha-Synuclein occurs physiologically as a helically folded tetramer that resists aggregation.* Nature, 2011. **477**(7362): p. 107-10.
94. Wang, W., et al., *A soluble alpha-synuclein construct forms a dynamic tetramer.* Proc Natl Acad Sci U S A, 2011. **108**(43): p. 17797-802.
95. Binolfi, A., F.X. Theillet, and P. Selenko, *Bacterial in-cell NMR of human alpha-synuclein: a disordered monomer by nature?* Biochem Soc Trans, 2012. **40**(5): p. 950-4.
96. Fauvet, B., et al., *alpha-Synuclein in central nervous system and from erythrocytes, mammalian cells, and Escherichia coli exists predominantly as disordered monomer.* J Biol Chem, 2012. **287**(19): p. 15345-64.
97. Burre, J., et al., *Properties of native brain alpha-synuclein.* Nature, 2013. **498**(7453): p. E4-6; discussion E6-7.
98. Abeliovich, A., et al., *Mice lacking alpha-synuclein display functional deficits in the nigrostriatal dopamine system.* Neuron, 2000. **25**(1): p. 239-52.
99. Perez, R.G., et al., *A role for alpha-synuclein in the regulation of dopamine biosynthesis.* J Neurosci, 2002. **22**(8): p. 3090-9.
100. Murphy, D.D., et al., *Synucleins are developmentally expressed, and alpha-synuclein regulates the size of the presynaptic vesicular pool in primary hippocampal neurons.* J Neurosci, 2000. **20**(9): p. 3214-20.
101. Burre, J., et al., *Alpha-synuclein promotes SNARE-complex assembly in vivo and in vitro.* Science, 2010. **329**(5999): p. 1663-7.

102. Jenco, J.M., et al., *Regulation of phospholipase D2: selective inhibition of mammalian phospholipase D isoenzymes by alpha- and beta-synucleins.* Biochemistry, 1998. **37**(14): p. 4901-9.
103. Zhu, M., et al., *Alpha-synuclein can function as an antioxidant preventing oxidation of unsaturated lipid in vesicles.* Biochemistry, 2006. **45**(26): p. 8135-42.
104. Chandra, S., et al., *Alpha-synuclein cooperates with CSPalpha in preventing neurodegeneration.* Cell, 2005. **123**(3): p. 383-96.
105. Ostrerova, N., et al., *alpha-Synuclein shares physical and functional homology with 14-3-3 proteins.* J Neurosci, 1999. **19**(14): p. 5782-91.
106. Ahn, M., et al., *Chaperone-like activities of alpha-synuclein: alpha-synuclein assists enzyme activities of esterases.* Biochem Biophys Res Commun, 2006. **346**(4): p. 1142-9.
107. Rekas, A., et al., *The chaperone activity of alpha-synuclein: Utilizing deletion mutants to map its interaction with target proteins.* Proteins, 2012. **80**(5): p. 1316-25.
108. Manda, K.M., et al., *The chaperone-like activity of alpha-synuclein attenuates aggregation of its alternatively spliced isoform, 112-synuclein in vitro: plausible cross-talk between isoforms in protein aggregation.* PLoS One, 2014. **9**(6): p. e98657.
109. Uversky, V.N., *A protein-chameleon: conformational plasticity of alpha-synuclein, a disordered protein involved in neurodegenerative disorders.* J Biomol Struct Dyn, 2003. **21**(2): p. 211-34.
110. Ahmad, B., Y. Chen, and L.J. Lapidus, *Aggregation of alpha-synuclein is kinetically controlled by intramolecular diffusion.* Proc Natl Acad Sci U S A, 2012. **109**(7): p. 2336-41.
111. Ferreon, A.C., et al., *Interplay of alpha-synuclein binding and conformational switching probed by single-molecule fluorescence.* Proc Natl Acad Sci U S A, 2009. **106**(14): p. 5645-50.
112. Sandal, M., et al., *Conformational equilibria in monomeric alpha-synuclein at the single-molecule level.* PLoS Biol, 2008. **6**(1): p. e6.
113. Brucale, M., et al., *Pathogenic mutations shift the equilibria of alpha-synuclein single molecules towards structured conformers.* Chembiochem, 2009. **10**(1): p. 176-83.
114. Trexler, A.J. and E. Rhoades, *Single molecule characterization of alpha-synuclein in aggregation-prone states.* Biophys J, 2010. **99**(9): p. 3048-55.
115. Zimmerman, S.B. and S.O. Trach, *Estimation of macromolecule concentrations and excluded volume effects for the cytoplasm of Escherichia coli.* J Mol Biol, 1991. **222**(3): p. 599-620.
116. Munishkina, L.A., et al., *The effect of macromolecular crowding on protein aggregation and amyloid fibril formation.* J Mol Recognit, 2004. **17**(5): p. 456-64.
117. Uversky, V.N., et al., *Accelerated alpha-synuclein fibrillation in crowded milieu.* FEBS Lett, 2002. **515**(1-3): p. 99-103.
118. van Raaij, M.E., et al., *Concentration dependence of alpha-synuclein fibril length assessed by quantitative atomic force microscopy and statistical-mechanical theory.* Biophys J, 2008. **95**(10): p. 4871-8.
119. Ferreira, S.T., A. Chapeaurouge, and F.G. De Felice, *Stabilization of partially folded states in protein folding/misfolding transitions by hydrostatic pressure.* Braz J Med Biol Res, 2005. **38**(8): p. 1215-22.
120. Uversky, V.N., J. Li, and A.L. Fink, *Pesticides directly accelerate the rate of alpha-synuclein fibril formation: a possible factor in Parkinson's disease.* FEBS Lett, 2001. **500**(3): p. 105-8.
121. Manning-Bog, A.B., et al., *The herbicide paraquat causes up-regulation and aggregation of alpha-synuclein in mice: paraquat and alpha-synuclein.* J Biol Chem, 2002. **277**(3): p. 1641-4.

122. Uversky, V.N., et al., *Synergistic effects of pesticides and metals on the fibrillation of alpha-synuclein: implications for Parkinson's disease.* Neurotoxicology, 2002. **23**(4-5): p. 527-36.
123. Hashimoto, T., et al., *Magnesium exerts both preventive and ameliorating effects in an in vitro rat Parkinson disease model involving 1-methyl-4-phenylpyridinium (MPP+) toxicity in dopaminergic neurons.* Brain Res, 2008. **1197**: p. 143-51.
124. Miyake, Y., et al., *Dietary intake of metals and risk of Parkinson's disease: a case-control study in Japan.* J Neurol Sci, 2011. **306**(1-2): p. 98-102.
125. Li, J., et al., *Rifampicin inhibits alpha-synuclein fibrillation and disaggregates fibrils.* Chem Biol, 2004. **11**(11): p. 1513-21.
126. Bieschke, J., et al., *EGCG remodels mature alpha-synuclein and amyloid-beta fibrils and reduces cellular toxicity.* Proc Natl Acad Sci U S A, 2010. **107**(17): p. 7710-5.
127. Singh, P.K., et al., *Curcumin modulates alpha-synuclein aggregation and toxicity.* ACS Chem Neurosci, 2013. **4**(3): p. 393-407.
128. Fujiwara, H., et al., *alpha-Synuclein is phosphorylated in synucleinopathy lesions.* Nat Cell Biol, 2002. **4**(2): p. 160-4.
129. Smith, W.W., et al., *Alpha-synuclein phosphorylation enhances eosinophilic cytoplasmic inclusion formation in SH-SY5Y cells.* J Neurosci, 2005. **25**(23): p. 5544-52.
130. Chen, L., et al., *Tyrosine and serine phosphorylation of alpha-synuclein have opposing effects on neurotoxicity and soluble oligomer formation.* J Clin Invest, 2009. **119**(11): p. 3257-65.
131. Paleologou, K.E., et al., *Phosphorylation at S87 is enhanced in synucleinopathies, inhibits alpha-synuclein oligomerization, and influences synuclein-membrane interactions.* J Neurosci, 2010. **30**(9): p. 3184-98.
132. Schmid, A.W., et al., *Alpha-synuclein post-translational modifications as potential biomarkers for Parkinson disease and other synucleinopathies.* Mol Cell Proteomics, 2013. **12**(12): p. 3543-58.
133. Li, W., et al., *Aggregation promoting C-terminal truncation of alpha-synuclein is a normal cellular process and is enhanced by the familial Parkinson's disease-linked mutations.* Proc Natl Acad Sci U S A, 2005. **102**(6): p. 2162-7.
134. Murray, I.V., et al., *Role of alpha-synuclein carboxy-terminus on fibril formation in vitro.* Biochemistry, 2003. **42**(28): p. 8530-40.
135. Ostrerova-Golts, N., et al., *The A53T alpha-synuclein mutation increases iron-dependent aggregation and toxicity.* J Neurosci, 2000. **20**(16): p. 6048-54.
136. Li, J., V.N. Uversky, and A.L. Fink, *Effect of familial Parkinson's disease point mutations A30P and A53T on the structural properties, aggregation, and fibrillation of human alpha-synuclein.* Biochemistry, 2001. **40**(38): p. 11604-13.
137. Greenbaum, E.A., et al., *The E46K mutation in alpha-synuclein increases amyloid fibril formation.* J Biol Chem, 2005. **280**(9): p. 7800-7.
138. Krasnoslobodtsev, A.V., et al., *alpha-Synuclein misfolding assessed with single molecule AFM force spectroscopy: effect of pathogenic mutations.* Biochemistry, 2013. **52**(42): p. 7377-86.
139. Ghosh, D., et al., *The Parkinson's disease-associated H50Q mutation accelerates alpha-Synuclein aggregation in vitro.* Biochemistry, 2013. **52**(40): p. 6925-7.
140. Conway, K.A., et al., *Acceleration of oligomerization, not fibrillization, is a shared property of both alpha-synuclein mutations linked to early-onset Parkinson's disease: implications for pathogenesis and therapy.* Proc Natl Acad Sci U S A, 2000. **97**(2): p. 571-6.

141. Badiola, N., et al., *Tau enhances alpha-synuclein aggregation and toxicity in cellular models of synucleinopathy.* PLoS One, 2011. **6**(10): p. e26609.
142. Masliah, E., et al., *beta-amyloid peptides enhance alpha-synuclein accumulation and neuronal deficits in a transgenic mouse model linking Alzheimer's disease and Parkinson's disease.* Proc Natl Acad Sci U S A, 2001. **98**(21): p. 12245-50.
143. Ono, K., et al., *Cross-seeding effects of amyloid beta-protein and alpha-synuclein.* J Neurochem, 2012. **122**(5): p. 883-90.
144. Mougenot, A.L., et al., *Transmission of prion strains in a transgenic mouse model overexpressing human A53T mutated alpha-synuclein.* J Neuropathol Exp Neurol, 2011. **70**(5): p. 377-85.
145. Alim, M.A., et al., *Tubulin seeds alpha-synuclein fibril formation.* J Biol Chem, 2002. **277**(3): p. 2112-7.
146. Liu, I.H., et al., *Agrin binds alpha-synuclein and modulates alpha-synuclein fibrillation.* Glycobiology, 2005. **15**(12): p. 1320-31.
147. Lindersson, E., et al., *p25alpha Stimulates alpha-synuclein aggregation and is co-localized with aggregated alpha-synuclein in alpha-synucleinopathies.* J Biol Chem, 2005. **280**(7): p. 5703-15.
148. Lindersson, E.K., et al., *alpha-Synuclein filaments bind the transcriptional regulator HMGB-1.* Neuroreport, 2004. **15**(18): p. 2735-9.
149. Israeli, E. and R. Sharon, *Beta-synuclein occurs in vivo in lipid-associated oligomers and forms hetero-oligomers with alpha-synuclein.* J Neurochem, 2009. **108**(2): p. 465-74.
150. Uversky, V.N., et al., *Biophysical properties of the synucleins and their propensities to fibrillate: inhibition of alpha-synuclein assembly by beta- and gamma-synucleins.* J Biol Chem, 2002. **277**(14): p. 11970-8.
151. McLean, P.J., et al., *TorsinA and heat shock proteins act as molecular chaperones: suppression of alpha-synuclein aggregation.* J Neurochem, 2002. **83**(4): p. 846-54.
152. Luk, K.C., et al., *Interactions between Hsp70 and the hydrophobic core of alpha-synuclein inhibit fibril assembly.* Biochemistry, 2008. **47**(47): p. 12614-25.
153. Rekas, A., et al., *Interaction of the molecular chaperone alphaB-crystallin with alpha-synuclein: effects on amyloid fibril formation and chaperone activity.* J Mol Biol, 2004. **340**(5): p. 1167-83.
154. Waudby, C.A., et al., *The interaction of alphaB-crystallin with mature alpha-synuclein amyloid fibrils inhibits their elongation.* Biophys J, 2010. **98**(5): p. 843-51.
155. Serpell, L.C., et al., *Fiber diffraction of synthetic alpha-synuclein filaments shows amyloid-like cross-beta conformation.* Proc Natl Acad Sci U S A, 2000. **97**(9): p. 4897-902.
156. Conway, K.A., J.D. Harper, and P.T. Lansbury, *Accelerated in vitro fibril formation by a mutant alpha-synuclein linked to early-onset Parkinson disease.* Nat Med, 1998. **4**(11): p. 1318-20.
157. Miake, H., et al., *Biochemical characterization of the core structure of alpha-synuclein filaments.* J Biol Chem, 2002. **277**(21): p. 19213-9.
158. Der-Sarkissian, A., et al., *Structural organization of alpha-synuclein fibrils studied by site-directed spin labeling.* J Biol Chem, 2003. **278**(39): p. 37530-5.
159. Tycko, R., *Solid-state NMR studies of amyloid fibril structure.* Annu Rev Phys Chem, 2011. **62**: p. 279-99.
160. Heise, H., et al., *Molecular-level secondary structure, polymorphism, and dynamics of full-length alpha-synuclein fibrils studied by solid-state NMR.* Proc Natl Acad Sci U S A, 2005. **102**(44): p. 15871-6.

161. Chen, M., et al., *Investigation of alpha-synuclein fibril structure by site-directed spin labeling.* J Biol Chem, 2007. **282**(34): p. 24970-9.
162. Vilar, M., et al., *The fold of alpha-synuclein fibrils.* Proc Natl Acad Sci U S A, 2008. **105**(25): p. 8637-42.
163. Comellas, G., et al., *Structured regions of alpha-synuclein fibrils include the early-onset Parkinson's disease mutation sites.* J Mol Biol, 2011. **411**(4): p. 881-95.
164. Pornsuwan, S., et al., *Long-range distances in amyloid fibrils of alpha-synuclein from PELDOR spectroscopy.* Angew Chem Int Ed Engl, 2013. **52**(39): p. 10290-4.
165. Lemkau, L.R., et al., *Site-specific perturbations of alpha-synuclein fibril structure by the Parkinson's disease associated mutations A53T and E46K.* PLoS One, 2013. **8**(3): p. e49750.
166. Dickson, D.W., et al., *Diffuse Lewy body disease: light and electron microscopic immunocytochemistry of senile plaques.* Acta Neuropathol, 1989. **78**(6): p. 572-84.
167. Kosaka, K., *Diffuse Lewy body disease in Japan.* J Neurol, 1990. **237**(3): p. 197-204.
168. Caughey, B. and P.T. Lansbury, *Protofibrils, pores, fibrils, and neurodegeneration: separating the responsible protein aggregates from the innocent bystanders.* Annu Rev Neurosci, 2003. **26**: p. 267-98.
169. Tsika, E., et al., *Distinct region-specific alpha-synuclein oligomers in A53T transgenic mice: implications for neurodegeneration.* J Neurosci, 2010. **30**(9): p. 3409-18.
170. Sandberg, A., et al., *Stabilization of neurotoxic Alzheimer amyloid-beta oligomers by protein engineering.* Proc Natl Acad Sci U S A, 2010. **107**(35): p. 15595-600.
171. Winner, B., et al., *In vivo demonstration that alpha-synuclein oligomers are toxic.* Proc Natl Acad Sci U S A, 2011. **108**(10): p. 4194-9.
172. El-Agnaf, O.M., et al., *Detection of oligomeric forms of alpha-synuclein protein in human plasma as a potential biomarker for Parkinson's disease.* FASEB J, 2006. **20**(3): p. 419-25.
173. Tokuda, T., et al., *Detection of elevated levels of alpha-synuclein oligomers in CSF from patients with Parkinson disease.* Neurology, 2010. **75**(20): p. 1766-72.
174. Hansson, O., et al., *Levels of cerebrospinal fluid alpha-synuclein oligomers are increased in Parkinson's disease with dementia and dementia with Lewy bodies compared to Alzheimer's disease.* Alzheimers Res Ther, 2014. **6**(3): p. 25.
175. Paleologou, K.E., et al., *Detection of elevated levels of soluble alpha-synuclein oligomers in post-mortem brain extracts from patients with dementia with Lewy bodies.* Brain, 2009. **132**(Pt 4): p. 1093-101.
176. Sharon, R., et al., *The formation of highly soluble oligomers of alpha-synuclein is regulated by fatty acids and enhanced in Parkinson's disease.* Neuron, 2003. **37**(4): p. 583-95.
177. Danzer, K.M., et al., *Different species of alpha-synuclein oligomers induce calcium influx and seeding.* J Neurosci, 2007. **27**(34): p. 9220-32.
178. Wright, J.A., X. Wang, and D.R. Brown, *Unique copper-induced oligomers mediate alpha-synuclein toxicity.* FASEB J, 2009. **23**(8): p. 2384-93.
179. Cappai, R., et al., *Dopamine promotes alpha-synuclein aggregation into SDS-resistant soluble oligomers via a distinct folding pathway.* FASEB J, 2005. **19**(10): p. 1377-9.
180. Lowe, R., et al., *Calcium(II) selectively induces alpha-synuclein annular oligomers via interaction with the C-terminal domain.* Protein Sci, 2004. **13**(12): p. 3245-52.
181. Volles, M.J., et al., *Vesicle permeabilization by protofibrillar alpha-synuclein: implications for the pathogenesis and treatment of Parkinson's disease.* Biochemistry, 2001. **40**(26): p. 7812-9.

182. Hogen, T., et al., *Two different binding modes of alpha-synuclein to lipid vesicles depending on its aggregation state.* Biophys J, 2012. **102**(7): p. 1646-55.
183. Pountney, D.L., N.H. Voelcker, and W.P. Gai, *Annular alpha-synuclein oligomers are potentially toxic agents in alpha-synucleinopathy. Hypothesis.* Neurotox Res, 2005. **7**(1-2): p. 59-67.
184. Choi, B.K., et al., *Large alpha-synuclein oligomers inhibit neuronal SNARE-mediated vesicle docking.* Proc Natl Acad Sci U S A, 2013. **110**(10): p. 4087-92.
185. Hinault, M.P., et al., *Stable alpha-synuclein oligomers strongly inhibit chaperone activity of the Hsp70 system by weak interactions with J-domain co-chaperones.* J Biol Chem, 2010. **285**(49): p. 38173-82.
186. Emmanouilidou, E., et al., *Cell-produced alpha-synuclein is secreted in a calcium-dependent manner by exosomes and impacts neuronal survival.* J Neurosci, 2010. **30**(20): p. 6838-51.
187. Lee, H.J., S. Patel, and S.J. Lee, *Intravesicular localization and exocytosis of alpha-synuclein and its aggregates.* J Neurosci, 2005. **25**(25): p. 6016-24.
188. Danzer, K.M., et al., *Exosomal cell-to-cell transmission of alpha synuclein oligomers.* Mol Neurodegener, 2012. **7**: p. 42.
189. Luk, K.C., et al., *Pathological alpha-synuclein transmission initiates Parkinson-like neurodegeneration in nontransgenic mice.* Science, 2012. **338**(6109): p. 949-53.
190. Lee, S.J., et al., *Cell-to-cell transmission of alpha-synuclein aggregates.* Methods Mol Biol, 2012. **849**: p. 347-59.
191. Luk, K.C., et al., *Exogenous alpha-synuclein fibrils seed the formation of Lewy body-like intracellular inclusions in cultured cells.* Proc Natl Acad Sci U S A, 2009. **106**(47): p. 20051-6.
192. Volpicelli-Daley, L.A., et al., *Exogenous alpha-synuclein fibrils induce Lewy body pathology leading to synaptic dysfunction and neuron death.* Neuron, 2011. **72**(1): p. 57-71.
193. Danzer, K.M., et al., *Seeding induced by alpha-synuclein oligomers provides evidence for spreading of alpha-synuclein pathology.* J Neurochem, 2009. **111**(1): p. 192-203.
194. Masuda-Suzukake, M., et al., *Prion-like spreading of pathological alpha-synuclein in brain.* Brain, 2013. **136**(Pt 4): p. 1128-38.
195. Luk, K.C., et al., *Intracerebral inoculation of pathological alpha-synuclein initiates a rapidly progressive neurodegenerative alpha-synucleinopathy in mice.* J Exp Med, 2012. **209**(5): p. 975-86.
196. Holliger, P. and P.J. Hudson, *Engineered antibody fragments and the rise of single domains.* Nat Biotechnol, 2005. **23**(9): p. 1126-36.
197. Kayed, R., et al., *Conformation dependent monoclonal antibodies distinguish different replicating strains or conformers of prefibrillar Abeta oligomers.* Mol Neurodegener, 2010. **5**: p. 57.
198. Emadi, S., et al., *Detecting morphologically distinct oligomeric forms of alpha-synuclein.* J Biol Chem, 2009. **284**(17): p. 11048-58.
199. Guilliams, T., et al., *Nanobodies raised against monomeric alpha-synuclein distinguish between fibrils at different maturation stages.* J Mol Biol, 2013. **425**(14): p. 2397-411.
200. Kasturirangan, S., et al., *Nanobody specific for oligomeric beta-amyloid stabilizes nontoxic form.* Neurobiol Aging, 2012. **33**(7): p. 1320-8.
201. De Genst, E., et al., *A nanobody binding to non-amyloidogenic regions of the protein human lysozyme enhances partial unfolding but inhibits amyloid fibril formation.* J Phys Chem B, 2013. **117**(42): p. 13245-58.

202. Gebauer, M. and A. Skerra, *Engineered protein scaffolds as next-generation antibody therapeutics.* Curr Opin Chem Biol, 2009. **13**(3): p. 245-55.
203. Jansson, B., M. Uhlen, and P.A. Nygren, *All individual domains of staphylococcal protein A show Fab binding.* FEMS Immunol Med Microbiol, 1998. **20**(1): p. 69-78.
204. Foster, T.J. and D. McDevitt, *Surface-associated proteins of Staphylococcus aureus: their possible roles in virulence.* FEMS Microbiol Lett, 1994. **118**(3): p. 199-205.
205. Nilsson, B., et al., *A synthetic IgG-binding domain based on staphylococcal protein A.* Protein Eng, 1987. **1**(2): p. 107-13.
206. Nord, K., et al., *Binding proteins selected from combinatorial libraries of an alpha-helical bacterial receptor domain.* Nat Biotechnol, 1997. **15**(8): p. 772-7.
207. Lofblom, J., et al., *Affibody molecules: engineered proteins for therapeutic, diagnostic and biotechnological applications.* FEBS Lett, 2010. **584**(12): p. 2670-80.
208. Feldwisch, J. and V. Tolmachev, *Engineering of affibody molecules for therapy and diagnostics.* Methods Mol Biol, 2012. **899**: p. 103-26.
209. Gronwall, C., et al., *Selection and characterization of Affibody ligands binding to Alzheimer amyloid beta peptides.* J Biotechnol, 2007. **128**(1): p. 162-83.
210. Wikman, M., et al., *Selection and characterization of HER2/neu-binding affibody ligands.* Protein Eng Des Sel, 2004. **17**(5): p. 455-62.
211. Orlova, A., et al., *Synthetic affibody molecules: a novel class of affinity ligands for molecular imaging of HER2-expressing malignant tumors.* Cancer Res, 2007. **67**(5): p. 2178-86.
212. Hoyer, W., et al., *Stabilization of a beta-hairpin in monomeric Alzheimer's amyloid-beta peptide inhibits amyloid formation.* Proc Natl Acad Sci U S A, 2008. **105**(13): p. 5099-104.
213. Luheshi, L.M., et al., *Sequestration of the Abeta peptide prevents toxicity and promotes degradation in vivo.* PLoS Biol, 2010. **8**(3): p. e1000334.
214. Hoyer, W. and T. Hard, *Interaction of Alzheimer's A beta peptide with an engineered binding protein--thermodynamics and kinetics of coupled folding-binding.* J Mol Biol, 2008. **378**(2): p. 398-411.
215. Gronwall, C. and S. Stahl, *Engineered affinity proteins--generation and applications.* J Biotechnol, 2009. **140**(3-4): p. 254-69.
216. Smith, G.P., *Filamentous fusion phage: novel expression vectors that display cloned antigens on the virion surface.* Science, 1985. **228**(4705): p. 1315-7.
217. Smith, G.P. and V.A. Petrenko, *Phage Display.* Chem Rev, 1997. **97**(2): p. 391-410.
218. Lam, S.L. and V.L. Hsu, *NMR identification of left-handed polyproline type II helices.* Biopolymers, 2003. **69**(2): p. 270-81.
219. McNulty, B.C., et al., *Temperature-induced reversible conformational change in the first 100 residues of alpha-synuclein.* Protein Sci, 2006. **15**(3): p. 602-8.
220. Hutchinson, E.G. and J.M. Thornton, *A revised set of potentials for beta-turn formation in proteins.* Protein Sci, 1994. **3**(12): p. 2207-16.
221. Bogan, A.A. and K.S. Thorn, *Anatomy of hot spots in protein interfaces.* J Mol Biol, 1998. **280**(1): p. 1-9.
222. Vilar, M., et al., *The fold of α-synuclein fibrils.* Proc Natl Acad Sci U S A, 2008. **105**(25): p. 8637-42.
223. Zibaee, S., et al., *Human beta-synuclein rendered fibrillogenic by designed mutations.* J Biol Chem, 2010. **285**(49): p. 38555-67.

224. Mittag, T. and J.D. Forman-Kay, *Atomic-level characterization of disordered protein ensembles.* Curr Opin Struct Biol, 2007. **17**(1): p. 3-14.
225. Esteban-Martin, S., et al., *Identification of fibril-like tertiary contacts in soluble monomeric alpha-synuclein.* Biophys J, 2013. **105**(5): p. 1192-8.
226. Kim, H.Y., et al., *Correlation of amyloid fibril beta-structure with the unfolded state of alpha-synuclein.* Chembiochem, 2007. **8**(14): p. 1671-4.
227. Fuxreiter, M., et al., *Preformed structural elements feature in partner recognition by intrinsically unstructured proteins.* J Mol Biol, 2004. **338**(5): p. 1015-26.
228. Csermely, P., R. Palotai, and R. Nussinov, *Induced fit, conformational selection and independent dynamic segments: an extended view of binding events.* Trends Biochem Sci, 2010. **35**(10): p. 539-46.
229. Cheon, M., et al., *Structural reorganisation and potential toxicity of oligomeric species formed during the assembly of amyloid fibrils.* PLoS Comput Biol, 2007. **3**(9): p. 1727-38.
230. Celej, M.S., et al., *Toxic prefibrillar α-synuclein amyloid oligomers adopt a distinctive antiparallel β-sheet structure.* Biochem J, 2012. **443**(3): p. 719-26.
231. Zibaee, S., et al., *Human β-synuclein rendered fibrillogenic by designed mutations.* J Biol Chem, 2010. **285**(49): p. 38555-67.
232. Koo, H.J., H.J. Lee, and H. Im, *Sequence determinants regulating fibrillation of human α-synuclein.* Biochem Biophys Res Commun, 2008. **368**(3): p. 772-8.
233. Lamberto, G.R., et al., *Structural and mechanistic basis behind the inhibitory interaction of PcTS on α-synuclein amyloid fibril formation.* Proc Natl Acad Sci U S A, 2009. **106**(50): p. 21057-62.
234. Rao, J.N., V. Dua, and T.S. Ulmer, *Characterization of α-synuclein interactions with selected aggregation-inhibiting small molecules.* Biochemistry, 2008. **47**(16): p. 4651-6.
235. Abe, K., et al., *Peptide ligand screening of alpha-synuclein aggregation modulators by in silico panning.* BMC Bioinformatics, 2007. **8**: p. 451.
236. Narayanan, V., Y. Guo, and S. Scarlata, *Fluorescence studies suggest a role for alpha-synuclein in the phosphatidylinositol lipid signaling pathway.* Biochemistry, 2005. **44**(2): p. 462-70.
237. Guo, Y. and S. Scarlata, *A loss in cellular protein partners promotes alpha-synuclein aggregation in cells resulting from oxidative stress.* Biochemistry, 2013. **52**(22): p. 3913-20.
238. Mirecka, E.A., et al., *Sequestration of a beta-hairpin for control of alpha-synuclein aggregation.* Angew Chem Int Ed Engl, 2014. **53**(16): p. 4227-30.
239. Grüning, C.S., et al., *Alternative conformations of the tau repeat domain in complex with an engineered binding protein.* Journal of Biological Chemistry, 2014.
240. Kitamoto, T., R. Iizuka, and J. Tateishi, *An amber mutation of prion protein in Gerstmann-Straussler syndrome with mutant PrP plaques.* Biochemical and Biophysical Research Communications, 1993. **192**(2): p. 525-31.
241. Daidone, I., et al., *β-hairpin conformation of fibrillogenic peptides: structure and alpha-beta transition mechanism revealed by molecular dynamics simulations.* Proteins, 2004. **57**(1): p. 198-204.
242. Dupuis, N.F., et al., *Human islet amyloid polypeptide monomers form ordered β-hairpins: a possible direct amyloidogenic precursor.* J Am Chem Soc, 2009. **131**(51): p. 18283-92.
243. Gill, A.C., *β-hairpin-mediated formation of structurally distinct multimers of neurotoxic prion peptides.* PLoS One, 2014. **9**(1): p. e87354.

244. Grabenauer, M., et al., *Oligomers of the prion protein fragment 106-126 are likely assembled from β-hairpins in solution, and methionine oxidation inhibits assembly without altering the peptide's monomeric conformation.* J Am Chem Soc, 2010. **132**(2): p. 532-9.
245. Mitternacht, S., et al., *Monte Carlo study of the formation and conformational properties of dimers of Aβ42 variants.* J Mol Biol, 2011. **410**(2): p. 357-67.
246. Reddy, A.S., et al., *Stable and metastable states of human amylin in solution.* Biophys J, 2010. **99**(7): p. 2208-16.
247. Rosenman, D.J., et al., *Aβ monomers transiently sample oligomer and fibril-like configurations: ensemble characterization using a combined MD/NMR approach.* J Mol Biol, 2013. **425**(18): p. 3338-59.
248. Dyson, H.J. and P.E. Wright, *Intrinsically unstructured proteins and their functions.* Nat Rev Mol Cell Biol, 2005. **6**(3): p. 197-208.
249. Huston, J.S., et al., *Protein engineering of antibody binding sites: recovery of specific activity in an anti-digoxin single-chain Fv analogue produced in Escherichia coli.* Proceedings of the National Acadademy of Sciences ot the United states of America, 1988. **85**(16): p. 5879-83.
250. Grönwall, C., et al., *Selection and characterization of Affibody ligands binding to Alzheimer amyloid β peptides.* J Biotechnol, 2007. **128**(1): p. 162-83.
251. Lindberg, H., et al., *Staphylococcal display for combinatorial protein engineering of a head-to-tail affibody dimer binding the Alzheimer amyloid-β peptide.* Biotechnology Journal, 2013. **8**(1): p. 139-45.
252. Robinson, C.R. and R.T. Sauer, *Equilibrium stability and sub-millisecond refolding of a designed single-chain Arc repressor.* Biochemistry, 1996. **35**(44): p. 13878-84.
253. Robinson, C.R. and R.T. Sauer, *Optimizing the stability of single-chain proteins by linker length and composition mutagenesis.* Proceedings of the National Acadademy of Sciences ot the United states of America, 1998. **95**(11): p. 5929-34.
254. Chi, Y.C., et al., *Residue histidine 50 plays a key role in protecting alpha-synuclein from aggregation at physiological pH.* J Biol Chem, 2014. **289**(22): p. 15474-81.
255. Park, S.M., et al., *Distinct roles of the N-terminal-binding domain and the C-terminal-solubilizing domain of alpha-synuclein, a molecular chaperone.* J Biol Chem, 2002. **277**(32): p. 28512-20.
256. Morales, R., I. Moreno-Gonzalez, and C. Soto, *Cross-seeding of misfolded proteins: implications for etiology and pathogenesis of protein misfolding diseases.* PLoS Pathog, 2013. **9**(9): p. e1003537.
257. Rebek, J., Jr., *Molecular recognition and self-assembly special feature: Introduction to the molecular recognition and self-assembly special feature.* Proc Natl Acad Sci U S A, 2009. **106**(26): p. 10423-4.
258. Guo, J.L., et al., *Distinct alpha-synuclein strains differentially promote tau inclusions in neurons.* Cell, 2013. **154**(1): p. 103-17.

Abbreviations

Aβ	Amyloid-β peptide
AD	Alzheimer's diseases
Ala	alanine
Asp	aspartate
CD	Circular Dichroism
CSF	cerebrospinal fluid
Cys	cysteine
e.g.	exempli gratia, for example
FTIR	Fourier Transform Infrared
Gly	glycine
GS3	Gly-Ser-Ser-Ser
His	histidine
HSP(s)	heat shock proteins
HSQC	heteronuclear single quantum coherence
IAPP	Islet amyloid polypeptide
IDP(s)	intrinsically disordered protein
Ile	isoleucine
ITC	isothermal titration calorimetry
kDa	kilo Dalton
LB	Lewy body
mRNA(s)	messenger RNA(s)
NAC	non-Aβ component
NMR	nuclear magnetic resonance
NTF(s)	neurofibrillary tangle(s)
PD	Parkinson's disease
Phe	phenylalanine
PrP	prion protein
SAXS	small-angle X-ray scattering
scFv	single chain fragment variant
SDS	sodium dodecyl sulfate
SEC	size exclusion chromatography
Ser	serine
SN	substantia nigra
SPA	staphylococcal protein A
T2D	Type 2 diabetes
ThT	Thioflavin T
Tyr	tyrosine
Val	valine

List of Figures and Tables

Acknowledgment

There are a number of people who helped me during my PhD study and without their support, this thesis would never have been written. Above all, I'm most grateful to my supervisor Dr. Wolfgang Hoyer for providing me the great opportunity for an exciting research, his kind help, support and patience. Furthermore, I thank my second supervisor and dean of Institure of Physical Biology, Professor Dr. Dieter Willbold and also Professor Dr. Detlev Riesner for providing researchers a warm and friendly atmosphere for reseach and their precious support and advices.

Thereafter, I thank my colleagues especially Clara Grüning, Aziz Gauhar and Dr. Ewa Mirecka for all friendly, collaborative and funny moments. Furthermore, I thank Dr. Mathias Stoldt, Professor Dr. Henrike Heise and Professor Dr. Torleif Härd, Dr. Oliver Bannach, Dr. Lothar Gremer for the valuable discussions and cooparations.

I thank all kind stuff in Institute of Physical biology especially Barbara Schulten, Elke Reinartz and Bernd Esters for their continuous support. I thank Mario Schneider, Oleksandr Brener, Lars Lüers, Jendrik Marbach, Steffen Hübinger, Stefan Klinker, Ehsan Amin and Kazem Nouri for all helps and funny moments.

Finally, my special thanks go to my family. I would like to dedicate this thesis to my parents for their nonstop loving, financial support and encouragement throughout my entire life. I'm thankful to my brothers and sisters for giving me motivation and positive thoughts.

Declaration

I do solemnly declare that my thesis is presentation of original research performed according to the “Principles of Good Scientific Practice” set out by Heinrich-Heine University of Düsseldorf. This thesis does not contain the data already pulished in public domain and it has never been submitted or accepted by any other insitutions for the award of any other degrees.

Düsseldorf, 25.11.2014

Hamed Shaykhalishahi